

ENHANCING EXPRESSION OF RECOMBINANT HEMOPROTEINS: PROGRESS
TOWARD UNDERSTANDING STRUCTURE/FUNCTION AND
THERAPEUTIC APPLICATION

Except where reference is made to the work of others, the work described in this dissertation is my own or was done in collaboration with my advisory committee.
This dissertation does not include proprietary or classified information.

Cornelius Varnado

Certificate of Approval:

Holly R. Ellis
Assistant Professor
Chemistry and Biochemistry

Douglas C. Goodwin, Chair
Associate Professor
Chemistry and Biochemistry

James H. Hargis
Professor
Chemistry and Biochemistry

Thomas Albrecht-Schmitt
Associate Professor
Chemistry and Biochemistry

Stephen L. McFarland
Dean
Graduate School

ENHANCING EXPRESSION OF RECOMBINANT HEMOPROTEINS: PROGRESS
TOWARD UNDERSTANDING STRUCTURE/FUNCTION AND
THERAPEUTIC APPLICATION

Cornelius Varnado

A Dissertation
Submitted to
the Graduate Faculty of
Auburn University
in Partial Fulfillment of the
Requirements for the Degree of
Doctor of Philosophy

Auburn, Alabama
August 7, 2006

ENHANCING EXPRESSION OF RECOMBINANT HEMOPROTEINS: PROGRESS
TOWARD UNDERSTANDING STRUCTURE/FUNCTION AND
THERAPEUTIC APPLICATION

Cornelius Varnado

Permission is granted to Auburn University to make copies of this dissertation at its discretion, upon request of individuals or institutions and at their expense.
The author reserves all publication rights.

Signature of Author

Date of Graduation

VITA

Cornelius Varnado, son of Alice Winding, was born in McComb, Mississippi on December 6, 1976. He graduated from South Pike High School, Magnolia, Mississippi, in May of 1995. He then attended Alcorn State University in Alcorn State, Mississippi and graduated with a Bachelor of Science in Chemistry in May of 2000. In August 2000, he entered graduate school at Auburn University in the Department of Chemistry and Biochemistry for a Ph.D. degree.

DISSERTATION ABSTRACT

ENHANCING EXPRESSION OF RECOMBINANT HEMOPROTEINS: PROGRESS
TOWARD UNDERSTANDING STRUCTURE/FUNCTION AND
THERAPEUTIC APPLICATION

Cornelius Varnado

Doctor of Philosophy, August 7, 2006
(B.S. Alcorn State University, Alcorn State, MS, May 2000)

209 Typed Pages

Directed by Douglas C. Goodwin

Nature has developed ways to control the essential need to activate oxygen. Hemoproteins perform this task using iron in a prosthetic group (e.g., iron-protoporphyrin-IX or heme). The environment surrounding the heme iron in hemoproteins dictates their activity and makes them a diverse group of enzymes. This makes hemoproteins good models for exploring the relationship between protein structure and function. The techniques necessary to pursue these studies are material-intensive. Commonly available systems for the expression of recombinant hemoproteins in *E. coli* are able to produce large quantities of protein. However, in many cases the vast majority of the protein lacks heme and are therefore inactive. A hemoprotein expression (HPEX) system was developed to resolve this problem. This system, based on the expression of an outer membrane heme receptor, was tested on two different hemoproteins, myoglobin

and catalase-peroxidase. In both cases, the system was successful, demonstrating a dramatic increase in the heme content of these proteins. Additional studies were carried out on the catalase-peroxidases. The ability of catalase-peroxidases to catalyze catalase *and* peroxidase activities using one active site make them ideal for studying the protein structure/function relationship. Moreover, a periplasm-targeted subset of these enzymes have been implicated as virulence factors. The first full characterization of a periplasmic catalase-peroxidase was carried out on KatP, an enzyme from the highly virulent pathogen *E. coli* O157:H7. Absorption and EPR spectra indicated a high-spin heme enzyme dominated by the hexacoordinate high-spin complex. Apparent k_{cat} values for catalase and peroxidase activities were higher for KatP than with other catalase-peroxidase. However, K_M values were also higher for KatP. Ferric KatP reacted with peracetic acid to form compound I and with CN^- to form a ferri-cyano complex consistent with other catalase-peroxidases. Peroxynitrite also supported compound I formation in this enzyme. This catalytic capability, combined with efficient catalase and peroxidase activities, and a periplasmic location may be advantageous for meeting an immune response that generates copious reactive oxygen and reactive nitrogen species. Crystal structures of catalase-peroxidases have revealed the presence of a three amino acid covalent adduct (Trp-Tyr-Met). It is essential for catalase activity. An SDS-PAGE method to monitor the establishment of the crosslink was developed. Using this method it was demonstrated that crosslink formation requires a redox active porphyrin. Substitution of the Tyr residue with Phe prevent formation of the crosslink and generates a protein that has no catalase activity, enhanced peroxidase activity, and increased susceptibility to peroxide-dependent inactivation.

ACKNOWLEDGEMENTS

The research conducted in this dissertation would not have been possible without the help and support of many people whom I wish to thank. First, I would like to thank my research advisor, Dr. Douglas C. Goodwin or ‘Doc’ as we called him in the lab. Doc has been a mentor as well as a friend. His patients and willingness to help guide me through my graduate career has given me a great foundation to build a career in science. I would like to thank my committee members, Drs. Holly Ellis, Thomas Albrecht-Schmitt, and James Howard Hargis for their constructive suggestions and all of their professional assistances. Thanks to all of my lab mates at Auburn University, especially Ruletha Baker, Yongjiang Li, Carma Cook, Robert Moore, Kristen Hertwig, Kimberley Laband, Robert Thomas, and J. Kenneth Roberts for all of the intelligent discussions, selfless help, and a pleasant lab environment. Special thanks to all of my family and friends for their continuous support, understanding, and encouragement. I especially want to thank my mom, Alice, whose display of strength, courage and values have made me the person who I am today. Finally, I would like to thank the Department of Chemistry and Biochemistry, Auburn University, the American Chemistry Society’s Petroleum Research Fund, and COSAM for their funding support for my research. I gratefully acknowledge the Southern Regional Education Board and Auburn University President’s Graduate Opportunity Program for their fellowship support during my graduate studies.

Style Manual Used: Biochemical and Biophysical Research Communications

Computer Software Used: Microsoft Word, Microsoft Excel, Prism, ChemDraw,
SwissPdb Viewer, MegaPov, Adobe Photoshop

TABLE OF CONTENTS

LIST OF TABLES.....	xii
LIST OF FIGURES.....	xiii
INTRODUCTION.....	1
CHAPTER ONE: LITERATURE REVIEW.....	7
Oxygen.....	7
Iron.....	10
Iron Cofactors.....	12
Hemoproteins.....	19
Summary.....	60
CHAPTER TWO: MATERIALS AND METHODS.....	63
Reagents.....	63
Construction of pHPEX Plasmids.....	64
Expression of KatG and Myoglobin.....	68
Cloning and Expression of KatP and KatG ^{Y226F}	71
Protein Characterization.....	75
CHAPTER THREE: RESULTS.....	83
HPEX System.....	83
KatP.....	105

Trp-Tyr-Met Covalent Adduct.....	123
CHAPTER FOUR: DISCUSSION.....	141
Expression of Recombinant Hemoproteins.....	142
Periplasmic Catalase-Peroxidase.....	151
Role of Trp-Tyr-Met Covalent Adduct.....	158
Summary.....	162
REFERENCES.....	166

LIST OF TABLES

Table 1.1.	Reduction Potentials of Some Oxygen Species and Other Compounds.....	8
Table 2.1	Plasmids and strains used for the development of the hemoprotein expression (HPEX) system.....	64
Table 3.1.	Catalase Kinetic Parameters for Recombinant KatG from Hemin-Supplemented Cultures of BL-21 (DE3) pHPEX3 and Unsupplemented Cultures of BL-21 (DE3) pLysS.....	96
Table 3.2.	Heme Absorption Maxima for Recombinant KatG from pHPEX3- and pLysS-Transformed <i>E. coli</i> BL-21 (DE3).....	97
Table 3.3.	Heme Absorption Maxima for KatP and KatG.....	110
Table 3.4.	Kinetic Parameters for the Catalase and Peroxidase Activities of KatG and KatP.....	114

LIST OF FIGURES

Figure 1.1.	Molecular Orbital Diagram of Molecular Oxygen.....	9
Figure 1.2.	Schematic Diagram of Reactive Oxygen Species (ROS) and their Interactions with Cells.....	13
Figure 1.3.	Iron-Sulfur Clusters and Mononuclear and Binuclear Non-Heme Iron Centers.....	15
Figure 1.4.	Biosynthetic Pathway for Heme.....	16
Figure 1.5.	Structure of Common Hemes.....	18
Figure 1.6.	Active Site Representation of Myoglobin.....	22
Figure 1.7.	T → R Transition in Hemoglobin.....	24
Figure 1.8.	Catalytic Cycle of Cytochrome P450.....	27
Figure 1.9.	Catalytic Cycle of Cytochrome Oxidase.....	31

Figure 1.10.	Active Site Comparison of Myoglobin vs. Peroxidase.....	35
Figure 1.11.	Catalytic Cycle of Peroxidase.....	37
Figure 1.12.	Catalytic Cycle of Catalase.....	40
Figure 1.13.	Catalytic Cycle of Catalase-peroxidase.....	45
Figure 1.14.	Active Site Comparison of Catalase-peroxidase and Class I Plant Peroxidases.....	47
Figure 1.15.	Autoxidation Reaction of Myoglobin and Hemoglobin.....	52
Figure 1.16.	Generation of ROS in Cytochrome P450.....	54
Figure 1.17.	Schematic Representation of the NADPH Oxidase.....	58
Figure 1.18.	Catalytic Cycle of Myeloperoxidase.....	60
Figure 2.1.	Oxidation of ABTS.....	78
Figure 2.2.	Trypsin Digest of Peptide Bond in Protein.....	80
Figure 3.1.	Schematic Representation of the Plasmids pHPEX1 (A),	

	pHPEX2 (B), pHPEX3 (C), and pHPEX-fur(D).....	84
Figure 3.2.	Diagnostic Restriction Digests of pHPEX1 (A), pHPEX2 (B), pHPEX3 (C), and pHPEX-fur (D).....	86
Figure. 3.3.	Heme Receptor Expression by Untransformed and pHPEX2- Transformed <i>E. coli</i> BL-21 (DE3).....	88
Figure 3.4.	Growth of Untransformed BL-21 (DE3) Cells in Minimal Media.....	89
Figure 3.5.	Growth of pHPEX2-Transformed BL-21 (DE3) Cells in Minimal Media.....	91
Figure 3.6.	UV-Visible Absorption Spectra of Catalase-Peroxidase Expressed in pHPEX3-Transformed Cells.....	92
Figure 3.7.	UV-Visible Absorption Spectra of Catalase-Peroxidase Expressed in pLysS-Transformed Cells.....	93
Figure 3.8.	Catalase Activity of KatG Expressed in pLysS- and pHPEX- Transformed System.....	94
Figure 3.9.	Ferric Minus Ferri-cyano Difference Spectra for Recombinant KatG Expressed in pHPEX3- and pLysS- Transformed Systems.....	98
Figure 3.10.	UV-Visible Absorption Spectra for Myoglobin Expressed in pHPEX3-Transformed Cells (Lysis cells).....	99

Figure 3.11.	Derivative UV-Visible Absorption Spectra for Myoglobin Expressed in pHPEX3-Transformed Cells (Whole cells).....	101
Figure 3.12.	Derivative UV-Visible Absorption Spectra for Myoglobin Expressed in pLysS-Transformed Cells (Whole cells).....	102
Figure 3.13.	Derivative UV-Visible Absorption Spectra for Myoglobin Expressed in pHPEX-fur-Transformed Cells (Whole cells).....	103
Figure 3.14.	Derivative UV-Visible Absorption Spectra for Myoglobin Expressed in BL-21(DE3)-Transformed Cells (Whole cells).....	104
Figure 3.15.	SDS Electrophoretic Separation of Total Cellular Protein from BL-21 DE3)pLysS Transformed pKatP3.....	106
Figure 3.16.	Heme Absorption Spectra for Ferric, Ferri-Cyano, and Ferrous Forms of KatP in Soret Region.....	108
Figure 3.17.	Heme Absorption Spectra for Ferric, Ferri-Cyano, and Ferrous Forms of KatP (480-680 nm).....	109
Figure 3.18.	EPR Spectrum of KatP and KatG.....	112
Figure 3.19.	Effect of H ₂ O ₂ Concentration on the Catalase Activity of KatG and KatP.....	113
Figure 3.20.	Effect of H ₂ O ₂ Concentration on the Peroxidase Activity of	

KatG and KatP.....	115
Figure 3.21. Effect of pH on the Catalase and Peroxidase Activity of KatP.....	117
Figure 3.22. KatP Formation of Compound I by Peracetic Acid.....	118
Figure 3.23. Absorption Changes Spectra for KatP Formation of Compound I by Peracetic Acid.....	119
Figure 3.24. Effect of Peracetic Acid Concentration on the Rate of Formation of Compound I.....	120
Figure 3.25. Effect of Cyanide Concentration on the Rate of Formation of the Fe ^{III} -CN Complex of KatP.....	121
Figure 3.26. Absorption Changes Spectra for KatP Formation of Ferri-cyano Complex.....	122
Figure 3.27. SDS-PAGE of Ni-NTA-Purified KatP	124
Figure 3.28. Trp-Tyr-Met Covalent Adduct of Catalase-Peroxidases.....	126
Figure 3.29. Absorption Spectra of Purified KatG.....	128
Figure 3.30. Effect of Heme and Peroxide on Migration of apo-KatG by SDS-PAGE.....	129

Figure 3.31. Matrix-Assisted Laser Desorption-Ionization Mass Spectrometry Schematic.....	132
Figure 3.32. MALDI Spectrum of Tryptic Digest of KatG without Covalent Adduct.....	134
Figure 3.33. MALDI Spectrum of Tryptic Digest of KatG with Covalent Adduct.....	135
Figure 3.34. SDS Electrophoretic Separation of Total Cellular Protein from BL-21 (DE3)pLysS Transformed pKatG ^{Y226F}	136
Figure 3.35. Effect of H ₂ O ₂ Concentration on the Catalase Activity of wtKatG and KatG ^{Y226F}	137
Figure 3.36. Effect of H ₂ O ₂ Concentration on the Peroxidase Activity of wtKatG and KatG ^{Y226F}	138
Figure 3.37. Effect of Heme and Peroxide on Migration of KatG ^{Y226F} by SDS-PAGE.....	140
Figure 4.1 Incorporation of Peroxynitrite in the Catalytic Cycle of Catalase-peroxidase.....	155
Figure 4.2. KatP Compound I Formation in the present of 200μm Peroxynitrite.....	156

Figure 4.3.	KatP Compound I Conversion to Compound II in the present of Peroxynitrite.....	157
Figure 4.4.	Active Site Representation of <i>E. coli</i> Catalase-Peroxidase.....	160
Figure 4.5.	Proposed Mechanism for Formation of Trp-Tyr-Met Adduct.....	163

INTRODUCTION

Hemoproteins are a very important class of enzymes found in nature and are involved in a wide range of biological processes including the metabolism of drugs and other xenobiotics, binding and transport of oxygen, respiratory electron transport, and detoxification of reactive oxygen species. As the name implies, hemoproteins are identified by the presence of a heme prosthetic group. This prosthetic group is central to the activity and/or regulation of the hemoproteins. The astounding feature is that this same prosthetic group can be directed to such a wide array of functions. Clearly, it is the protein structure around the heme group which directs the heme to a prescribed function specifically and efficiently. Ideally, if we can understand how the structures of proteins do this, we can better understand how to manipulate or control their many functions or even engineer new heme-based catalysts with new/superior properties. The best models to further investigate hemoprotein structure and function will be those that provide, first of all, insight into poorly defined aspects of the structure function equation. Second, the best models will be those for which deeper understanding of their structure and mechanism has direct benefit to unraveling serious biomedical problems.

Catalase-peroxidases stand out in both respects. First, the catalase-peroxidases have substantial biomedical importance. They are involved in the activation of the drug isoniazid, which is a front line antibiotic against *Mycobacterium tuberculosis*.

Mutation to *Mycobacterium tuberculosis* catalase-peroxidase figures prominently in the development of resistance to isoniazid. Indeed, over 70% of INH resistant tuberculosis strains carry mutations, which affect the function of catalase-peroxidase. Furthermore, the presence of a periplasmic version of this enzyme has been identified as unique to virulent pathogenic bacteria such as *Escherichia coli* O157:H7, *Yersinia pestis*, and *Legionella pneumophila*. The distinct absence of this periplasmic enzyme in the non-pathogenic relatives of these organisms implicates it as a virulence factor.

The mechanisms by which distant protein structures alter the catalytic properties of the heme prosthetic group are poorly defined. In this respect, the catalase-peroxidases also present an ideal model for study. The catalase-peroxidases have an active site which is virtually superimposable on those of several monofunctional peroxidases. Yet, only the catalase-peroxidases possess substantial catalase activity. Because of the high similarity of the active sites, influence by structures peripheral to the active site are likely to be the influential factors in this obvious functional disparity. Clearly, catalase-peroxidases provide an ideal system to evaluate a poorly understood aspect of enzyme structure and function and apply this understanding to important biomedical problems.

In order to study hemoproteins, large quantities of these proteins are needed for the material-intensive techniques necessary to pursue such studies. To date, the most productive, most efficient, and least expensive methods to produce the quantities of protein required are through the expression of recombinant forms in *Escherichia coli*. Unfortunately, for hemoproteins this is often hindered by the fact that a vast majority of the protein produced lacks the heme prosthetic group required for activity [1-6]. Simply

stated, the rate of protein synthesis is much greater than the rate of heme biosynthesis. These difficulties have prompted attempts to better match rates of heme biosynthesis and protein expression. One approach is to reduce the rate of protein expression [6] such that heme biosynthetic rates can keep pace. This is effective for producing hemoproteins with the full complement of correctly bound heme, but the decrease in expression rates may be inconvenient. An alternative approach is to increase the rate of heme biosynthesis. Production of δ -aminolevulinic acid (δ -ALA) is the rate-limiting step in the heme biosynthetic pathway [7]. Therefore, the most common method is to add large quantities of δ -ALA to expression cultures, stimulating heme production and resulting in higher heme content for the target recombinant hemoproteins [1, 3, 5]. Unfortunately, the amount of δ -ALA added to cultures is quite large, adding considerable expense to protein expression procedures. The simplest approach would be to add heme to the culture medium during expression of the target protein. This is hindered by the limited ability of many laboratory strains of *E. coli* to use exogenously added heme as an iron source for growth [8-10]. Conversely, through expression of outer membrane-bound heme receptors many pathogenic bacteria effectively overcome this limitation [8, 9, 11-19]. One example is *E. coli* 0157:H7, which uses a TonB-dependent outer membrane-bound heme receptor for heme acquisition [8, 11, 12, 20]. Most importantly, it has been shown that common laboratory strains of *E. coli* need only produce a heme receptor in order to gain full ability to import heme into the cell [8-10].

In order to aid the evaluation of the catalase-peroxidase structure/function relationship, an *E. coli*-based hemoprotein expression (HPEX) system was developed. This system is based on a series of plasmids (pHPEX) that contain the gene for the heme

receptor from *E. coli* O157:H7 (*chuA*). Transformation of our *E. coli* expression strains with pHPEX plasmids results in the ability to retrieve heme from the surrounding medium. Heme so collected is then incorporated into the active site of the target recombinant hemoprotein as it is expressed. Thus, this HPEX system is designed to yield target hemoproteins without limiting the rate of protein expression. The expression of the heme receptor by pHPEX along with hemin added to the expression medium resulted in the expression of KatG protein with full heme content and activity. The addition of the iron uptake regulator domain in pHPEX1-fur and the *lacUV5* promoter to pHPEX2 resulted in the control of the heme receptor expression by iron dependence or IPTG induction. The expression of T7 lysozyme by pHPEX3 inhibited the leakage expression of toxic protein under the common *lac* promoter.

The cellular locations of many catalase–peroxidases have not been unequivocally established. Many appear to be cytoplasmic [21, 22], and the vast majority lacks a signal peptide sequence associated with targeting to the periplasm. However, a small number of exceptions have recently been identified [23-25]. However, they are exclusively present in highly virulent pathogenic bacteria, including *E. coli* O157:H7 [12], *Y. pestis* [25], and *L. pneumophila* [23]. In these three cases, the periplasmic catalase–peroxidases are proposed to be virulence factors [23, 25-27].

The mechanisms by which these periplasmic catalase–peroxidases may contribute to virulence have not been determined, necessitating comprehensive studies to evaluate their potentially important roles. Although one of these enzymes has been isolated [25, 27], the periplasmic catalase–peroxidases remain poorly characterized. This study reports the overexpression, purification, and characterization of the periplasmic catalase–

peroxidase from enterohemorrhagic *E. coli* O157:H7. This enzyme bears the name KatP because it is encoded on a large plasmid (pO157) associated with virulence [24]. The isolation and characterization of this enzyme provides important additional information and resources to evaluate the mechanisms by which these novel periplasmic catalase–peroxidases may contribute to bacterial virulence.

The addition of a histidine tag to KatP enabled the complete isolation of expressed KatP using affinity and hydrophobic interaction chromatography. Absorption spectra of KatP were typical for catalase-peroxidases. KatP showed comparable catalase and peroxidase activities to other catalase-peroxidases. The k_{cat} values for KatP catalase and peroxidase activities were somewhat higher than other enzymes. On the other hand, K_M values were considerably higher for KatP. KatP also showed the typical sharp but distinct pH dependence for catalase and peroxidase activities. KatP formation of compound I and CN^- binding rates were also similar. The strong catalase and peroxidase activities of KatP, combined with its unique periplasmic location and its ability to react with peroxynitrite may position it ideally for use by this and other pathogens in meeting a host immune response.

The crystal structures of catalase-peroxidases each show a three amino acid covalent adduct [28-30]. The function of this Trp-Tyr-Met covalent adduct is not fully understood. However, its role in the function of catalase-peroxidase is being evaluated [31-34]. Mutation of the Tyr or Trp residue of the covalent adduct results in a loss of catalase activity [31, 33-37]. On the other hand, peroxidase activity is maintained. This indicates that the formation of compound I is not affected by the covalent adduct. The covalent adduct seems to have an effect on the reduction of compound I back to the ferric

form of the enzyme which is where catalase and peroxidase activities differ. This study looks at the formation of the covalent adduct and its effect on catalase-peroxidase.

High-level expressions of KatP appeared to result in production of the enzyme with and without the covalent adduct. Purified KatP evaluated by SDS-PAGE electrophoresis shows two protein bands. Each band was identified as KatP determined by MS. The upper band contained no heme, determined by FPLC, and had no activity, but the lower band had both heme and activity. The results with KatP reflected a general trend observed in the laboratory with KatG. That is, the greater the heme content, the greater the proportion of protein migrating with a lower apparent molecular weight. Reconstitution of apoKatG with heme resulted in the partial conversion of catalase-peroxidase to its cross-linked form. The conversion is enhanced upon the addition of peracetic acid. Conversely, reconstitution of KatG with a redox inactive cofactor (e.g., Zinc-protoporphyrin IX), no cross-link was formed, indicating that formation of the three-amino acid covalent adduct was heme and peroxidase dependent. In order to further investigate this adduct, the variant Y226F was generated and evaluated by electrophoresis and steady-state kinetics. Purified Y226F showed only one KatG protein band evaluated by SDS-PAGE. The Y226F variant essentially lost all catalase activity. However, peroxidase activity was retained. This further validates the necessity of the cross-link for catalase activity. Probing of this covalent adduct could very well prove to be novel in the understanding of the relationship between the structure and function of enzymes.

CHAPTER ONE

LITERATURE REVIEW

Oxygen

Molecular oxygen (O_2) is vital for a range of organisms, serving as a terminal electron acceptor in numerous oxidation reactions, not the least of which is the respiratory electron transport system. In order to obtain as much ATP as possible from a carbon source, the terminal oxidant must be a strong oxidizing agent. The standard potential for reduction of O_2 to H_2O indicates that O_2 is a very good oxidant (Table 1.1). Thermodynamically speaking, O_2 should be able to accept electrons from almost any biological molecule. However, the chemical reactivity of molecular oxygen or dioxygen with most organic, and by extension, biological molecules at ambient temperatures is essentially nonexistent [38]. The low reactivity of dioxygen is due to the presence of two unpaired electrons in the antibonding orbital (π_{2p}^*) (Fig.1.1). These unpaired electrons for dioxygen (+1/2, +1/2) give a spin quantum number of one, and a spin multiplicity of three ($2s + 1$), which makes it a triplet molecule in its ground state. In order to

Reactions	E ^{o'} (Volts)	Reference
•OH + e ⁻ + H ⁺ → H ₂ O	2.31	[39]
H ₂ O ₂ + 2 e ⁻ + 2H ⁺ → 2H ₂ O	1.35	[40]
O ₂ ^{•-} + e ⁻ + 2H ⁺ → H ₂ O ₂	0.94	[41]
RS [•] (cysteine) + e ⁻ → RS ⁻	0.84	[42]
O ₂ + 4 e ⁻ + 4H ⁺ → 2H ₂ O	0.82	[39]
PUFA [•] (<i>bis</i> -allylic) + H ⁺ → PUFA-A	0.60	[43]
O ₂ + 2 e ⁻ + 2H ⁺ → H ₂ O ₂	0.33	[39]
Ascorbate [•] + H ⁺ → ascorbate monoanion	0.28	[43]
Ubiquinone + H ⁺ → Semiubiquinone	-0.04	[44]
NAD ⁺ + 2 e ⁻ + H ⁺ → NADH	-0.32	[41]
Riboflavin → Riboflavin ^{•-}	-0.32	[45]
O ₂ + e ⁻ → O ₂ ^{•-}	-0.33	[40]
Fe(III) transferrin → Fe(II) transferrin	-0.40	[46]

E^{o'} = standard reduction potential (1atm, pH 7)

Table 1.1. Reduction Potentials of Some Oxygen Species and Other Compounds

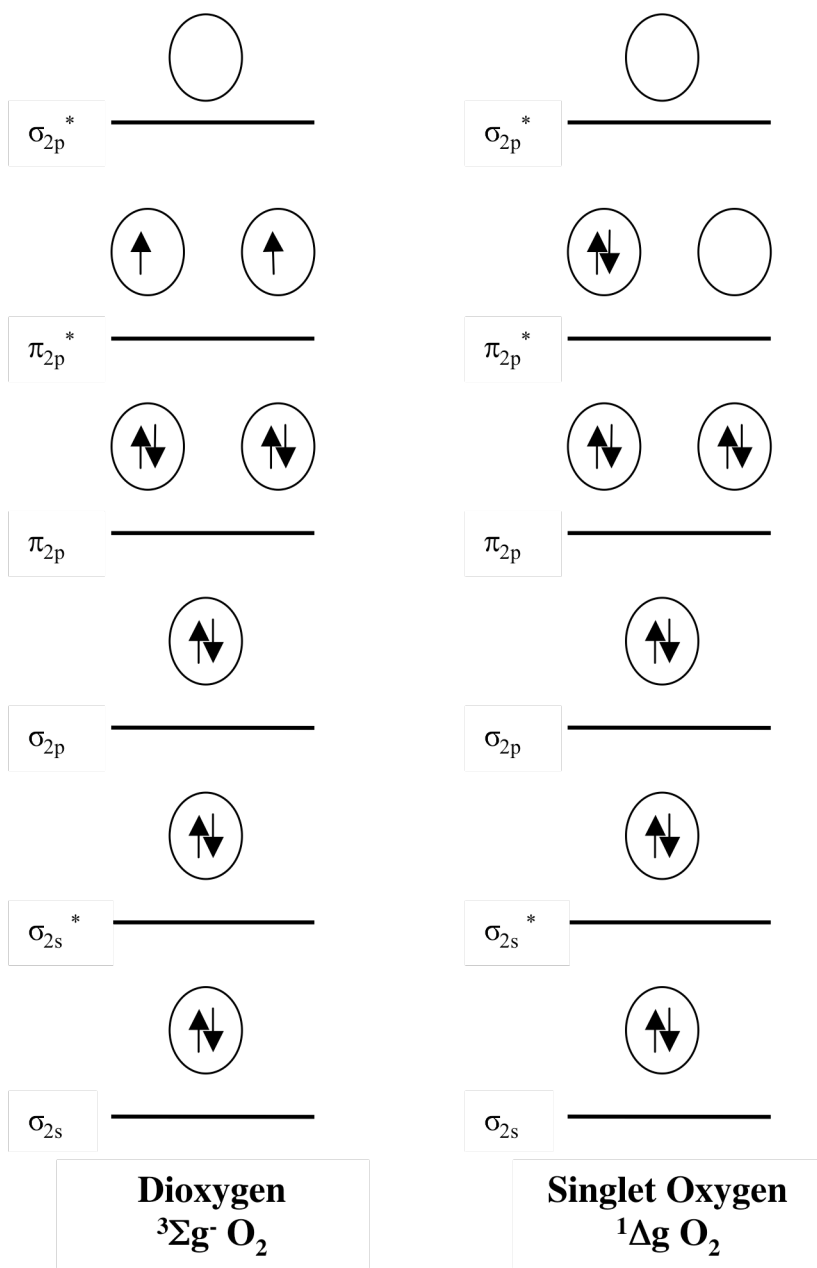


Figure 1.1. Molecular Orbital Diagram of Molecular Oxygen

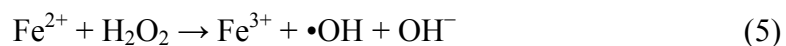
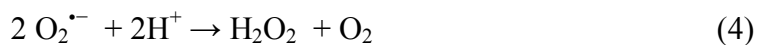
maintain spin conservation during a reaction, oxygen must either react with another unpaired electron or produce a triplet ground state product. Stable triplet states are unusual. Oxygen reaction with most molecules is considered to be spin-forbidden in that most molecules are in a singlet ground state [41]. The reaction of singlet molecules with triplet molecules does not occur at appreciable rates because of this high kinetic barrier. On balance, this is an advantageous arrangement. Without this kinetic barrier, the indiscriminant and rapid oxidation of nearly all biological molecules would occur, making life in an aerobic atmosphere impossible. Nevertheless, to take advantage of the properties of O₂ in biological system, the kinetic barrier must be overcome. As it is, the rate of O₂ reaction with singlet molecules is too slow to be of any use to a living organism. The difficulty comes in how to reduce this barrier in a controlled and selective manner.

Iron

In order to lower the high kinetic barriers required for the reaction of triplet oxygen, transition metals are frequently used. Transition metals such as iron (Fe), copper (Cu), and manganese (Mn), which have partially filled d-orbitals, can exist in several oxidation and spin-states. Transition metals can donate and accept electrons with oxygen forming a metal-dioxygen complex. This complex gives transition metals the ability to act as an efficient catalyst of redox reactions by giving dioxygen an electron environment like singlet oxygen (Fig. 1.1). Bonding of the metal with oxygen allows for electron

acceptance and lowers the activation energy of triplet oxygen to overcome the kinetic barriers. The interaction of metals with dioxygen is of great interest and has been well studied since its discovery in the mid 1800s [47].

Iron, one of the most abundant elements, is an essential component of virtually all life forms. Iron, under typical physiological conditions, is observed to cycle between its two dominant oxidation states ferrous (Fe^{2+}) or ferric (Fe^{3+}). The utility of iron in the catalytic activation of dioxygen can be seen even in the simplest system. For example, consider the reactions of a low molecular weight Fe complex like Fe-EDTA, where RH is an organic electron donor (reaction 2-5). The final reaction in the sequence, known as the



Fenton reaction, produces hydroxyl radical ($\cdot\text{OH}$) (reaction 5), the most active of all so-called reactive oxygen or partially-reduced oxygen species (e.g., $\text{O}_2^{\cdot-}$, H_2O_2 , $\cdot\text{OH}$) [48-50].

Hydroxyl radicals participate in hydrogen abstraction, electron transfer, or addition reactions with a truly broad range of compounds, and this at near diffusion-limited rates [51, 52]. Clearly, the transition metal-dependent activation of dioxygen can be used for chemical transformations. However, this type of mechanism provides little if

any control, leading to the indiscriminant oxidation of system components. Evidence that such mechanisms of oxygen activation are detrimental to biological molecules and living cells is abundant. Indeed hydroxyl radicals have been shown to alter the structure and disrupt the function of all classes of biological molecules (e.g., lipid, protein, carbohydrate, and nucleic acid) (Fig. 1.2)[50, 53, 54].

Iron Cofactors

Clearly iron can activate molecular oxygen toward many types of oxidative transformations. However, the issue still remains of controlling its reactivity making it specific and useful rather than indiscriminant and harmful for living organisms. This must be achieved by controlling the environment of the iron. Nature has developed several ways to control iron and its interactions with dioxygen. The first evidence of biological control of iron is in the vanishingly low concentrations of “free” or low molecular weight complexes of iron observed within most organisms [55]. The vast majority of iron found in living systems is associated, in one form or another, with proteins. Clearly, the protein environment of the iron is a key factor in determining its reactivity.

The environment of the iron can be evaluated at several levels. The first, and most obvious, is its immediate environment, which is summed up in its nature as a cofactor. In almost all cases, a protein associated with iron relies on the metal for its activity. The iron, therefore, is participating as a cofactor. The three most common

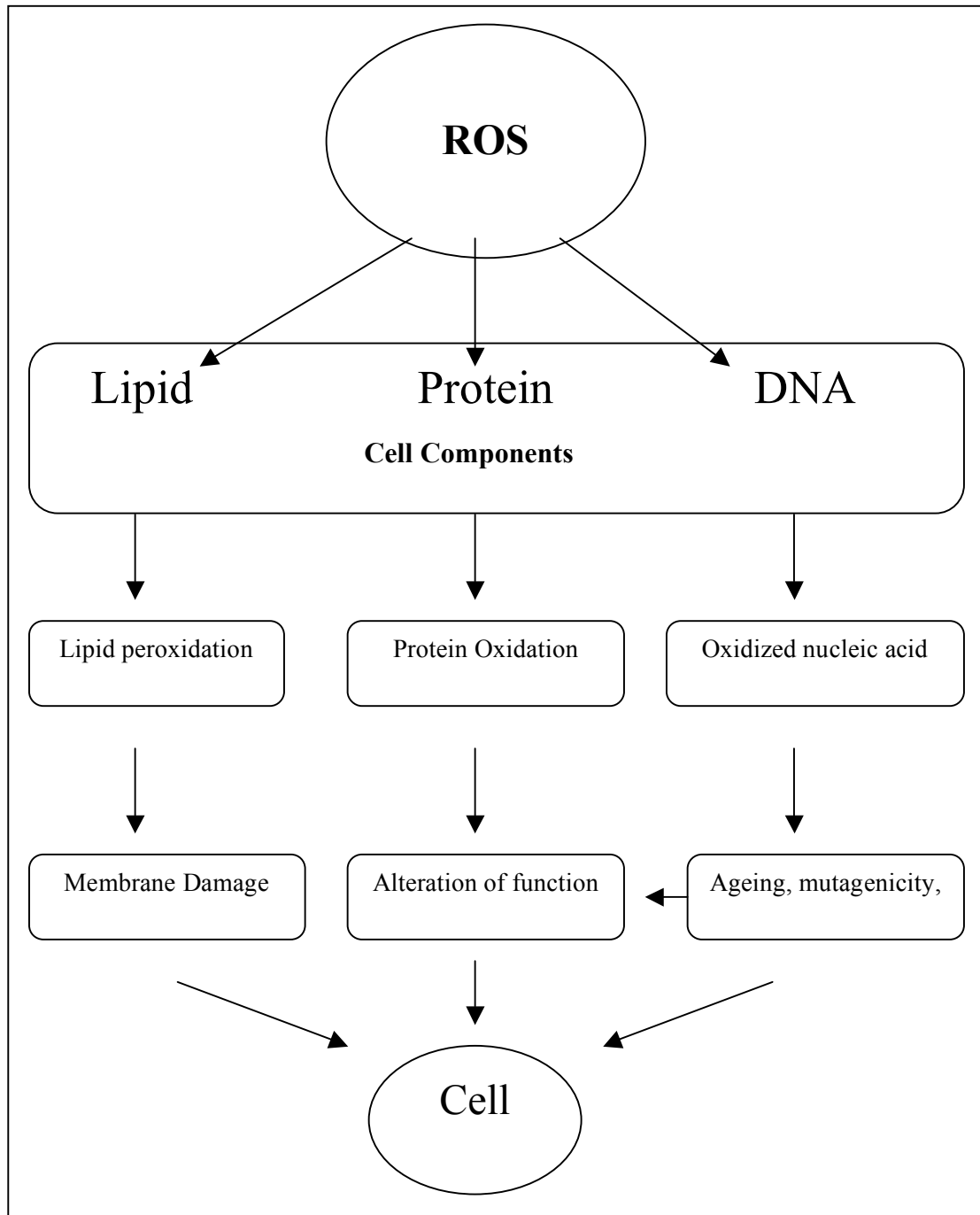


Figure 1.2. Schematic Diagram of Reactive Oxygen Species (ROS) and their Interactions with Cells.

forms of iron-dependent cofactors are heme iron, non-heme iron, and iron-sulfur clusters. Iron-sulfur clusters are a form of non-heme iron cofactor, but they constitute such a widely used catalytic strategy in biology that they can be considered as a separate group. Commonly observed arrangements include FeS, Fe₂S₂, Fe₃S₄, and Fe₄S₄ (Fig. 1.3). Other non-heme iron centers are typically directly ligated by several amino acid side chains from the surrounding protein. Common motifs include mononuclear iron centers observed in proteins like tyrosine hydroxylase and TauD as well as the binuclear centers observed in enzymes like methane monooxygenase and ribonucleotide reductase (Fig. 1.3). Finally, hemes are also widely utilized as cofactors in biological systems. Though the other iron-dependent cofactors play very important roles in biological function, the focus of this literature review will be on the heme-type iron cofactors.

Heme cofactors are synthesized via a common pathway using the universal tetrapyrrole precursor δ -aminolevulinic acid (δ -ALA). The synthesis of δ -ALA is the rate-limiting step in the biosynthetic pathway (Fig. 1.4) [56, 57]. Whether derived from glycine and succinyl-CoA or glutamate (as in some prokaryotes), δ -ALA undergoes a series of six reactions, yielding protoporphyrin IX, the most common biological porphyrin. Protoporphyrin IX is then charged with a single Fe atom by the enzyme ferrochelatase to form the most commonly observed heme cofactor, iron-protoporphyrin IX also known as heme *b* (Fig. 1.4). This synthetic pathway is highly similar across all species with some differences in the subcellular location of the steps [56, 57]. In prokaryotes, this pathway takes place in the cytosol. However, in eukaryotes, δ -ALA is synthesized in the mitochondrial matrix along with the final three steps involving coproporphyrinogen III synthesis to heme. Each of the other steps occurs in the cytosol.

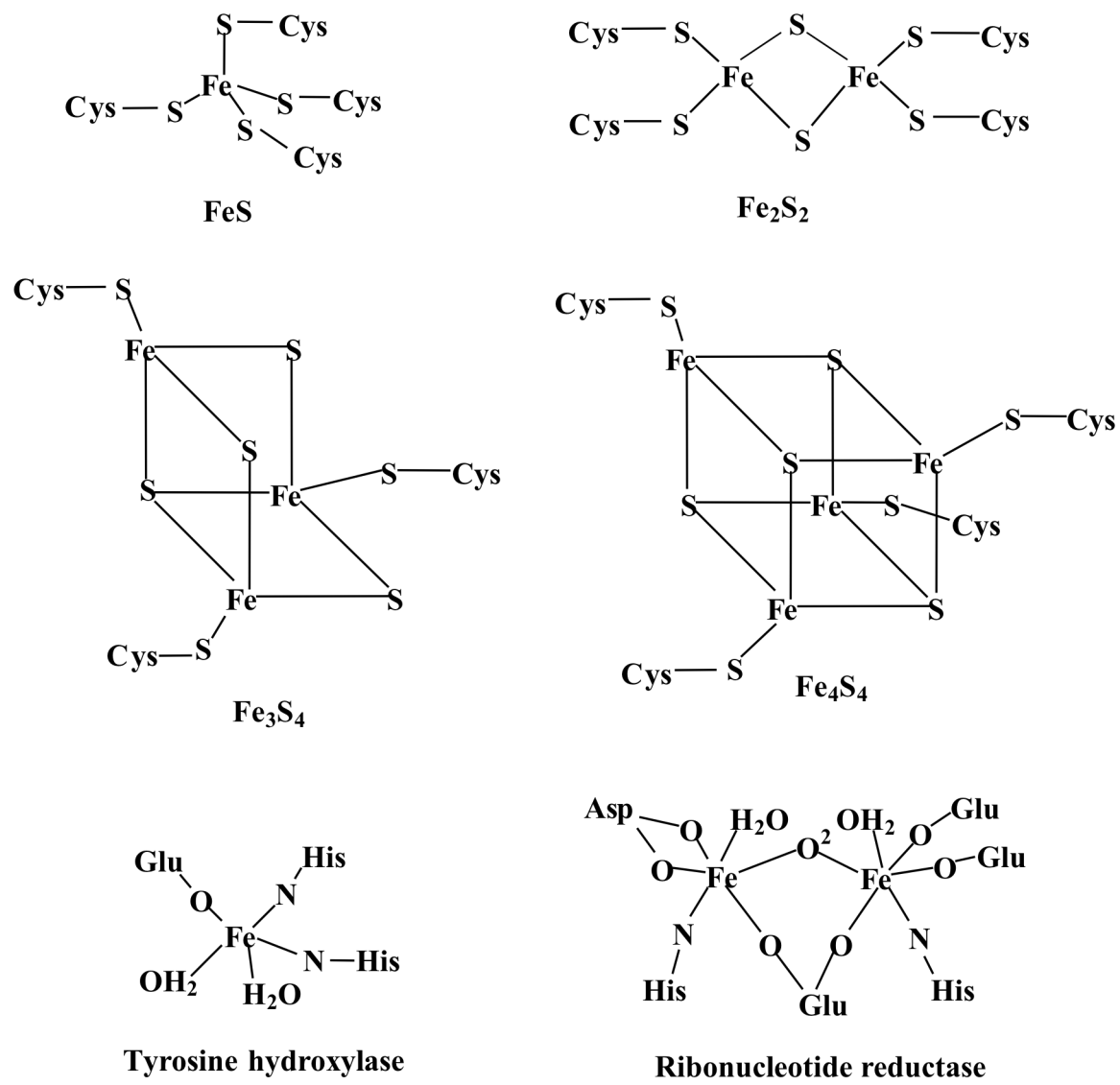


Figure 1.3. Iron-Sulfur Clusters and Mononuclear and Binuclear Non-Heme Iron Centers

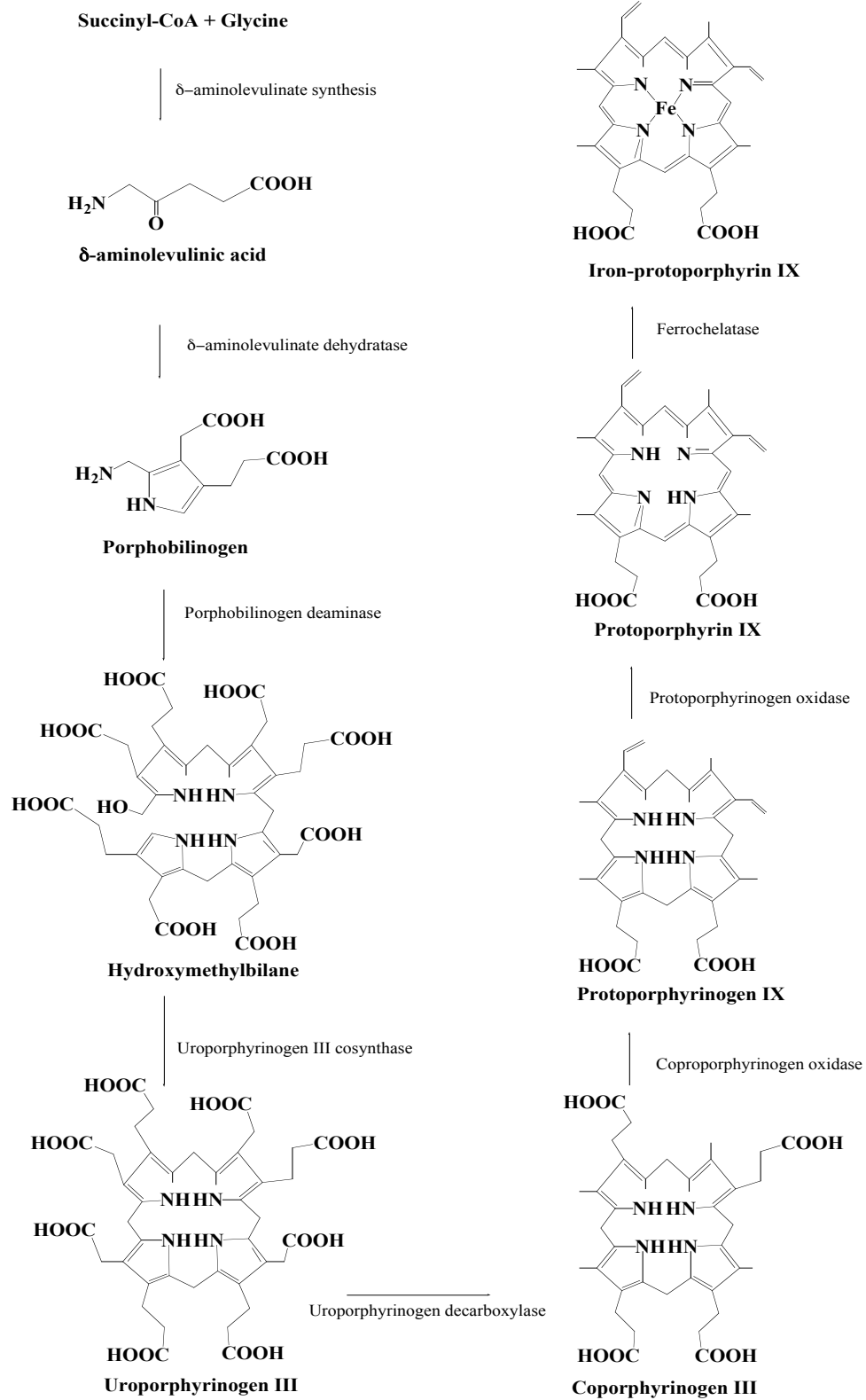


Figure 1.4. Biosynthetic Pathway for Heme.

In plants, the mitochondria do not contain the enzyme required for coproporphyrinogen III conversion to protoporphyrinogen IX and requires a precursor form in plastids.

Heme cofactors are utilized for a truly diverse range of biological processes. This requires a complex regulation of the environment of the heme iron, and this regulation occurs at numerous levels. Most simply, there are structural perturbations of the cofactor itself. In all heme structures, iron is complexed to the macrocycle by four equatorial nitrogens from four pyrroles. This leaves two additional ligand binding sites. The most commonly observed oxidation states for heme are the ferric and ferrous state (-200 mV) but free heme is dominated by the ferric state under atmospheric conditions [58]. The ferrous form of heme iron in heme proteins is properly referred to as heme. Likewise, when the heme iron is in its ferric form, the proper term is hemin.

There are three main types of heme found in proteins, all derived from protoporphyrin IX (Fig. 1.5). Heme *b* is the most abundant form of heme and is found in hemoglobins, myoglobins, catalases, and peroxidases among others. Heme *a* is different from heme *b* at two carbon positions of the porphyrin ring: the oxidization of one of its methyl side chains into a formyl group and the replacement of one of the vinyl side chains by an isoprenoid side chain as found in cytochrome-*c* oxidase (Fig. 1.5). The formyl group is more electron-withdrawing than the methyl group. The long alkyl group makes heme *a* hydrophobic and is also more electron-withdrawing than the vinyl group [59]. This gives heme *a* a higher reduction potential. Both heme *a* and heme *b* are not covalently bound to the proteins that rely on them. Heme *c* differs from *b* and *a* in that it is covalently attached by two thioether bonds between the protein and the vinyl group of the heme by the cysteine sulfurs of a CXXCH binding motif (Fig. 1.5) [60]. The

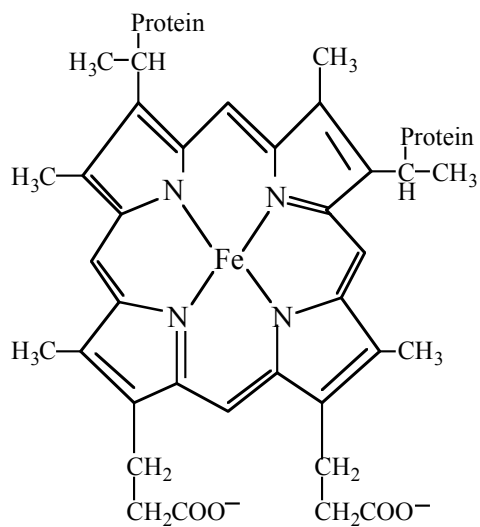
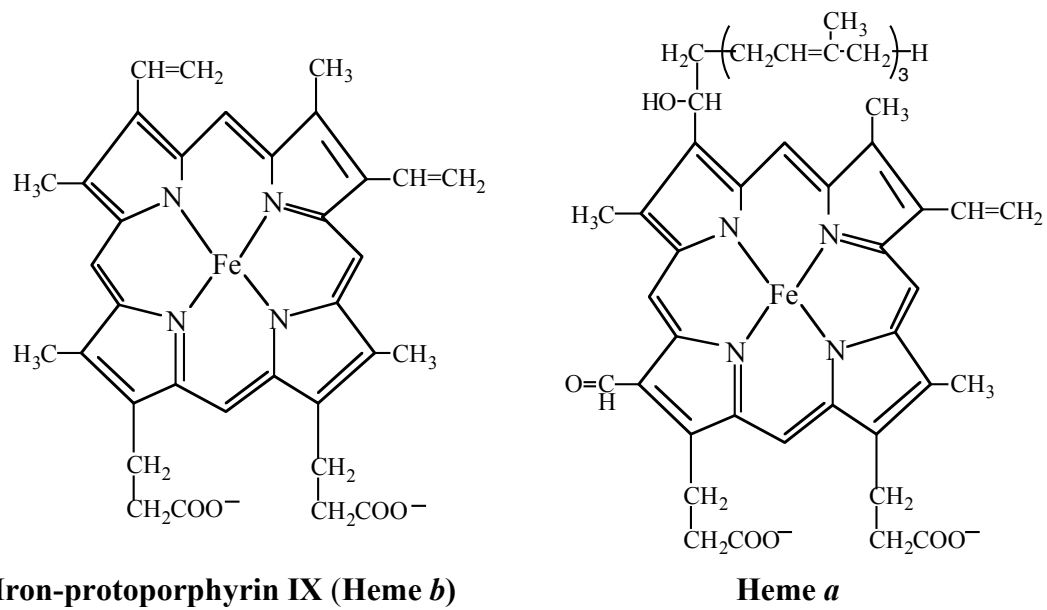


Figure 1.5. Structure of Common Hemes

presence of the thioether bond may add stability to the protein. The loss of the thioether bond in cytochrome *c*₅₅₂ results in destabilization of the protein [61]. However, the reduction potential doesn't seem to be affected by the presence or absence of the thioether linkage.

Hemoproteins

Heme is a highly reactive molecule because of its iron center. As with free iron, heme can be very toxic to cells, tissues, and organs as a result of the open accessibility to the heme iron [57]. The heme structure alone is not sufficient to control and direct the reactivity of the iron-O₂ interaction. For this reason, virtually all heme is found complexed with proteins as a prosthetic group, hence their designation as hemoproteins. The importance of hemoproteins in biology cannot be overstated. They participate in sensing, storing and transporting of O₂, metabolism of drugs and other xenobiotics, electron transfer, production and decomposition of reactive oxygen species, and production, sensing, and degradation of nitric oxide. In all of these cases, the heme is central to the activity of the protein in question. Clearly, this diversity of chemical transformations cannot be explained solely by the structure of the heme. In many cases, the proteins in these processes are using the same type of heme. The protein structure surrounding the heme dictates its function and this occurs at several levels.

The most obvious is the immediate coordination environment of the heme moiety. Heme iron has two open coordination sites above and below the plane of the porphyrin

ring which ligands can bind. The character of the axial ligands can profoundly change the function of the heme. For instance, the globin proteins, which bind, transport, and store oxygen have a histidine as the fifth ligand bound to the Fe proximal side. The sixth coordination site is open to allow binding of O₂ or H₂O (when O₂ is absent) as the sixth ligand [62]. O₂ is then transported as a non-reactive species. In the peroxidase proteins, histidine is also the fifth ligand but these proteins do not typically bind oxygen. Instead, they bind peroxide and reduce it to H₂O. On the other hand, cytochrome P450 is a monooxygenase. It has a cysteine ligand bound to the Fe proximal side with oxygen or water as the other ligand [63]. The proximal ligand along with the H-bonding networks associated with the ligand play a key part in the activity of hemoproteins. The reduction potentials of human myoglobin (+50 mV), cytochrome P450_{cam} (high spin, -170 mV; low spin, -270 mV), horseradish peroxidase (-250 mV), and catalase (<-500 mV) are different as a result of the nature of the ligands[64]. The reduction potential of the heme iron, of course, dictates the stability of its oxidation states – a critical consideration in the reactivity of a hemoprotein.

Binding of O₂ by the Globins

Though the most famous examples of the globins are mammalian hemoglobin and myoglobin, globins have been identified in bacteria, fungi, and plants as well. The globins are known for their ability to sense, store, and/or transport O₂. They have also been shown to possess NO dioxygenation activity (reaction 6). In order to achieve all of



these functions, the heme iron must be in its reduced form rather than its oxidized form because O₂ only binds to heme in the ferrous form not the ferric form. The ligation environment of heme in the globins favors the reduced state. As discussed previously, the reduction potential of the heme in these types of proteins is relatively high (~ +50 mV). This is due to the proximal histidine ligand bound to the heme iron and its H-bonding interactions (Fig. 1.6). In the globins, the proximal histidine forms a weak H-bond with a backbone carbonyl. Relatively speaking, the very weak H-bond means that the histidine ligand retains neutral character. This increases the stability of the ferrous oxidation state relative to the ferric. This is evident in the relatively high reduction potential. However, more is required for effective O₂ binding than heme in its ferrous state. The protein environment outside of the iron ligands also plays an important role. A histidine on the distal side of the heme in the globins is positioned close to the heme iron. This histidine forms a strong hydrogen bond to dioxygen (2 Å), when it is bound, stabilizing the Fe-O₂ complex [65]. Amino acids like valine and leucine are also positioned in the distal pocket. These inhibit binding of other ligands and help to protect the active site against side reactions involving the bound O₂. The ability of hemoglobin and myoglobin to bind oxygen in an un-reactive environment using iron provides an excellent example of how the Fe-O₂ interaction is controlled by protein environment.

It is because of the proteins structural features far from the heme group that hemoglobin and myoglobin can be allies in the transport and storage of oxygen. Hemoglobin is found in high concentration in the red blood cells while myoglobin is

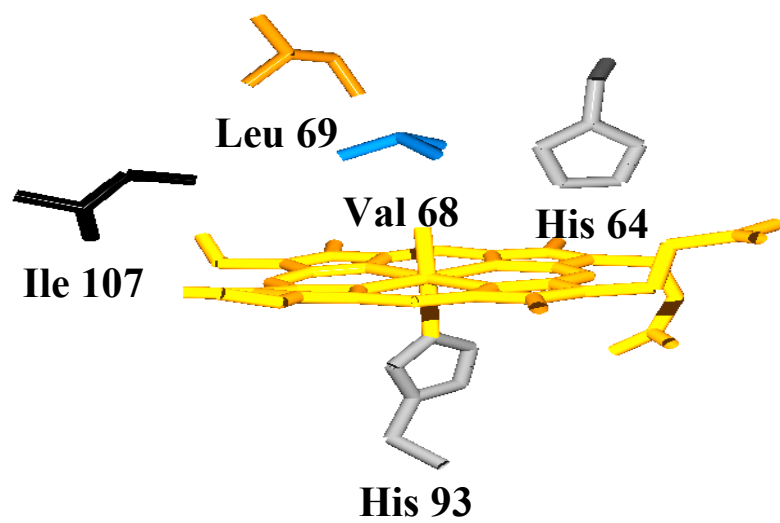


Figure 1.6. Active Site Representation of Myoglobin [66].

found in muscle tissue. The heme in both hemoglobin and myoglobin is coordinated to the protein through a proximal histidine ligand revealed by X-ray crystallography [67, 68]. Oxygen is left to bind to the one remaining Fe coordination position on the distal side of the heme. X-ray structural analysis has shown that hemoglobin contains two α and β chains each resembling myoglobin. The architecture of the heme pocket gives the globin proteins the ability to reversibly bind O_2 . The distal histidine in its hydrophobic environment is a key amino acid in that its hydrogen bonding network helps to stabilize oxyheme against superoxide-releasing autoxidation and also contribute to CO vs. O_2 discrimination [69]. Both globins possess all of these features; however, hemoglobin and myoglobin do not bind to oxygen at the same rate. Binding curve plots show myoglobin binding to oxygen with high affinity according to a hyperbolic curve [70]. This indicates that myoglobin will bind oxygen when oxygen partial pressure is high and release oxygen when oxygen partial pressure is low. On the other hand, hemoglobin produces a sigmoid (S-shaped) curve [71]. This indicates a change in hemoglobin affinity for oxygen or cooperative oxygen binding. Hemoglobin affinity for oxygen rises with increasing oxygen concentration. This cooperative binding is due to a transition between its tertiary structures. When oxygen is bound to the iron, a 0.6\AA shift is observed in helix F (Fig.1.7) [72]. This shift in the iron atom gives rise to a conformational change resulting in a heme environment with an enhanced ligand affinity. This is called an oxy or relaxed (R) state. When oxygen is not bound, it is called a deoxy or tense (T) structure (Fig.1.7). It is clear that the high affinity of oxygen binding for myoglobin makes it ideal for oxygen storage. On the other hand, the ability of hemoglobin to bind oxygen more

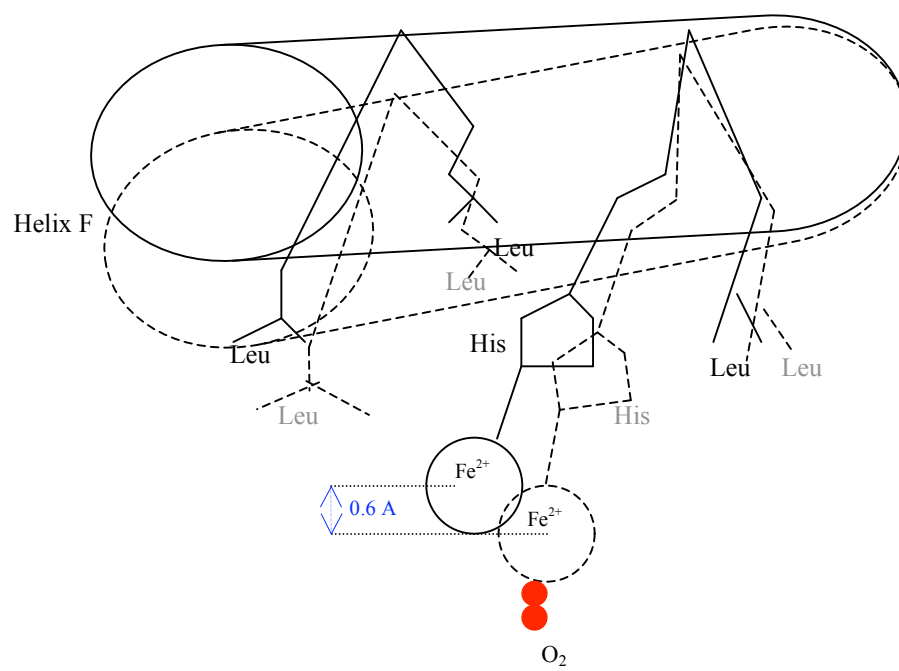
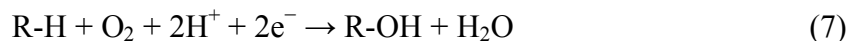


Figure 1.7. T → R transition in hemoglobin. R state is with O₂ bound.

when oxygen is available and release oxygen when it is not makes it ideal for oxygen transport.

Cytochrome P450

Cytochrome P450 (P450) is a large family of hemoproteins found in a wide range of eukaryotes and prokaryotes. With over 450 different enzymes identified, most P450s are membrane-bound proteins. Cytochromes P450 have been shown to catalyze many reactions including hydroxylations, epoxidations, dealkylations, sulfoxidations, dehalogenations, and oxidative deamination. In humans, P450s play a critical role in cellular metabolism, which includes: 1) the conversion of cholesterol to androgen, estrogen, gluco- and mineral-corticoids, 2) the synthesis and degradation of prostaglandins and other unsaturated fatty acids, 3) the conversion of vitamins to their active forms, 4) the metabolism of cholesterol to bile acids, and 5) a number of reactions involved in the metabolism of xenobiotics. Generally speaking, the P450s are mono-oxygenases and are diverse in their ability to incorporate one of the two oxygen atoms of O₂ into a variety of substrates while the other oxygen atom is reduced by two electrons to water. An example hydroxylation is given in reaction 7.



The first P450 was identified by Klingenberg in 1958. It exhibited an unusual absorption band at 450 nm when reduced and exposed to CO [73]. This hemoprotein was assigned the name cytochrome P450 as a result. Like many hemoproteins, the P450s use heme *b* as a prosthetic group. However, cytochromes P450 differ from most hemoproteins in that they have a proximal cysteine ligand. The substantial electron density of the thiolate ligand preferentially stabilizes the Fe^{III} over the Fe^{II} oxidation state as reflected in the low reduction potential (~ -300 mV for the low-spin form). As a consequence higher oxidation states, like the ferryl-oxo porphyrin radical intermediate, are stabilized as well, contributing to the P450's ability to heterolytically cleave oxygen-oxygen bonds (reaction 8). The globins are not able to achieve this.



The catalytic cycle of P450 starts with a low-spin, six-coordinate ferric heme with water as the distal ligand (Fig. 1.8) [74]. When the substrate binds, water is released and the heme becomes a high-spin, five-coordinate ferric species that leaves an open site available for oxygen to bind (a). An external electron donor is also needed. The cofactor NAD(P)H used by P450 reductase serves as an electron delivery system to reduce the P450 heme to a ferrous species so that O₂ can bind (b). The binding of oxygen yields an oxygen-P450-substrate complex, which is unstable and undergoes molecular

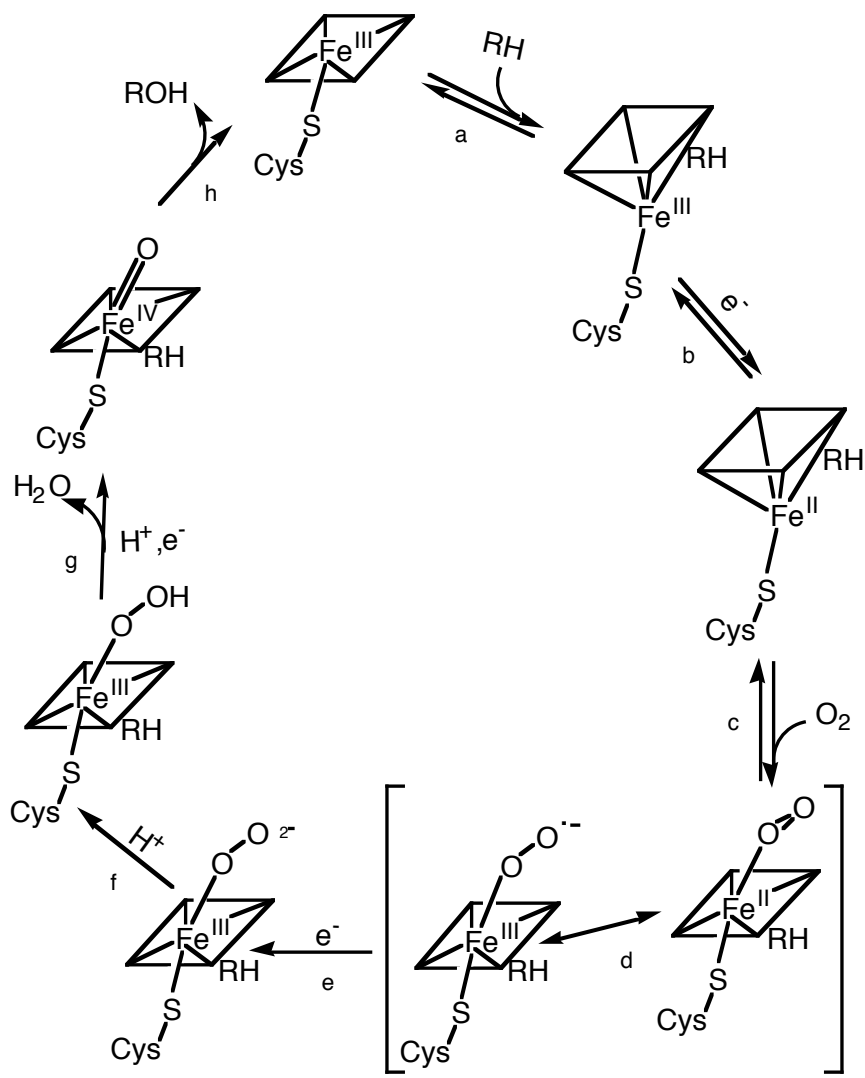


Figure 1.8. Catalytic Cycle of Cytochrome P450.

rearrangement between a ferrous- O_2 (c) and a ferric-superoxide species (d). The addition of a second electron by NAD(P)H, which is the rate-limiting step, generates a ferric peroxide adduct (e) [74]. This intermediate is protonated to a hydroperoxide intermediate (f). Oxygen is then protonated a second time (g). This leads to the heterolytic cleavage of oxygen resulting in the release of water and the generation of an ferryl-oxo intermediate, which is similar to the peroxidase enzyme iron-oxo intermediate called compound I. This intermediate is believed to be responsible for the production of the hydroxylated substrate (h).

Cytochrome Oxidase

Cytochrome oxidase, also known as cytochrome *c* oxidase or cytochrome *aa₃*, is a complex of metalloproteins that play a fundamental role in oxygen reduction in cellular respiration of eukaryotes and prokaryotes. Clearly, cytochrome oxidase is an essential enzyme for most aerobic life forms. Indeed, it is the protein of cellular respiration that interacts directly with the terminal electron acceptor, molecular oxygen. This enzyme is an integral membrane protein that facilitates a transmembrane proton gradient by using the driving force of reduction of O_2 to H_2O to carry out the translocation of protons across the membrane. Consuming more than 90 % of O_2 taken in by living organisms, cytochrome oxidase gives cells the ability to oxidize foodstuff by catalyzing one-electron oxidation of four cytochromes *c* resulting in the four-electron reduction of O_2 (reaction 10).



The ability of cytochrome oxidase to reduce O_2 to H_2O makes it unique compared to other hemoproteins that bind molecular oxygen like the globins. Cytochrome oxidase contains two heme *a* (*a* and *a*₃) molecules and two copper (Cu_a and Cu_b) ions at its catalytic core. As established by McMunn, Warburg, and Keilin between 1884-1933, this enzyme has spectroscopic properties of cytochromes but binds to oxygen like the oxidases. To account for both of these properties, it was named cytochrome oxidase [75]. However, it wasn't until 1938 that Keilin and Hartree discovered the essential role of cytochrome *c* as an electron donor to the terminal oxidase [75]. They decided to call the enzyme cytochrome *c* oxidase. Keilin and Hartree studies of cytochrome oxidases also showed some dissimilarity between the two hemes. One heme seemed to bind oxygen, carbon monoxide, and cyanide while the other one did not [75]. Heme *a* was obtained as the name for the one that did not bind oxygen and *a*₃ given to the other.

Both heme *a* and *a*₃ from cytochrome oxidase have a high reduction potential (+230 and +390 mV, respectively) as a result of the long alkyl group and formyl group which makes heme *a* more electron-withdrawing than both heme *b* and *c* [76]. The crystal structure of cytochrome oxidase shows heme *a* as a six-coordinate low-spin heme with two histidine residues as axial iron-ligands [77]. Conversely, heme *a*₃ is a five-coordinate high-spin heme. This difference in coordination environment has much to do with differing roles of these hemes in cytochrome oxidase catalysis. The absence of a sixth ligand to the heme *a*₃ iron allows for oxygen to bind as a ligand. Whereas heme *a*

simply acts as an electron transfer conduit delivering electrons to the heme a_3 and Cu_b as appropriate.

The reaction of cytochrome oxidase requires the cooperation of four redox centers. Cytochrome oxidase is composed of as many as thirteen subunits with the redox centers located within subunits I and II [78]. Heme a and a_3 and Cu_b are located in subunit I, while Cu_a is found in subunit II. Heme a_3 and Cu_b form a binuclear catalytic center for O_2 reduction to H_2O . Heme a and Cu_a are connected through a series of hydrogen bonds which allows for the transfer of electrons from cytochrome c to the catalytic center. The reduction of O_2 to H_2O requires eight general steps (Fig. 1.9) [79]. Cu_b , coordinated to the catalytic center by the bonding of three histidines residues, is reduced by one electron from Cu^{II} to Cu^{I} (a). The hexa-coordinate ferric heme a_3 is then reduced by one electron to the Fe^{II} state (b). This reduction enables O_2 to bind, forming a dioxygen complex involving $\text{Fe}^{\text{II}}_{a_3}$ and Cu^{I}_b (c). The reduction of the dioxygen complex results in an iron peroxy intermediate (d). Cu_b is then reduced by one electron followed by a proton uptake, giving rise to a $\text{Fe}^{\text{III}}_{a_3}\text{-O}^{\cdot-}\text{-OH}$ intermediate along with Cu^{I}_b (e). A second protonation coincides with the heterolytic bond cleavage of O-O , giving a ferryl-oxo state for heme a_3 and H_2O bound to Cu^{II}_b (f). Heme a_3 is then reduced by one electron initiating a proton rearrangement (g). This rearrangement gives both iron and copper with hydroxide ligands. Introduction of two more protons yields two H_2O molecules and a return to the resting state of the enzyme (h).

A rapid transfer of electrons from heme a traps O_2 in the iron-copper center allowing for further reduction of oxygen. Indeed, the reaction of cytochrome oxidase is

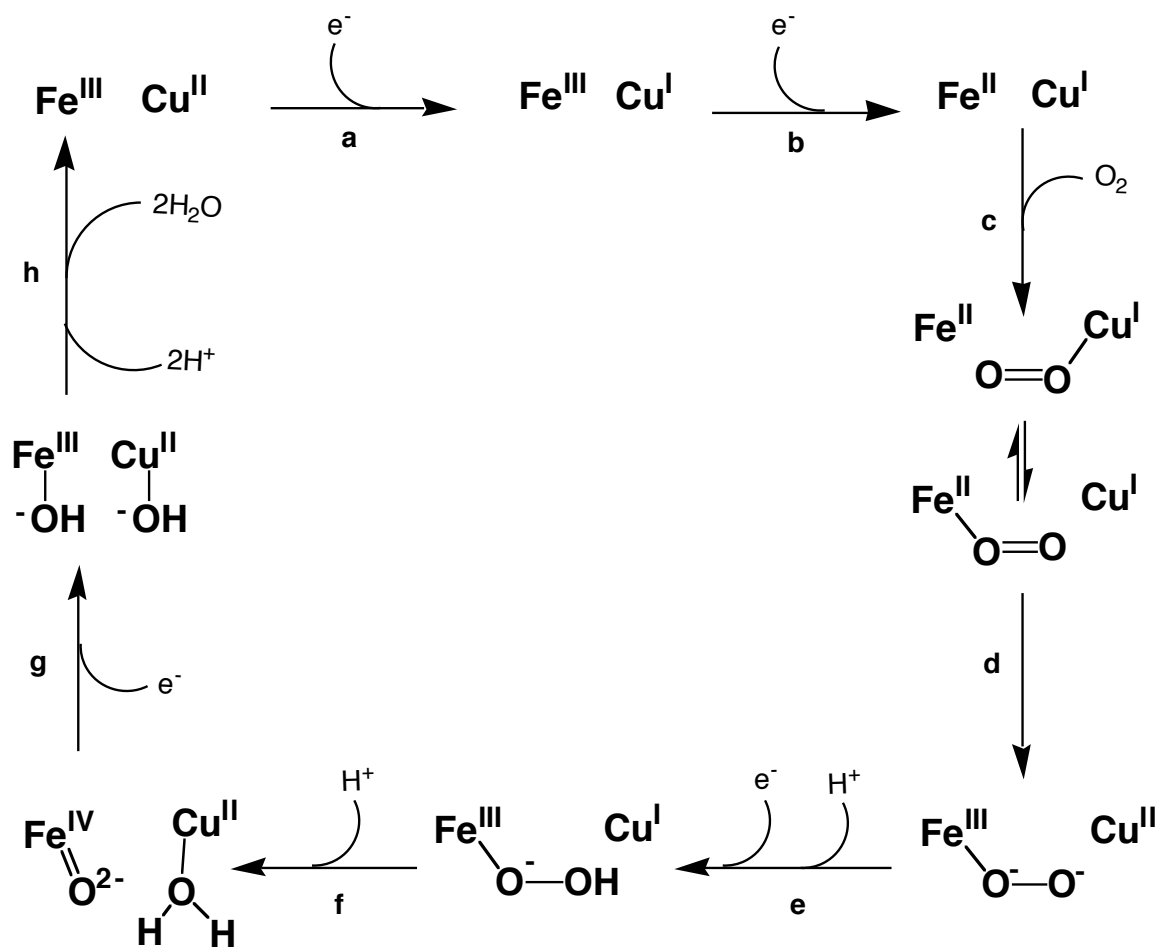


Figure 1.9. Catalytic Cycle of Cytochrome Oxidase. The Fe refers to the iron of heme a_3 and the Cu refers to the Cu_b center.

one of the fastest in biology with an apparent second order rate constant of about $10^8 \text{ M}^{-1} \text{ s}^{-1}$ [80, 81]. This rapid reduction of O_2 to H_2O decreases the life span of the catalytic intermediates containing partially reduced oxygen species, which minimizes their release into the surrounding environment. The bi-heme and bi-copper complex gives cytochrome oxidase the ability to effectively and efficiently utilize the terminal oxidant, O_2 , by binding and reducing it by four electrons to H_2O . However, other redox centers in the electron transport chain may leak electrons to O_2 producing reactive oxygen species (e.g., $\text{O}_2^{\bullet-}$) [82]. Other hemoproteins including superoxide dismutases, catalase, and peroxidase are used as a defense against $\text{O}_2^{\bullet-}$.

Peroxidases

Peroxidases are a large class of enzymes found among many living organisms. This wide distribution implicates these enzymes as important for most living systems. Most contain heme, and these are divided into two superfamilies: mammalian peroxidases and peroxidases found in plants, microorganisms, and fungi (the so-called plant peroxidases) [83]. A small third group includes chloroperoxidase and the di-heme cytochrome *c* peroxidase.

Mammalian peroxidases include lactoperoxidase, myeloperoxidase and prostaglandin H synthase. The second group is further divided into three classes. Mitochondrial yeast cytochrome *c* peroxidase, chloroplast and cytosolic ascorbate peroxidases, and the gene-duplicated bacterial catalase-peroxidases make up class I.

Class II are monomeric glycoproteins with four conserved disulfide bridges and two conserved calcium coordination sites, and are comprised of the secretory fungal peroxidases like lignin and manganese peroxidase [84]. The classical or secretory plant peroxidases, such as the well-known enzyme horseradish peroxidase, form class III. They are also monomeric glycoproteins with four conserved disulfide bridges and two conserved calcium binding sites. However, the location of the disulfide bridges is different from the class II enzymes.

In the overall reaction of most peroxidases, peroxide is reduced to H₂O using two donated electrons (reaction 11). Peroxidases also participate in a variety of biosynthetic and/or degradative functions using peroxide as an oxidant. On one hand, the consumption of peroxide protects the cell against accumulation of these dangerously reactive compounds. However, the identity of the electron donor also contributes a large part of the particular biological function of each peroxidase. For instance, peroxidases catalyze the dehydrogenation of monolignols, a precursor in the biosynthesis of the cell-wall polymers known as lignin [85]. On the other hand, in white rot fungi, peroxidases help to catalyze the degradation of the plant polymer lignin using H₂O₂ and veratryl alcohol or Mn^{II} [86].



Like the globins and P450s, peroxidases contain the non-covalently bound heme *b*. As in the globins, a histidine serves as the proximal ligand to the heme iron [87].

Water may serve as the sixth ligand, but this varies from peroxidase to peroxidase. This, of course, raises the very important question: What about the structures of these proteins account for their different activities and functions? First, although both groups of proteins share a common proximal histidine ligand, the environment of that ligand is quite different in peroxidases as compared to the globins (Fig. 1.10). In peroxidases, there is a strong hydrogen bond between the δ -N of the histidine ligand and a strictly conserved aspartate residue. The strong H-bond imparts a substantial anionic character (i.e., electron density) to the histidine ligand. Thus, the higher oxidation states of the heme iron tend to be favored. Indeed, the reduction potential for a typical peroxidase is \sim -250 mV [64]. Conversely, the histidine ligand of the globins participates in an H-bond with a backbone carbonyl oxygen. The considerably weaker H-bond ensures that this proximal ligand retains a more neutral character. Thus, the reduction potential of the heme iron is considerably higher \sim +50 mV[64]. In its resting state, peroxidases are a ferric heme protein unable to bind oxygen, whereas the globins are found in the ferrous state, and therefore able to accept O₂ as a sixth ligand. A common distal histidine is also found in both groups. In peroxidases, the distal histidine serves as a general acid-base catalyst to transfer a proton from the peroxide oxygen-1, bound to the heme, to oxygen-2 to promote the heterolytic cleavage of the peroxide O-O bond. However, the distal histidine in myoglobin forms an H-bond with the O₂ to help stabilize oxyheme. Another unique feature of the distal cavity of peroxidases is the presence of an arginine and tryptophan. The positive charge arginine stabilizes the developing negative charge on oxygen-2.

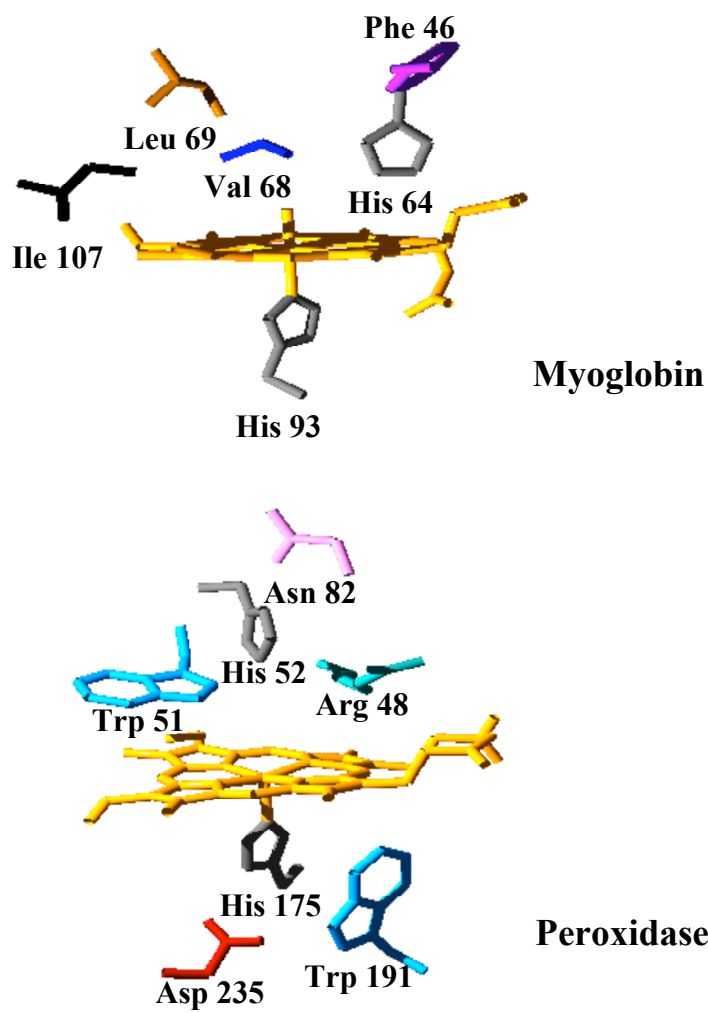


Figure 1.10. Active Site Comparison of Myoglobin vs. Peroxidase [66, 88].

While the peroxidases are involved in a variety of functions, the catalytic cycle of many of them are highly similar. The resting state of the enzyme is found as a high-spin ferric heme. The heme iron is oxidized by two electrons by H_2O_2 , resulting in the heterolytic cleavage of the O-O bond (Fig. 1.11)[89, 90]. This leads to the release of one equivalent of H_2O and the generation of the intermediate known as compound I, which has a formal oxidation state of +5. Compound I is a ferryl-oxo porphyrin π -cation radical intermediate with an oxygen from hydrogen peroxide still bound. In some cases, like cytochrome c peroxidase, the radical is transferred to a near-by amino acid side chain [91]. Compound I is then reduced by one electron by an exogenous electron donor to yield a ferryl-oxo intermediate called compound II and one equivalent of the substrate radical. Although similar to compound I, compound II does not contain the π -cation radical and has a formal oxidation state of +4 [89]. Compound II is finally reduced back to the ferric or resting state of the enzyme by a second equivalent of exogenous electron donor. Thus, a second equivalent of substrate radical is generated.

The peroxidases are known to undergo H_2O_2 -dependent inactivation. In the presence of excess H_2O_2 , compound II is oxidized, resulting in the formation of compound III (formal oxidation state of +6) and water (reaction 12) [92]. Because the structure and oxidation state of compound III is similar to those of oxymyoglobin or oxyhemoglobin, it is often called 'oxyperoxidase' [92, 93]. Though the reaction of compound II with H_2O_2 is the most commonly observed route to compound III, the production of compound III has also been shown to occur by two additional pathways [94]. Ferrous peroxidase can react with O_2 (reaction 13), and ferric peroxidase may react

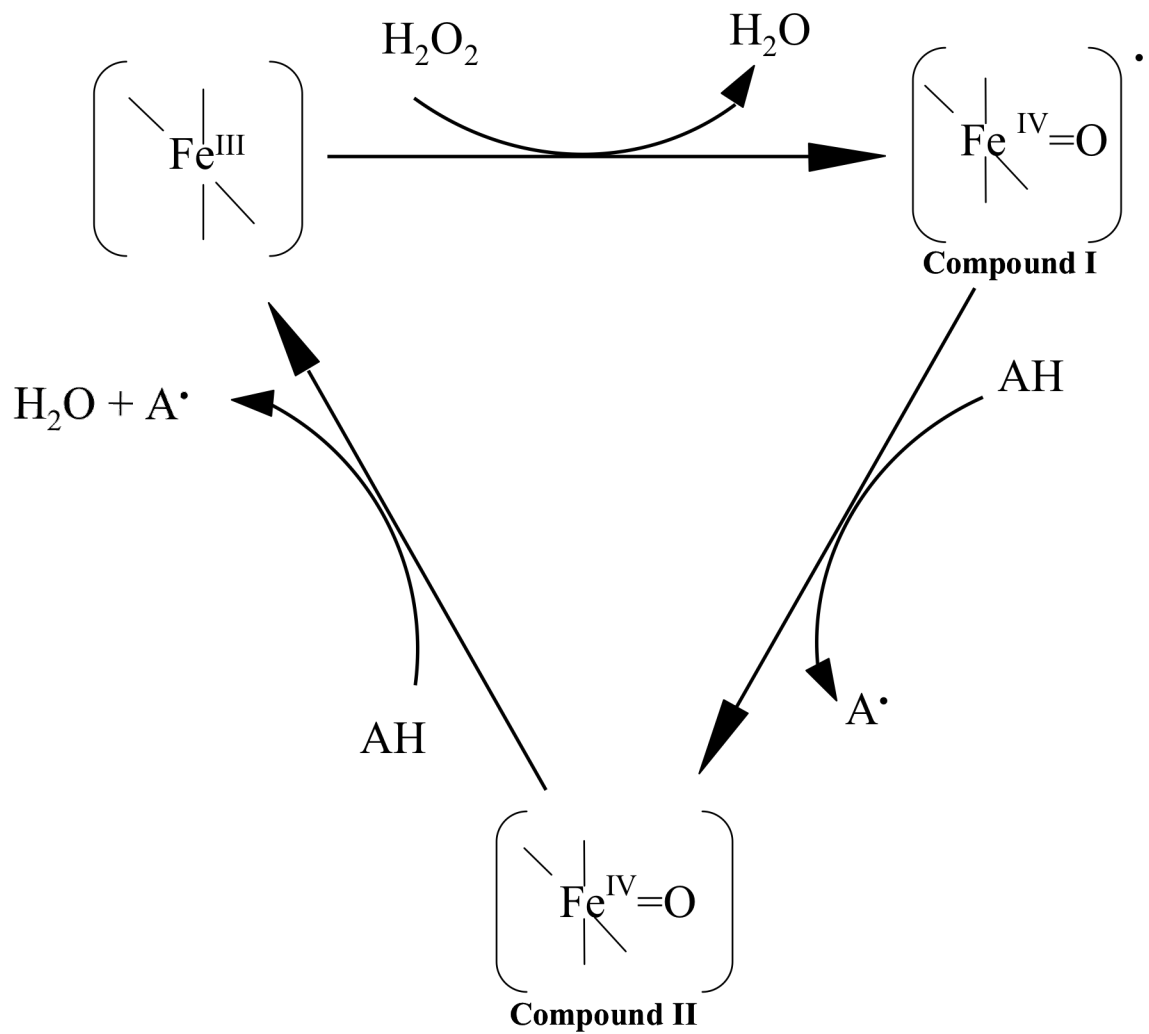
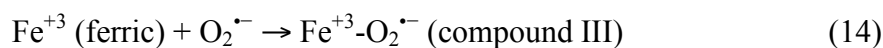
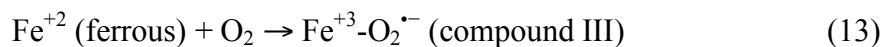
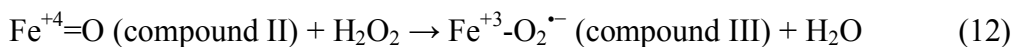


Figure 1.11. Catalytic Cycle of Peroxidase.



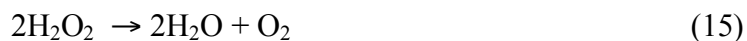
with $\text{O}_2^{\bullet-}$ (reaction 14). The formation of compound III from the reaction of compound II is slow and has an estimated second-order rate constant of $25 \text{ M}^{-1} \text{ s}^{-1}$ [95]. While compound III is an inactivated intermediate of peroxidases, compound III spontaneously decomposes to the ferric or resting form of the enzyme with a first-order rate constant of 10^{-3} s^{-1} [95]. Nevertheless, in the presence of high H_2O_2 concentrations, this inactive compound III intermediate tends to accumulate.

Unfortunately, in the presence of excess H_2O_2 , compound III will undergo additional reactions that lead to irreversible inactivation [93, 96]. The mechanism of this irreversible inactivation is unclear. The presence of the reducing substrate may play an important role in the inhibition of this inactivating pathway by limiting the buildup of compound II.

Catalases

Like the peroxidases, catalases are a class of hemoproteins that degrade hydrogen peroxide. Although catalases were named by Loew in 1901, it wasn't until 1923 that Warburg discovered the presence of iron at the active site [97]. Stern later identified heme *b* as the prosthetic group of all then known catalases [98]. The overall reaction of

catalase involved the degradation of two molecules of hydrogen peroxide to water and oxygen (reaction 15).



The primary role of catalase is proposed to be the protection of organisms from H_2O_2 and/or the reactive oxygen species generated from H_2O_2 . The catalytic cycle of catalases is similar in many respects to peroxidases. However, in the case of catalase, H_2O_2 is used both as an oxidant and reductant. The cycle is initiated by the oxidation of the ferric heme by one molecule of H_2O_2 to an oxyferryl porphyrin cation radical intermediate or compound I (Fig. 1.12) [99]. This results in the heterolytic O-O cleavage and the release of one equivalent of H_2O . Compound I is reduced by to the ferric form of the enzyme by a second molecule of H_2O_2 , releasing a second equivalent of H_2O and a molecule of O_2 .

Catalases, also called hydroperoxidases, are categorized into three main groups. The most widespread and extensively characterized group is the monofunctional catalases. The second group is the bifunctional catalase-peroxidases. This class of enzyme is closely related by sequence and structure to plant peroxidase and will be discussed in more detail in a later section. The last group includes the nonheme or Mn-containing catalase. Other heme-containing proteins also exhibit low levels of catalase activity including chloroperoxidases, plant peroxidases, and myoglobins [100]. This is likely due to the presence of heme. However, at best, these enzymes show 1000 fold

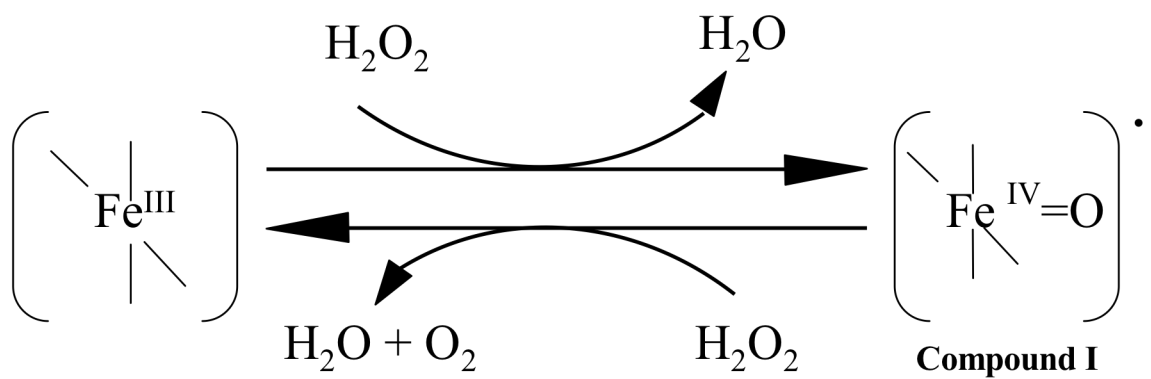


Figure 1.12. Catalytic Cycle of Catalase.

lower catalase activity than monofunctional catalases. Phylogenetic analysis of monofunctional catalases has revealed a division into three classes.

Clade I are mostly plant enzymes with one branch of bacterial catalases [101]. Clade II contains the large subunit catalases. All Clade II enzymes are of bacterial or fungal origin with the exception of one archaeobacterial enzyme. Clade III contains the small subunit catalases. These are widely distributed in bacteria, archaeobacteria, fungi and other eukaryotes including mammals. The most noticeable difference between small and large catalases is the presence in large catalases of an extra carboxyl-terminal domain, of about 150 residues, that resemble flavodoxin along with the absence of NADPH [102].

Like the peroxidases, most catalases contain heme *b*. However, the large subunit catalase or clade II contains a chlorin as the prosthetic group rather than heme *b* [103]. Heme *b* is believed to be bound first to the enzyme followed by a self-catalyzed reaction using the first H₂O₂ molecules bound to the enzyme [104]. Ring III of heme *b* is converted to cis-hydroxy γ -spirolactone. This modified heme is termed heme *d*. As with most hemoproteins, catalases have a distal histidine. However, the distal histidine is coplanar with the heme [99]. This orientation favored intensive π - π interactions between the essential histidine and the porphyrin [100]. This favors catalase activity by decreasing the reactivity of compound I with other substrates.

The heterolytic O-O cleavage by hemoproteins requires the heme iron to have a low reduction potential in order to stabilize the higher oxidation states of iron. In the peroxidases and P450s, this is accomplished by the proximal anionic histidine and thiolate (cysteine) heme iron ligand respectively as previously discussed. Catalases have

a tyrosine proximal iron ligand different from the peroxidases and the P450s. The proximal tyrosine is presented as a phenolate anion with the assistance of an adjacent arginine side chain. The anionic character of the phenolate ligand contributes to the very low reduction potential (<-500 mV) of catalases [105].

Most catalases exist as homotetramers with a characteristic globule for each subunit. Each subunit is comprised of four domains: The N-terminal arm, the β -barrel domain, the domain connection, sometimes referred to as 'wrapping domain' and the α -helical domain [103, 106, 107]. As previously mentioned, a small group contains an extra domain on the C-terminus that resembles a flavodoxin. While the β -barrel is well conserved, the α -helical domain has more variability. The N- and C-terminal domains have the most divergences. The heme of catalase is deeply buried in the core of the subunits.

The N-terminal arm extends for more than 50 residues and is the first region of catalases. It contains a 20-residue helix, which is the first secondary structure common to all catalases [108]. The essential distal histidine is located at the C-terminal end of the N-terminal arm. The second region is the β -barrel domain, which is an eight-stranded antiparallel β -barrel with six α -helical insertions [99]. It represents the core of each subunit and forms the distal side of the heme pocket. It also participates in the binding of NADPH in small subunit enzymes [109]. NADPH serves to protect catalase from inactivation by transferring electrons to the heme. Catalases become inactive when compound I undergoes a one-electron reduction to compound II. Compound II is reduced, or its formation is prevented when NADPH is bound to the enzyme.

The third region is the wrapping domain. This domain is a link between the β -barrel and α -helical domain. It contains some of the residues of the proximal side of the heme pocket. The fourth region is the α -helical domain. This domain interacts with the β -barrel and helps to stabilize its structure. It is also involved in the binding of NADPH. In the large subunit enzymes, a fifth domain links the α -helical domain to the C-terminal domain. This domain structure resembles flavodoxin and is called the flavodoxin domain. A flavodoxin domain may indicate a potential point of binding for flavin mononucleotide to serve as an electron transfer source as with NADPH. However, at this time its role in catalase function is not understood.

Catalase-Peroxidases

Catalase-peroxidases are a member of the Class I plant peroxidases and possess the unique ability to use one active site to catalyze two distinct activities (catalase and peroxidase). This is compared to monofunctional catalases, which have virtually no peroxidase activity, and typical peroxidases, which have virtually no catalase activity. With either activity, H_2O_2 is catalytically removed. These enzymes have been identified in a wide range of bacteria and a few fungi. It is suggested that catalase–peroxidase forms part of an essential defense against the deleterious effects of H_2O_2 and other reactive hydroperoxides [21, 23, 110]. In fact, the loss of catalase-peroxidase in *Mycobacterium tuberculosis* has been shown to decrease its ability to deal with reactive species generated by the host oxidative burst defense resulting in death [112].

Like most catalases and all plant peroxidases, catalase-peroxidases have heme *b* as a prosthetic group in a ferric high spin form. Histidine is the fifth ligand. The catalytic cycle for both catalase and peroxidase is initiated by the reduction of H₂O₂ by two electrons to H₂O with the five-coordinate ferric heme forming the iron-oxygen complex of the enzyme called compound I (Fig. 1.13). The two activities differ in their ability to reduce compound I back to its original ferric form. For catalase, compound I is reduced by two electrons to return to the ferric state by a second equivalent of H₂O₂. This results in the production of O₂ and a second equivalent of H₂O. In the case of peroxidase, two one-electron steps reduce the enzyme back to the ferric form. In the first step, compound I is reduced by one electron by an exogenous electron donor to produce compound II. Compound II is then reduced by one electron to produce the ferric form of the enzyme by a second equivalent of the exogenous electron donor. This two-step reduction results in the production of a second equivalent of H₂O and two equivalents of the electron donor radical.

Compared to catalases and peroxidases, catalase-peroxidases are a relative new enzyme class and have not been as extensively studied. Although the first catalase-peroxidase was discovered in 1979, a full sequence was not known until 1988 [111, 112]. These enzymes are now classified as class I plant peroxidases because of the similarity of their sequence and structure. Crystal structures of the enzyme started appearing in the early 2000s [28-30]. Catalase-peroxidases are found as a dimer or a tetramer with each subunit composed of 20 α -helices joined by linkers and three or four β -strands [113]. This gives catalase-peroxidases a very different tertiary/quaternary structure from monofunctional catalases, which have four distinct regions as previously mentioned.

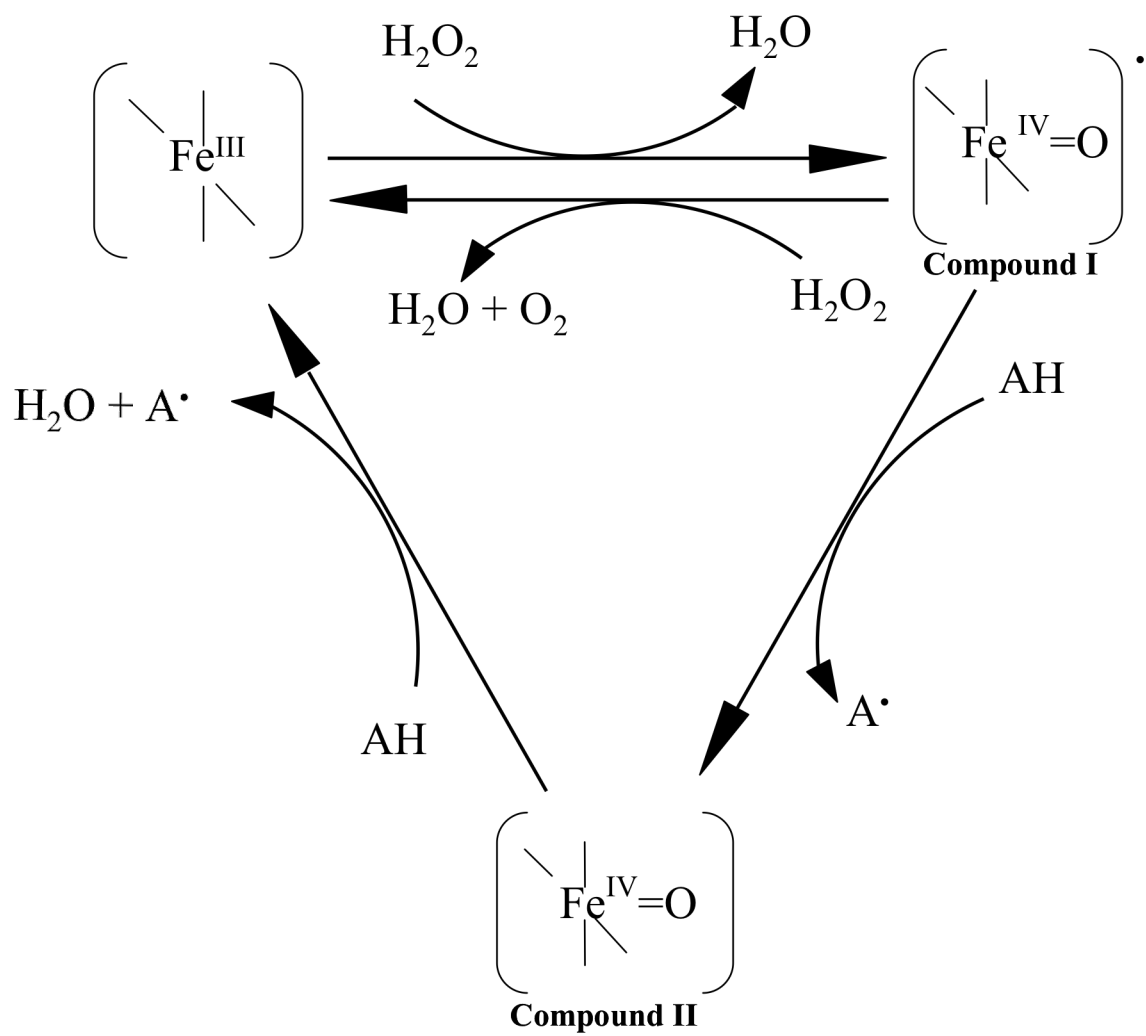


Figure 1.13. Catalytic Cycle of Catalase-peroxidase.

Indeed, there is no sequence or structural similarity between the catalase-peroxidases and monofunctional catalases. Clearly, the catalase activity of these bifunctional enzymes arises from a different structural strategy.

On the other hand, comparison of these bifunctional enzymes to *monofunctional peroxidases* reveals some striking similarities. In addition to the same heme group and fifth ligand (histidine), the other key residues in the active sites of catalase-peroxidases are virtually superimposable on those of monofunctional peroxidases (Fig. 1.14). This indicates that structural components external to this sphere of active site functional groups modulates the active site to impart catalytic abilities that do not typically come with peroxidase enzymes. Importantly, this opens a doorway to evaluating how active site capabilities are influenced by distant protein structures, a poorly understood aspect of enzyme structure/function.

In this regard, catalase-peroxidases have structural components that are distinctly absent from monofunctional peroxidases. Many of these unique features are external to the active site. It is believed that catalase-peroxidases arose through gene duplication, which resulted in a gene with two sequence-related domains (N-terminal and C-terminal) [114]. This is different from most peroxidases, which only have a single domain. Both domains are similar to monofunctional class I plant peroxidases. The active site is located in the N-terminal domain. However, the C-terminal domain doesn't have an active site and has undergone a greater evolutionary drift. The active site is more deeply buried than peroxidase but is accessed through a channel laterally like peroxidase rather than perpendicularly as in the monofunctional catalases. The C-terminal domain helps support the architecture of the active site by preventing the

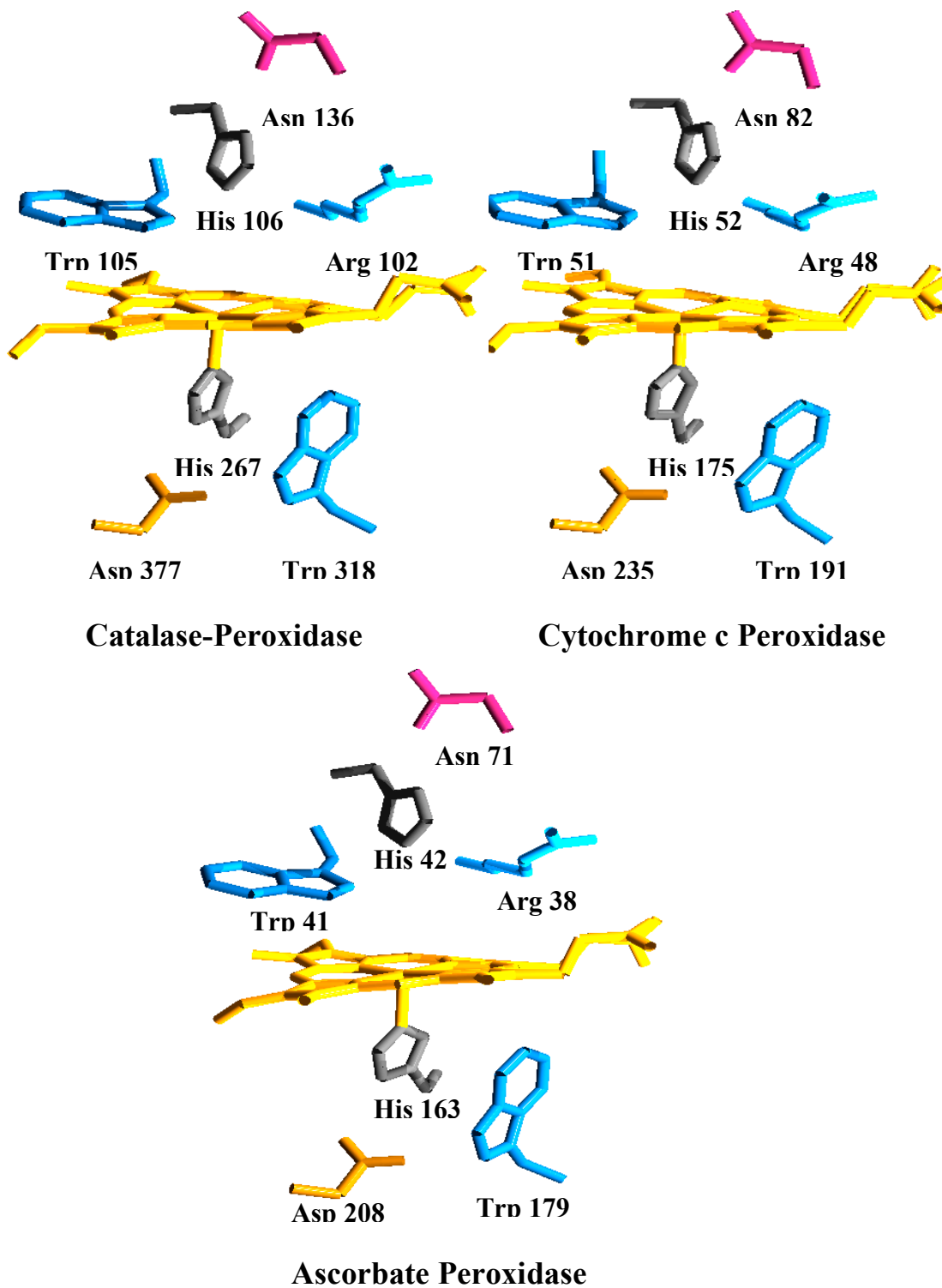


Figure 1.14. Active Site Comparison of Catalase-peroxidase and Class I Plant Peroxidases [29, 88, 115].

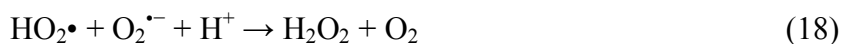
essential distal histidine from coordinating to the heme iron. Removal of the C-terminal domain results in the collapse of the active site and a complete loss of activity [116]. In lignin and manganese peroxidases, a Ca^{2+} ion helps support the architecture of the active site [117, 118]. However, the C-terminal domain likely has additional roles. Another difference from plant peroxidases revealed by sequence and structure analysis is the presence of two interhelical insertions (~35 amino acids) found in the N-terminal domain of catalase-peroxidases (an FG insertion found in the connector of the F and G helices, and an DE insertion found in connector of the D and E helices) [119]. Loss of the FG insertion results in the selective decrease of catalase activity [120, 121]. The FG insertion is believed to help peroxides access the active site and its loss interferes with the accessibility of the active site and the H-bonding network. The DE insertion has more of an influence on catalase-peroxidases. Our laboratory has also observed that the loss of the DE insertion results in a change of the active site environment and complete loss of catalase activity [120, 121]. One role of the DE insertion was revealed by crystal structures and electron density maps of catalase-peroxidases [28-30]. The presence of a three amino acid covalent adduct (Trp-Tyr-Met) is found in the distal heme pocket. The central amino acid Tyr is located on the DE insertion. Removal of the DE insertion interrupts this covalent adduct. The activity of the enzyme is affected by the presence of this adduct and requires the presence of heme for its formation. Interruption of this three amino acid covalent adduct results in the loss of catalase activity indicating one role of this adduct is to protect the catalase activity of the enzyme. The presence of this adduct also seems to be a characteristic common to all catalase-peroxidases. The key to understanding what makes catalase-

peroxidases unique in their function is held in these structures and how they affect the active site. The study of catalase-peroxidases will provide valuable insight to the general question of how an entire enzyme structure important for determining its catalytic capabilities, even those structures that are distant from the active site.

In addition to the knowledge of enzyme structure/function that can be gained from the study of catalase-peroxidases, these enzymes have roles in important biomedical processes that further increase the benefits to be gained from understanding the link between their structure and catalytic abilities. Tuberculosis is one of the most deadly infectious diseases in developing countries and is estimated to have infected one-third of the world's population [122]. Isoniazid (INH) has been a first-line antibiotic used against *Mycobacterium tuberculosis* infections since its discovery in 1952 [123]. It is known that INH is a prodrug which is converted to an active form by *M. tuberculosis* catalase-peroxidase (KatG) [124]. Activated INH inhibits the pathway for mycolic acid biosynthesis leading to the death of the organism. However, there are some key questions that need to be answered: 1) How does KatG activate INH? 2) What is its active form? 3) How do alterations of KatG gene by mutations lead to interrupted INH activation? These are important biomedical questions that relate to the structure/function relationship in catalase-peroxidases.

Catalase-peroxidases and Reactive Oxygen Species

The need to direct the reactivity of oxygen is essential for survival in an aerobic environment. While nature has gone to great lengths to ensure the interaction of Fe with O₂ is controlled and specific by the storage of Fe in complexes and proteins as pointed out earlier, ROS are still inevitably generated. A key role for catalases, peroxidases, and catalase-peroxidases is to remove reactive oxygen species (particularly but not exclusively H₂O₂) to prevent the damaging consequences of ROS. The partial reduction of O₂, starting with O₂^{•-}, can lead to the production of H₂O₂ and eventually to •OH if it goes unchecked (reactions 16-19). In this regard, there are two general sources for ROS. The first is “misfiring” that occur in electron transfer processes in biology, particularly where Fe



and O₂ interactions occur. In this respect, hemoproteins provide some examples of these types of “misfiring”. In some instances, much higher levels of ROS in addition to reactive nitrogen species are produced as part of a host defense against infection by microorganisms. The biological context of catalase-peroxidases can be understood to some degree in terms of these situations where ROS are generated.

Misfires in Hemoproteins Reaction

The globins are known to generate ROS through an autoxidation reaction (Fig. 1.15) [125]. Autoxidation reactions are found in nature in all oxygen binding hemoproteins [126]. However, there is no clear mechanism for this reaction. The reversible binding of O₂ to the globins first results in a ferrous-heme-oxygen complex. This oxygenated form of the protein can form a resonance hybrid with the ferric superoxo state. The release of superoxide anion results in the ferric form of the globin proteins, which are called met (e.g., metmyoglobin and methemoglobin) (Fig. 1.15). The heme can eventually be reduced back to the ferrous state. On the other hand, the ferric enzyme cannot bind O₂ and is physiologically inactive.

The rate of autoxidation is influenced by three factors: partial pressure of O₂, pH, and the different globin proteins. Studies on the effect of partial pressure of O₂ studies on autoxidation indicate an increase in rate up to a maximum when half the protein is saturated with O₂ [127, 128]. A 2-3 fold decrease in the rate is observed at higher partial pressures. High O₂ pressure may serve to protect the protein from autoxidation. Changes in pH are also known to affect the rate of autoxidation. At high concentration of both hydrogen and hydroxyl ions, an increase in the rate of autoxidation is observed [127, 129]. Although it is not understood why the increase occurs at high hydroxyl ions, Weiss theorizes that at low pH, a loss of hydrogen bonding between the distal histidine and Fe^{II}-O₂ results in the equilibrium protonation of Fe^{II}-O₂ to Fe^{II}-O₂H⁺ [130]. This leads to

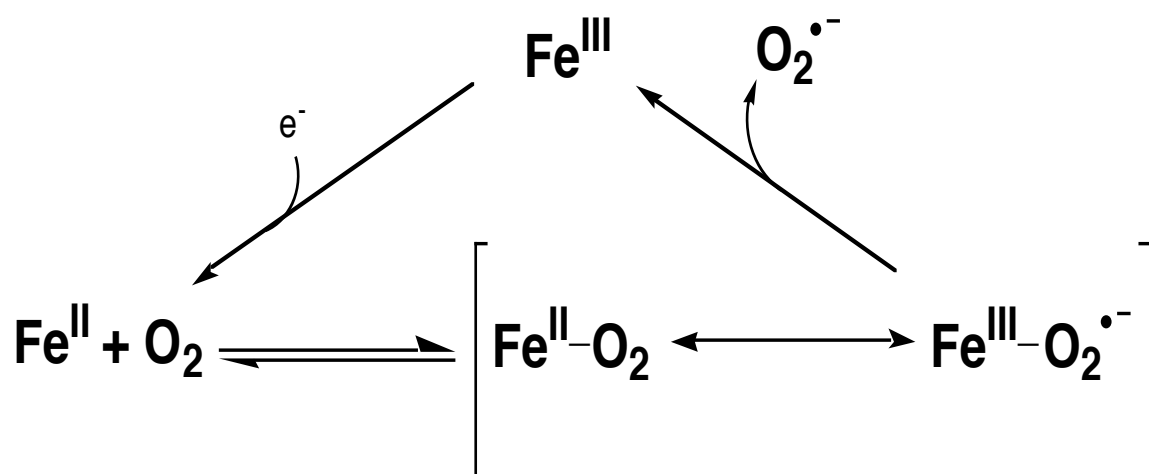


Figure 1.15. Autoxidation Reaction of Myoglobin and Hemoglobin.

the formation of the met species. The rate of autoxidation will also vary between different globin proteins [131, 132].

The cytochrome P450s catalyze the insertion of an oxygen atom into different substrates. Electron transfer to oxygen, which ultimately leads to substrate oxidation, controls this reaction. Uncoupling of the catalytic cycle can result in the production of ROS rather than the target product [133, 134]. One type of uncoupling outcome is the autoxidation decay of the one-electron reduced ternary complex to release superoxide (Fig. 1.16 (i)). This is reminiscent of globin autoxidation and comes as a result of slow delivery of the second electron to the oxygen. Superoxide subsequently produces hydrogen peroxide. Alternatively, the protonation of the ferri-peroxo complex leads to the release of hydrogen peroxide (j).

The presence of a substrate has a substantial effect on the production of ROS by cytochrome P450. Indeed, it has been estimated that in liver microsomal cytochrome P450 as much as 55% of the consumed oxygen appears as hydrogen peroxide in the presence of substrate and 100% in its absence [135]. The presence of substrate serves to increase the rate of the first electron transfer. Cytochrome *b₅* may also play a role in the coupling of cytochrome P450. Although not essential for activity, cytochrome *b₅* increases the activity of cytochrome P450, which decreases the production of ROS [136, 137]. However, it is not clear whether cytochrome *b₅* functions as an electron carrier or helps stabilize a particular cytochrome P450 conformation. In any case, cytochromes P450 and others like them can be a source of partially reduced oxygen species.

Autoxidation of cytochromes P450 and the globins are two examples among many of generation of ROS by “misfiring”. Living organisms must have ways to remove

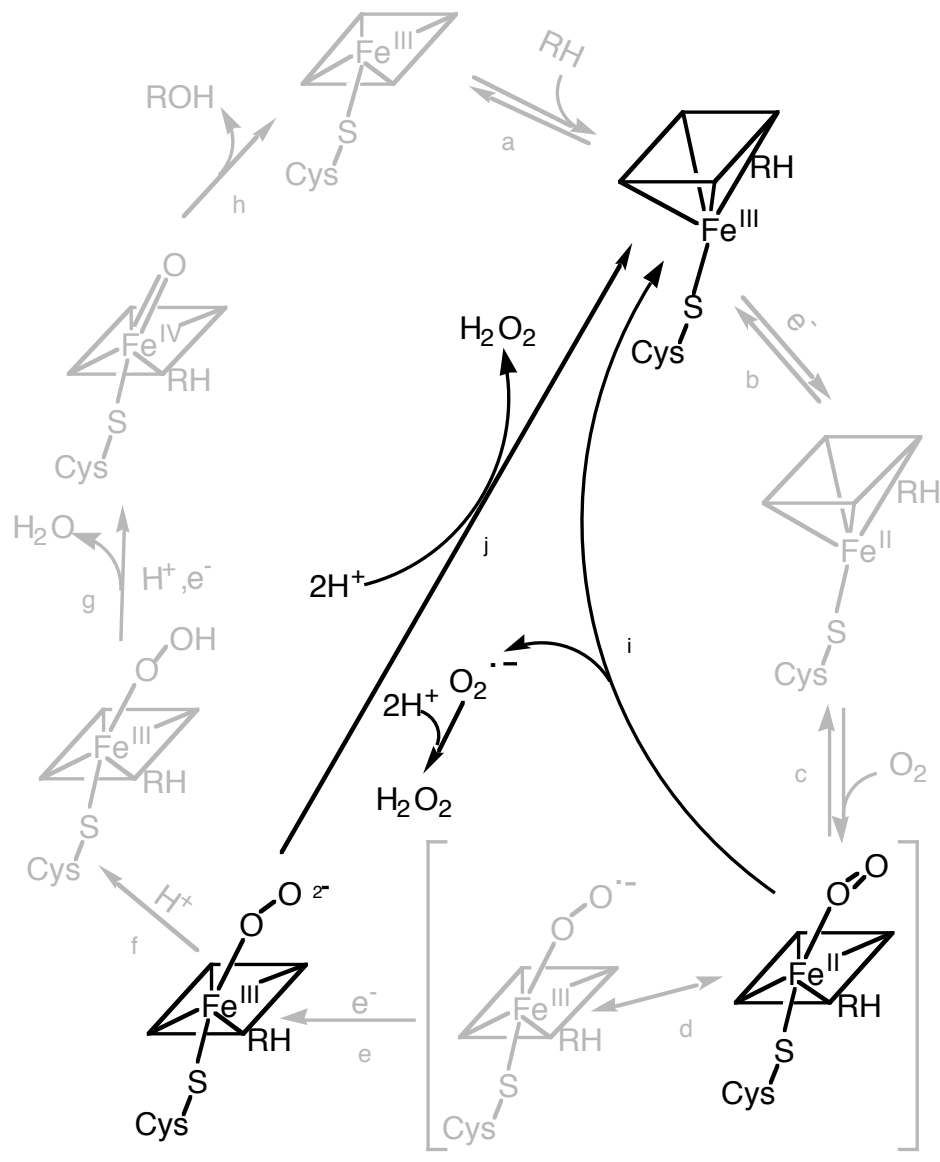


Figure 1.16. Generation of ROS in Cytochrome P450.

these ROS when they are generated. Systems to prevent formation of $\bullet\text{OH}$ are ubiquitous. Superoxide dismutase catalyzes removal of $\text{O}_2\bullet^-$ to produce O_2 and H_2O_2 . However, the presence of H_2O_2 can easily be reduced to $\bullet\text{OH}$, posing enormous risks. Therefore, catalase or peroxidase is essential for safe removal of partially reduced oxygen species. Catalase-peroxidases appear to fill this role in numerous bacteria.

Although most catalase-peroxidases are found in the cytoplasm, some bacterial have a second catalase-peroxidase located in the periplasmic space [22-24]. This seems to be overkill for bacterial protection against H_2O_2 . Why would a second catalase-peroxidase be necessary? In each case, this periplasmic catalase-peroxidase is found in a highly pathogenic bacterial species, including *Escherichia coli* O157:H7, *Yersina pestis* and *Legionella pneumophila*. Importantly, the non-pathogenic counterparts to these organisms do not have a periplasmic catalase-peroxidase, indicating that the periplasmic form may be a virulence factor. Sequence analysis has revealed a signal peptide present in the periplasmic enzymes, which was not found with the cytoplasmic catalase-peroxidases [24, 25, 27]. Periplasmic catalase-peroxidases also show a higher sequence homology with each other than with the cytoplasmic enzymes. The potential role of the periplasmic catalase-peroxidases from (KatP) as a virulence factor is further supported by the following: In *E. coli* O157:H7, catalase-peroxidase is encoded on the pO157 plasmid - a large plasmid associated with virulence [24]. In *Y. pestis*, KatY is expressed corresponding with a temperature shift from 26 °C to 37 °C [138]. This corresponds to a transfer of the bacterium from flea to mammalian host. In *L. pneumophila*, KatA seems to impart characteristics that help it survive and grow inside the macrophage host [23]. The mechanism by which these periplasmic catalase-peroxidases contribute to the

virulence of *E. coli* O157:H7, *Y. pestis* and *L. pneumophila* is not understood. It is proposed that periplasmic catalase-peroxidases may serve as the first line of defense against reactive oxygen species (ROS) and reactive nitrogen species (RNS) generated by the immune response [27].

Immune Response

Generation of ROS and RNS are a fundamental part of the immune response, in which the body defends itself against microorganisms, viruses, and other foreign substances [139]. ROS are also found to be generated in plants as a defensive response to pathogen attack [140]. In an immune response, neutrophil cells initiate respiratory burst, using hemoproteins to generate ROS and RNS. NADPH oxidase and myeloperoxidase are two hemoproteins used by the immune system.

NADPH oxidase, also known as respiratory burst oxidase, is responsible for this process. NADPH oxidase is a multi-enzyme complex membrane protein that catalyzes the one electron reduction of oxygen to superoxide ($O_2^{\bullet-}$) [141]. The overall reaction is:

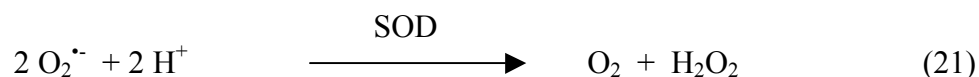


The cofactor NADPH is required as a source of electrons. The NADPH oxidase transfers an electron from NADPH to O_2 . As a result, $O_2^{\bullet-}$ is produced along with

oxidized NADP⁺. O₂^{•-} is the first step in the generation of a wide array of reactive oxidants.

The NADPH oxidase complex is comprised of two membrane components: p22 and gp91 (Fig. 1.17). These two components form cytochrome b₅₅₈. Cytochrome b₅₅₈ carries its name because in its reduced form, it has a characteristic absorption peak at 558 nm. Cytochrome b₅₅₈ is a heterodimer with two hemes. One heme is located within gp91 where O₂ binds while the other heme is shared between p22 and gp91 [142]. In anaerobic conditions, the hemes low midpoint potential of -245mV prevents the direct reduction of O₂ to O₂^{•-} by reduced cytochrome [143-145]. However, cytochrome is rapidly oxidized in aerobic conditions [146]. Although a three-dimensional structure of the cytochrome has yet to be solved, sequence comparisons indicates the presence of a flavin binding site [147]. The NADPH complex is also comprised of three cytosolic components and a G protein: p67, p47, p40, and rac1 or rac2 (Fig 1.17) [148]. When activated, the cytosolic proteins move to the membrane to form the active NADPH oxidase (Fig 1.17). While gp91 serves as the electron transporter of NADPH oxidase, the other components serve to regulate the transfer of electrons

The oxidative burst is only the first step in the antibacterial defense. Indeed, O₂^{•-} is a weak microbicidal alone [149]. If O₂^{•-} is reduced by a second electron, H₂O₂ will be generated (reaction 3). In the immune response, this is accomplished by superoxide dismutase (SOD) (reaction 21). Along with O₂^{•-}, H₂O₂ also has a relatively weak



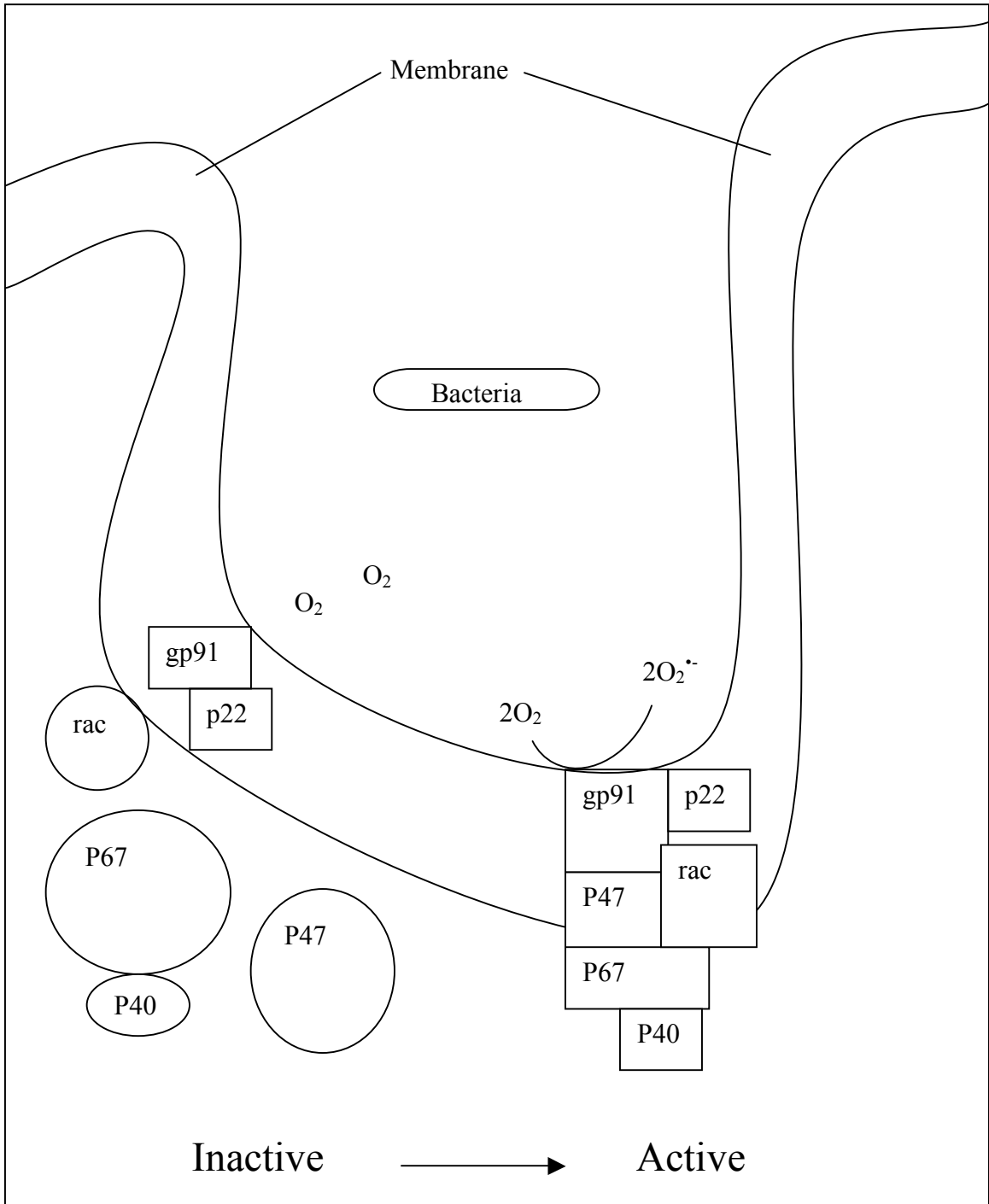


Figure 1.17. Schematic Representation of the NADPH oxidase.

microbicidal effect and needs to be activated to a more reactive oxidant [150]. One possibility is the generation of $\bullet\text{OH}$ by the 1 e^- reduction of H_2O_2 , but this is not the principal strategy of neutrophils. Instead, H_2O_2 is used as an oxidant to generate HOCl . Central to this process in neutrophils is myeloperoxidase. Myeloperoxidase is a heme-containing peroxidase that reacts with H_2O_2 (Fig. 1.18). As with other peroxidases, this reaction results in the formation of the ferryl-oxo porphyrin/protein radical intermediate compound I. Compound I is then reduced by a halide ion, Cl^- in particular, to generate the corresponding hypochlorous acid (i.e., HOCl) and the ferric enzyme. Hypochlorous acid is a strong oxidizing agent and can react with many biomolecules leading to the death of the invading cells [150].

Macrophages also generate large quantities of $\text{O}_2^{\bullet-}$ by way of an oxidative burst mechanism. In these cells, however, there is very little production of HOCl . Instead, $\text{NO}\bullet$ is rapidly generated by inducible nitric oxide synthase (iNOS). The $\text{O}_2^{\bullet-}$ generated by NADPH oxidase and $\text{NO}\bullet$ generate by iNOS react at diffusion controlled rates to generate peroxynitrite (ONOO^-) [151, 152]. Peroxynitrite is a highly bactericidal agent, many times more potent than H_2O_2 [153]. Peroxynitrite is a peroxide and has been shown to interact with peroxidases-type enzymes in a fashion similar to H_2O_2 . In the process, ONOO^- is reduced to the much less harmful NO_2^- anion [151, 154].

The placement of an enzyme in the periplasmic space that rapidly consumes H_2O_2 and ONOO^- may provide a distinct selective advantage for pathogens who must encounter activated macrophages and neutrophils from a host organism. The key to survival for microorganisms in host organisms is to have a good defense against the

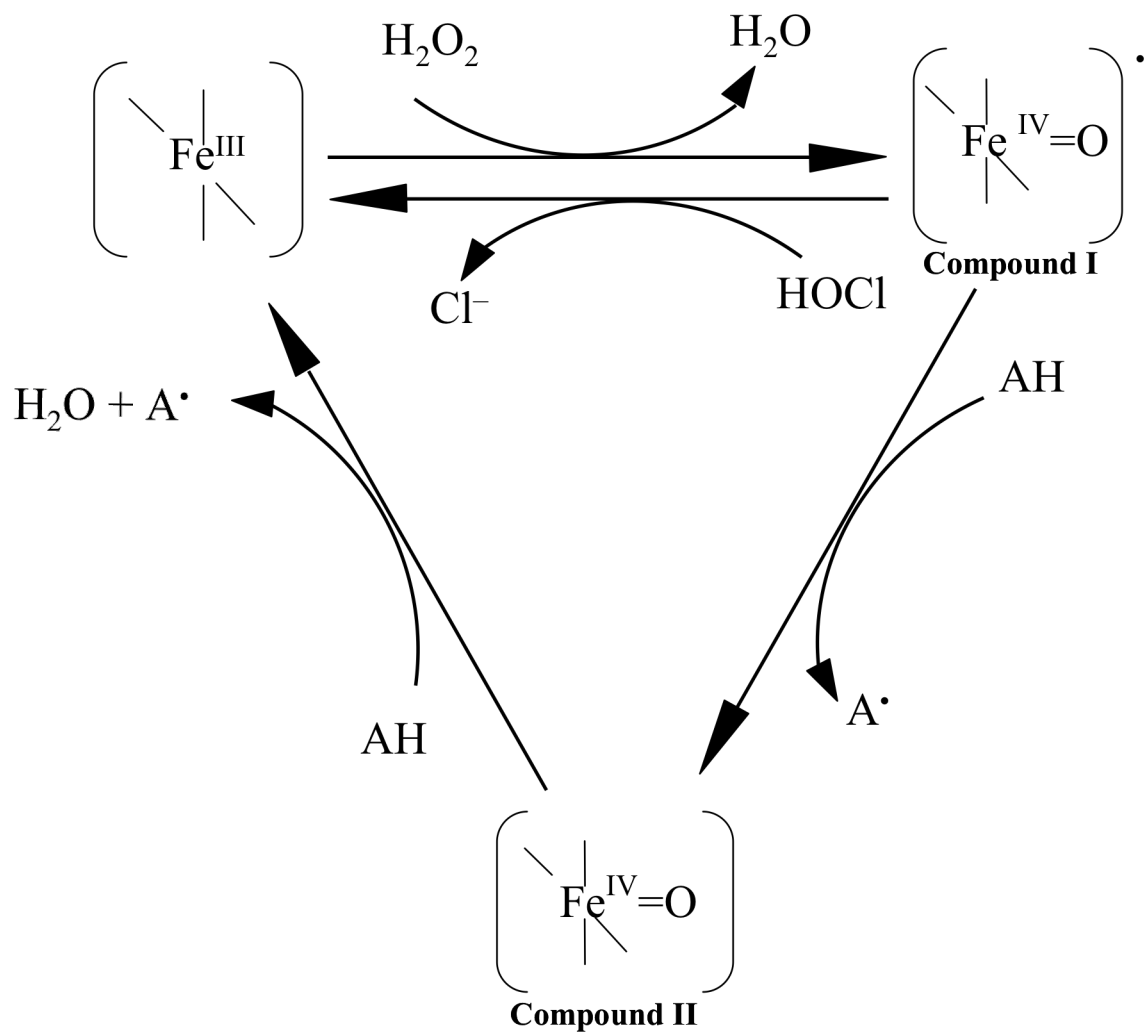


Figure 1.18. Catalytic Cycle of Myeloperoxidase.

immune response. The reduction of $O_2^{\cdot-}$ by superoxide dismutase is counter productive in producing the more powerful oxidant H_2O_2 , which regulates the production of HOCl. HOCl is too powerful of an oxidant to control, making the most efficient way to counteract the immune response by neutrophil cells the decomposition of H_2O_2 .

Summary

Hemoproteins are important in the essential need to activate oxygen. The presence of heme is critical to the function of hemoproteins. However, there are many factors that contribute to the diversity of hemoprotein activities including the structure of heme, heme iron ligands, and the environment surrounding the heme. The diversity of hemoproteins makes them a good model in the evaluation of the relationship between protein structure and function. In this dissertation a development of an expression system for the enhancement of recombinant hemoproteins expression is used as a tool to aid in the study of that relationship in these important proteins.

Catalase-peroxidases are a group of hemoproteins that give bacteria an enhanced capacity to combat ROS. The ability of catalase-peroxidases to use one active site, which is almost identical to monofunctional peroxidases, for two distinct activities also make them an ideal system to study protein structure and function relationship. In this dissertation the presence of a periplasmic catalase-peroxidase found in pathogenic bacteria is evaluated with its potential role in bacterial virulence in mind. The role of a

three amino acid covalent adduct is also evaluated so as to better understand the protein structure and function relationship.

CHAPTER TWO

MATERIALS AND METHODS

Reagents

The following compounds or materials, cataloged by source, were obtained. Hydrogen peroxide (30%), peracetic acid, δ -amino levulinic acid, hemin, imidazole, Sephacryl 300 HR, phenyl-Sepharose resin, 2,2'-bipyridyl, phenylmethylsulfonyl fluoride (PMSF), ampicillin, chloramphenicol, ferrous ammonium sulfate, sodium hydrosulfite, trifluoroacetic acid, and 2,2'-azino-bis(3-ethylbenzthiazoline-6-sulfonic acid) (ABTS) were purchased from Sigma (St. Louis, MO). Isopropyl- β -D-thiogalactopyranoside (IPTG), acetonitrile, kanamycin monosulfate, potassium ferricyanide, sodium hydroxide, and tetracycline hydrochloride were obtained from Fisher (Pittsburgh, PA). Bugbuster and benzonase were purchased from Novagen (Madison, WI). Pyridine was purchased from ACROS (New Jersey). Zinc (II) protoporphyrin IX (ZnPPIX) was purchased from

Frontier Scientific (Logan, UT). All restriction enzymes were purchased from New England Biolabs (Beverly, MA) and all oligonucleotide primers were purchased from Invitrogen (Carlsbad, CA). The *E. coli* strains BL-21 (DE3) pLysS, and XL-1 Blue were obtained from Stratagene (La Jolla, CA) as was Pfu polymerase. Nickel–nitrilotriacetic acid (Ni–NTA) resin was obtained from Qiagen (Valencia, CA). All buffers and media were prepared using water purified through a Millipore Q-PakII or a Barnstead EASY pure II system (18.2 MΩ/ cm resistivity).

Construction of pHPEX Plasmids

A description and abbreviations of plasmids and *E. coli* strains described in this work are summaries in Table 2.1. The pHPEX1 plasmid was constructed by first amplifying the heme receptor gene (*chuA*) from *E. coli* O157:H7 by PCR. This was accomplished using primers HPEX a01 (TAA CAA AAC *CAT GGC* AAT TGC AAG GGA TAA CGC) and HPEX a02 (GTG TGT AGG *AAT TCA* TTG TCT CTC TTC CTT CCA G) with internal restriction endonuclease recognition sequences (*italics*) for *NcoI* and *EcoRI*, respectively. The PCR product included the entire coding sequence plus 295 bp upstream of the ATG start codon and 50 bp downstream of the TAA stop codon. The *chuA* PCR product and the low-copy number plasmid, pACYC184, were digested with *NcoI* and *EcoRI* and isolated by agarose gel electrophoresis. Digested products were excised and extracted from the gel by Qiagen QIAquick gel extraction kit protocol. In

Plasmid	Starting construct	Modifications	Size (bp)
pHPEX1	pACYC184	<i>chuA</i> inserted, Cam ^r interrupted	6224
pHPEX2	pHPEX1	<i>lacUV5</i> inserted 5' to <i>chuA</i>	5547
pHPEX3	pHPEX2	T7 lysozyme (<i>lysS</i>) inserted	5400
pHPEX-fur	pHPEX1	<i>fur</i> inserted 5' to <i>chuA</i>	6243
pKatG1	pET20b(+)	<i>E. coli</i> KatG inserted (C-term 6 His-tag)	5765
Strain	Genotype		
BL-21 (DE3)	<i>E.coli</i> B F ⁻ <i>dcm ompT hsdS</i> (F _B m _b) <i>gal</i> (DE3)		
BL-21 (DE3) pLysS	BL-21 (DE3) [pLysS Cam ^r]		
BL-21 (DE3) pHPEX2	BL-21 (DE3) [pHPEX2 Tet ^r]		
BL-21 (DE3) pHPEX3	BL-21 (DE3) [pHPEX3 Tet ^r]		
BL-21 (DE3) pHPEX-fur	BL-21 (DE3) [pHPEX-fur Tet ^r]		

Table 2.1 Plasmids and strains used for the development of the hemoprotein expression (HPEX) system.

order to ligate DNA together, T4 DNA ligase was added to extracted DNA and incubated at 37°C for 1 hr. according to standard procedures [155]. The ligation products were then used to transform *E. coli* (XL-1 Blue). Transformants were selected on the basis of tetracycline resistance. Plasmid isolated from candidate colonies was analyzed by *AvaI* and *BssHII* restriction digest to ensure the correct construction of pHPEX1. The entire *chuA* gene was sequenced to ensure that no accidental mutations occurred during the procedure.

The pHPEX2 plasmid was constructed from pHPEX1. The natural *chuA* upstream regulatory elements present in pHPEX1 were replaced by the *lacUV5* promoter using the Seamless Cloning™ procedure (Stratagene). This protocol incorporates the restriction enzyme recognition sequence for *Eam1104 I* (5'-CTCTTC-3'). *Eam1104 I* is a type IIS restriction enzyme that cuts outside its recognition sequence as illustrated below. It cuts one nucleotide downstream of the recognition sequence on one strand and four nucleotides on the complementary strand, leaving a three nucleotide overhang that can be designed by the user for ligation. During amplification, 5-methyldeoxycytosine is included so that it is incorporated into the newly synthesized DNA. This serves to protect already-existing *Eam1104 I* sites against cleavage and ensure that only the restriction sites in the primers are hydrolyzed by *Eam1104 I*.

The portion of pHPEX1 to be retained for pHPEX2 was amplified using primers HPEX a05 (TGG AGA CTC TTC ATG TCA CGT CCG CAA TTT ACC TCG)



(*Eam1104 I* recognition site in italics) and HPEX a06 (CGT GGT *CTC TTC* GGA GGG TTC CAC TCT CTG TTG C). The *lacUV5* promoter was amplified from the pBT plasmid using primers *lacUV5 a00* (GGT TTC TTT *CTC TTC* CAC ATA CGC TGT TTC CTG TGT GAA A) and *lacUV5 a01* (GTT ACC TCT *CTT CAC* TCA GTT GGT AGC TCA GAG AAC C). Both PCR products were hydrolyzed with *Eam1104 I* and ligated together with T4 DNA ligase. The ligation products were then used to transform *E. coli* (XL-1 Blue). Transformants were selected on the basis of tetracycline resistance. Plasmid isolated from candidate colonies was analyzed by *ClaI* restriction digest to ensure the correct construction of pHPEX2. The entire *chuA* gene and *lacUV5* promoter were sequenced to ensure no accidental mutations occurred during PCR amplification.

The pHPEX3 plasmid was constructed by incorporating the gene for T7 lysozyme into the pHPEX2 plasmid. This was also accomplished by Seamless CloningTM. The portion of pHPEX2 to be retained for pHPEX3 was amplified by the primers HPEX a07 (GAA CGG GGC GGA *CTC TTC* CAA AAA GAT GCC AGG AAG ATA C) and HPEX a08 (CAC ATT CTT *GCT CTT* CTG GGG AAT GCT CAT CCG GAA TTC). The T7 lysozyme gene was amplified from the pLysS plasmid using the primers T7 LYS a01 (GTC CTG TCT *CTT CGC* CCC ATT GGC TGC CTC CCA CA) and T7 LYS a00 (GAG GAT CCG *CTC TTC* CTT TGA TAG ATT AAA AAG GAA AGG AGG). Both PCR products were hydrolyzed with *Eam1104 I* and ligated together with T4 DNA ligase. The ligation products were then used to transform *E. coli* (XL-1 Blue). Transformants were selected on the basis of tetracycline resistance. Plasmid isolated from candidate colonies was analyzed by *BsaI* and *BssHIII* restriction digest to ensure the correct construction of pHPEX3.

Finally, the pHPEX-fur plasmid was constructed by incorporating the iron uptake regulator into the pHPEX1 plasmid. This was accomplished using primers FURINS 1(CAT GGA TAA TAA TTC TCA TTA TA) and FURINS 2 (CAT GTA TAA TGA GAA TTA TTA TC), which contain the fur box and an *Nco*I overhang. The FURINS primers were annealed together by first heating equal quantities together at 90 °C for 5 min. and then cooling to 37 °C for 5 min. The duplex was then stored at 4 °C until used. The pHPEX1 plasmid was digested with *Nco*I. Both products were ligated together with T4 DNA ligase. The ligation products were then used to transform *E. coli* (XL-1 Blue). Transformants were selected on the basis of tetracycline resistance. Plasmid isolated from candidate colonies was analyzed by *Bst* BI and *Nco* I/*Kpn* I restriction digest to ensure the correct construction of pHPEX-fur. DNA sequencing was performed to ensure that the fur box was inserted once and in the proper orientation.

Expression of KatG and Myoglobin

Expression of KatG for Heme Evaluation

The pET-based plasmid pKatG1 for the expression of recombinant histidine-tagged *E. coli* catalase–peroxidase was used to transform two *E. coli* strains, BL-21 DE3 pLysS and BL-21 DE3 pHPEX3, and transformants were selected based on ampicillin or tetracycline resistance. Expression of KatG was carried out in Luria–Bertani broth (2 L). Cells were grown to mid-log phase ($OD_{600}=0.5$) and expression of KatG was induced by

addition of IPTG (1 mM). At the time of induction, KatG cultures were supplemented with 8 μ M hemin. Cultures were grown at 37 °C with constant shaking for four hours. At four hours post-induction, cells were harvested by centrifugation (13,000g), and the cell pellets were stored at -80 °C until purification.

To evaluate KatG expression, a quantity of cells sufficient to yield a 0.05 OD₆₀₀ reading (when diluted to 1 ml) was treated with an equal volume of 10% trichloroacetic acid (4 °C) and centrifuged in a microcentrifuge at maximum rcf for 5 min. The supernatant was discarded and the pellet was washed with 1 ml acetone. The pellets were then dried and resuspended in SDS-PAGE loading buffer, adjusting the pH as appropriate with trizma base. Samples were then separated by SDS-PAGE using a 7.6% acrylamide resolving gel.

Cell pellets were resuspended in Bugbuster (Novagen) reagent supplemented with benzonase (250 U) and PMSF (0.1 mM). The cell lysate was then centrifuged at 16,000g. The supernatant was loaded onto a Ni-NTA column by recirculating the solution at 1 ml/min through the column bed overnight. The column was then washed with 50 mM phosphate buffer, pH 8.0/200 mM NaCl/2 mM imidazole. Protein was eluted with 50 mM phosphate buffer, pH 8.0/200 mM NaCl/100 mM imidazole.

Expression of Myoglobin for Heme Evaluation

The pET-based plasmid pMb1 for the expression of recombinant sperm whale myoglobin (pMb1) was generously provided by the laboratory of John S. Olson at Rice

University and was used to transform four *E. coli* strains (BL-21 DE3, BL-21 DE3 pLysS, BL-21 DE3 pHPEX3, and BL-21 DE3 pHPEX-fur). Transformants were selected based on kanamycin or tetracycline resistance as appropriate. Expression of Mb was carried out in Luria–Bertani broth (10 mL). Cells were grown to mid-log phase ($OD_{600}=0.5$), and expression of Mb was induced by addition of IPTG (1 mM) or 2,2'-bipyridine (0.15 mM). At the time of induction, Mb cultures were supplemented with 8 μ M hemin. Cultures were grown at 37 °C with constant shaking for four hours. At four hours post-induction, cells were harvested by centrifugation (13,000g), and the cell pellets were stored at 4 °C.

To evaluate Mb expression, a quantity of cells sufficient to yield a 0.05 OD_{600} reading (when diluted to 1 ml) was treated with an equal volume of 10% trichloroacetic acid (4 °C) and centrifuged in a microcentrifuge at maximum rcf for 5 min. The supernatant was discarded and the pellet was washed with 1 ml acetone. The pellets were then dried and resuspended in SDS–PAGE loading buffer, adjusting the pH as appropriate with trizma base. Samples were then separated by SDS–PAGE using a 12% acrylamide resolving gel.

Cloning and Expression of KatP and KatG^{Y226F}

Cloning of KatP

Construction of the KatP plasmids was performed in our lab by Kristen Hertwig with the assistance of Dr. Douglas Goodwin. The *katP* gene was amplified from pO157 plasmid isolated from *E. coli* O157:H7 using primers O157a02 (CCT CCC TCA GTT CTC GAG TTT ATT GTT TAA ATC AAA CCG ATC) and O157a03 (CCC TTA ATC CGG AGA TCT TCA TAT GAT AAA AAA AAC TCT TCC). The resulting PCR product and pET20b(+) were digested with *Bgl*III and *Xho*I, and the fragments were separated by agarose gel electrophoresis. The bands were excised from the gel and extracted according to standard procedures [155]. The DNA fragments were then ligated and used to transform *E. coli* (XL-1 Blue). Transformants were selected based on ampicillin resistance and screened by restriction digests. The resulting construct (pKatP1) was used as a template for site-directed mutagenesis by the Quik-Change™ procedure (Stratagene, La Jolla, CA). The primers O157m01(+) (CGG AAC ATA CAG GAC CTA TGA TGG CCG GG) and O157m01(–) (CCC GGC CAT CAT AGG TCC TGT ATG TTC CG) were used to make a silent mutation to the codon for Thr 110 and thus remove an internal *Nde*I restriction site. The resulting PCR product was treated with *Dpn*I and used to transform *E. coli* (XL-1 Blue) by electroporation. Transformants were selected by ampicillin resistance and candidate plasmids were screened by restriction digest with *Nde*I. The resulting construct (pKatP2) and pET20b(+) were digested with *Nde*I and *Xho*I and the fragments were separated by agarose gel electrophoresis. The

bands corresponding to the *katP* gene and the pET plasmid were excised from the gel, extracted, and ligated together as described above. The resulting construct (pKatP3) was used to transform *E. coli* (XL-1 Blue). Transformants were screened by diagnostic restriction digests and candidate plasmids were subjected to DNA sequence analysis to ensure that no accidental mutations had accumulated during the cloning procedure. The final plasmid (pKatP3) was constructed such that the protein would be expressed with a C-terminal six-histidine tag.

Expression of KatP

The pKatP3 plasmid was used to transform *E. coli* (BL-21 DE3 pLysS), and transformants were selected based on ampicillin resistance. Expression of KatP was carried out in Luria–Bertani broth (2L). Cells were grown to mid-log phase ($OD_{600}=0.5$) and expression of KatP was induced by addition of IPTG (1 mM). At the time of induction, KatP cultures were also supplemented with δ -amino levulinic acid (0.5 mM) and ferrous ammonium sulfate (0.5 mM). Cultures were grown at 37 °C with constant shaking for four hours. At four hours, post-induction cells were harvested by centrifugation (13,000g), and the cell pellets were stored at –80 °C until purification.

To evaluate KatP expression, a quantity of cells sufficient to yield a 0.05 OD_{600} reading (when diluted to 1 ml) was treated with an equal volume of 10% trichloroacetic acid (4 °C) and centrifuged in a microcentrifuge at maximum rcf for 5 min. The supernatant was discarded and the pellet was washed with 1 ml acetone. The pellets were

then dried and resuspended in SDS–PAGE loading buffer, adjusting the pH as appropriate with trizma base. Samples were then separated by SDS–PAGE using a 7.6% acrylamide resolving gel.

Purification of KatP

Cell pellets were resuspended in Bugbuster (Novagen) reagent supplemented with benzonase (250 U) and PMSF (0.1 mM). The cell lysate was then centrifuged at 16,000g. The supernatant was loaded onto a Ni–NTA column by recirculating the solution at 1 ml/min through the column bed overnight. For KatP, the column was then washed with Buffer A (50 mM phosphate buffer, pH 8.0; 200 mM NaCl) supplemented with 2 mM imidazole. A second wash was then performed with Buffer A supplemented with 20 mM imidazole. Finally, protein was eluted off the column with Buffer A supplemented with 200 mM imidazole. Excess imidazole was then removed either by dialysis against Buffer A lacking imidazole or by gel filtration chromatography.

This initial purification procedure resulted in two-KatP proteins one of which contained heme and displayed peroxidase and catalase activities. The other lacked heme and showed no activity. We were able to isolate the active fraction using either a phenyl-sepharose column or FPLC anion exchange chromatography. For anion exchange, protein from the initial purification of KatP was loaded onto a UNO Q1 column (Bio-Rad, Hercules, CA). Separation was accomplished using a two buffer system: 50 mM Tris, pH 8.1 (Buffer I), and 50 mM Tris, pH 8.1/375 mM, NaCl (Buffer II). The initial

buffer condition of the column was 100% Buffer I/0% Buffer II. Following a 0.45 min isocratic period, buffer conditions were ramped to 67% Buffer I/33% Buffer II over 0.58 min. The buffer composition was then changed to 50% Buffer I/50% Buffer II over 8 min and then up to 40% Buffer I/60% Buffer II over the next 1.25 min. Finally, 0% Buffer I/100% Buffer II was passed over the column for 0.75 min, followed by 100% Buffer I/0% Buffer II for 2 min.

For separation using phenyl-sepharose, ammonium sulfate was added to partially purified KatP up to 20% saturation. This solution was used to load a phenyl-sepharose column. Following a wash step, active KatP was eluted from the column by a linear gradient from buffer 20% saturated with ammonium sulfate to buffer without ammonium sulfate. Fractions were evaluated for catalase activity and active fractions were analyzed for purity by SDS-PAGE. Pure and active fractions were collected and concentrated.

Cloning and Expression of KatG^{Y226F}

KatG Tyr 226 was mutated to Phe using a “Quik Change” procedure from Stratagene. Primers ECCPm 23(+) (GAG ATG GGT CTG ATC TTC GTT AAC CC) and ECCPm 23(-) (GGG TTA ACG AAG ATC AGA CCC ATC TC) were used to produce the Y226F substitution. Nucleotide substitutions designed to produce the mutation are underlined. The resulting PCR product was digested with *Dpn* I to remove the starting template and then used to transform *E. coli* (XL-1 Blue) by electroporation. Transformants were selected by ampicillin resistance and candidate plasmids were

evaluated by *Hpa* I digest. Primers were designed to make a unique restriction site making the digest possible. Positive candidates were subjected to DNA sequence analysis to ensure that no unintended mutations had accumulated during the site-directed mutagenesis procedure. Plasmids verified to carry the correct mutation were used to transform *E. coli* (BL-21 [DE3] pLysS). Expression of Y226F was accomplished by the same method as wtKatG except that some of the protein was expressed in inclusion bodies. Expression of some proteins at high rates can allow for aggregation due to hydrophobic effects before proper folding leading to formation of inclusion bodies. Expression was carried out at lower temperature (18 °C) in order to slow down expression and allow more protein to be produced in their native conformation. Protein was expressed for six hours following induction with IPTG. Purification of Y226F was carried by the same procedures as wtKatG.

Protein Characterization

UV-Visible Absorption Spectra

Spectral recordings of catalase-peroxidase preparations were carried out by scanning between 700 and 250 nm using Gilford Response-I or Shimadzu UV 1601 UV-Vis spectrophotometer. All spectral measurements were carried out at room temperature in 100 mM phosphate buffer, pH 7.0. The molar absorptivity of catalase-peroxidase (143 mM⁻¹ cm⁻¹) at 280 nm was estimated according to the method of Gill and von Hippel

[156]. The heme concentration was estimated by the pyridine hemichrome assay [157]. Briefly, to ensure that all the heme iron was in its oxidized (ferric) state, 50 mM potassium ferricyanide was added to heme/hemoprotein in 20% pyridine/ 0.1M NaOH solution. Ferric solution was used for baseline. The heme iron was then reduced to its ferrous form by addition of sodium hydrosulfite (~5mg). A spectrum was then recorded from 560-530 nm. The maximum absorption difference from the spectrum (typically Abs at 555 nm – Abs at 540 nm) was divided by the appropriate molar absorptivity ($\Delta\epsilon$ 20.7 mM⁻¹ cm⁻¹) to calculate heme concentration. Ferri-cyano catalase-peroxidase was prepared by addition of 2 mM NaCN to ferric catalase-peroxidase. Ferrous catalase-peroxidase was obtained by addition of dithionite to ferric catalase-peroxidase. The so-called Reinheitszahl (RZ) values were calculated with ferric catalase-peroxidase. This entails measuring the ratio of absorbance due to the heme (408 nm) over that of the protein (280 nm).

Catalase and Peroxidase Activity

Catalase activity was evaluated by monitoring the decrease in H₂O₂ concentration with time at 240 nm. The molar absorptivity of H₂O₂ at 240 nm is 39.4 M⁻¹ cm⁻¹ [158]. Unless otherwise indicated, all assays were carried out at 23 °C in 100 mM phosphate buffer, pH 7.0. All activities were normalized on the basis of heme content as determined by the pyridine hemichrome assay [157].

Peroxidase activity was evaluated by monitoring the production of 2,2'-azino-bis(3-ethylbenzthiazoline-6-sulfonic acid) radical (ABTS^{•+}) over time at 417 nm. The peroxidase activity of catalase-peroxidases generates the one-electron oxidation product of ABTS (ABTS^{•+}) (Fig. 2.1). The molar absorptivity of ABTS^{•+} at 417 nm is 34.7 mM⁻¹cm⁻¹ [159]. All assays were carried out at 23 °C in 50 mM acetate buffer, pH 5.0.

pH-Dependence of Catalase-Peroxidase Activity

The pH profile for catalase activity of KatP was measured from pH 6.0 to 8.0 by the decrease in H₂O₂ concentration with time at 240 nm. The effect of pH on peroxidase activity for KatP was measured by monitoring the production of ABTS^{•+} over time at 417 nm between pH 4.0 and 6.0. All activities were normalized based upon heme content as determined by the pyridine hemichrome assay [157].

Transient-State Kinetics

All stopped-flow measurements were performed using an SX.18MV Rapid Reaction Analyzer from Applied Photophysics (Surrey, UK) in single-mixing mode. Full spectral recordings of ferric KatP reaction with peracetic acid or cyanide were obtained by diode array. Rate constants for either reaction were determined by single-wavelength

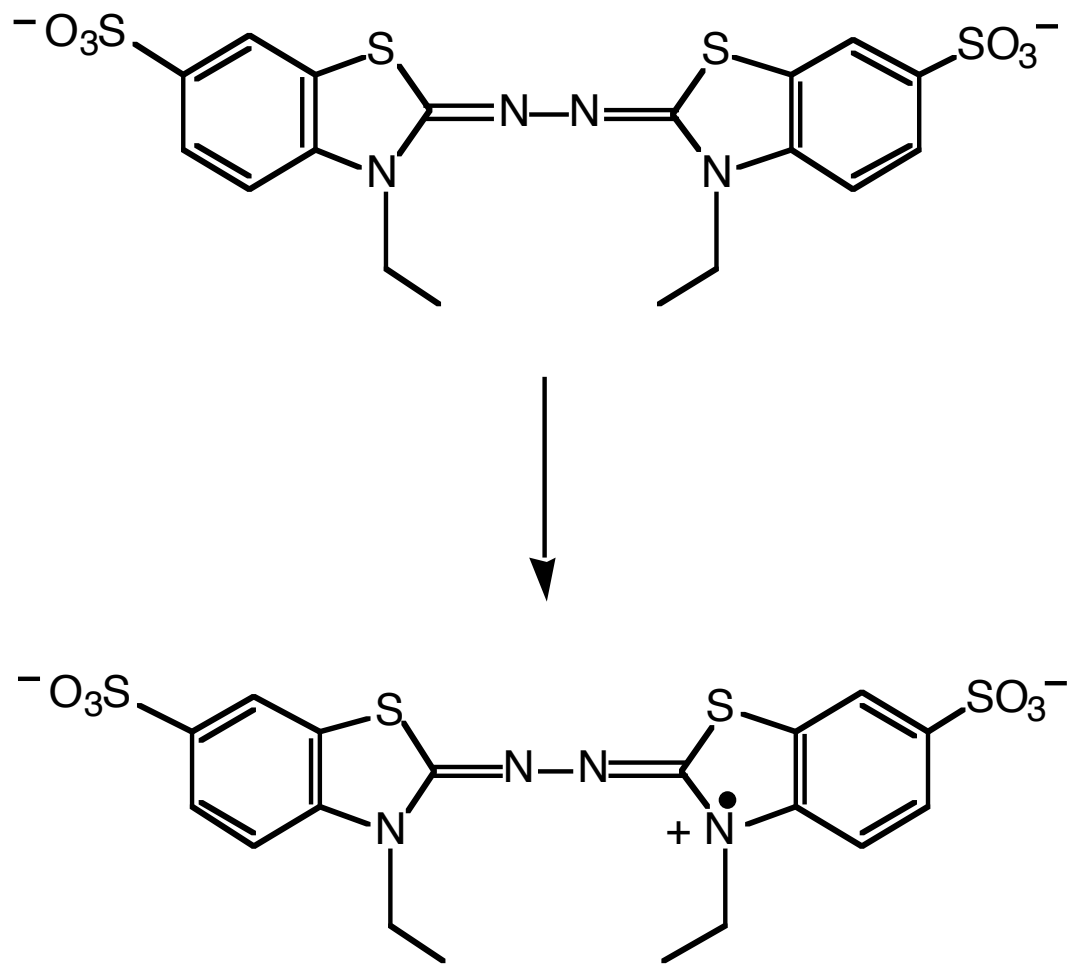


Figure 2.1. Oxidation of ABTS.

measurements at 403 nm. In either case, one syringe contained 2 μ M holo KatP as determined by heme content [2, 157]. The second syringe contained varying concentrations of peracetic acid or potassium cyanide. Reactions were carried out in 100 mM phosphate buffer, pH 7.0. The temperature for all reactions was maintained at 25 °C using a circulating water bath.

In Gel Digestion of KatG

Apo and holo KatG protein was separated using sodium dodecyl sulfate (SDS)-polyacrylamide gel electrophoresis (PAGE) with 7.6% (w/v) acrylamide gel. In gel digestion of protein was achieved by adapting methods described by Hellman and Rosenfeld [160, 161]. Protein was excised from the gel, and gel pieces were diced in a 1.7 μ l microfuge tube. To gel pieces, 200 μ l of 25mM NH_4HCO_3 / 50% acetonitrile was added and vortexed for 10 min to remove Coomassie stain from protein. This was repeated twice each time discarding the supernatant. Gel pieces were dried completely in a Savant SC110 Speed Vac. Trypsin (1 μ g) was added to gel pieces followed by incubation on ice to rehydrate. Trypsin is a serine protease, which cleaves peptide bonds on the carboxyl side of basic amino acid residues like lysine or arginine in proteins (Fig. 2.2). Trypsin was allowed to digest the protein in gel by incubating at 37 °C for 4- 8 hrs. Digested protein was then extracted from gel by adding 50% acetonitrile/ 5% formic acid and vortexing for 20-30min. This mixture was sonicated, and the process was repeated. Extracted digest volume was reduced to the appropriate volume (10-50 μ l).

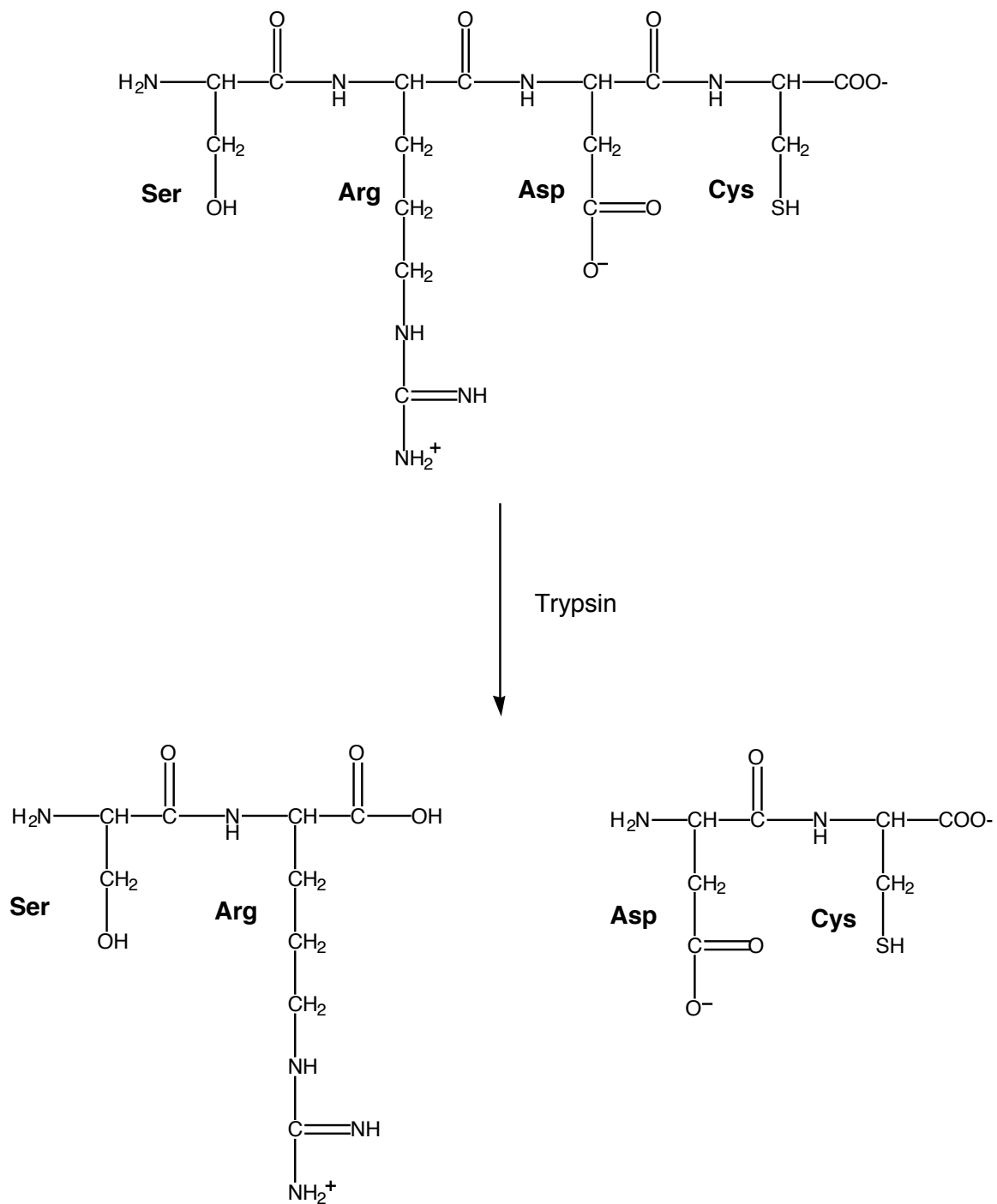


Figure 2.2. Trypsin digest of peptide bond in protein.

Digested samples were prepared for MALDI using 2, 5-dihydroxybenzoic acid (DHBA) as the matrix. For sample preparation, 1.0 μ l of digested solution was mixed with 1.0 μ l of matrix (160 mg/ml DHBA in water: acetonitrile 3:1, 2% formic acid). The samples (1 μ l) were loaded onto a Bruker stainless steel Micro SCOUT plate. Samples were air dried at room temperature.

Peptide Mass Identification Using MALDI-TOF MS

Mass spectrometric measurements of KatG after trypsin digestion were carried out on a Bruker Microflex Matrix-Assisted Laser Desorption-Ionization Time of Flight mass spectrometer (MALDI TOF-MS). The spectrometer was equipped with a microSCOUT ion source, a class III B ultraviolet laser, a 2-GHz digitizer, and a multichannel plate detector. Measurements were carried out in a positive ionization mode using a reflector voltage of 24 kV. Mass spectra were assembled as a sum of ion signals acquired from 50-100 laser pulses. Spectra were calibrated using Bruker peptide calibration standard as a reference. Peptide masses from mass spectra were searched against SwissPort 45.5 protein database.

Electron Paramagnetic Resonance Spectroscopy

EPR spectra of KatP were recorded on a Bruker EMX spectrometer equipped with an Oxford ESR 900 cryostat and ITC temperature controller. Spectrometer settings were as follows: temperature, 10 K; microwave frequency, 9.38 GHz; microwave power, 0.10 mW; receiver gain, 6.32×10^4 ; modulation frequency, 100 kHz; modulation amplitude, 10 G; conversion time, 163.84 ms; and time constant, 163.84 ms.

CHAPTER THREE

RESULTS

HPEX System

The pHPEX Plasmids

A low-copy number plasmid, pACYC184, was selected as the basis for the pHPEX constructs to avoid competition for replication machinery by the plasmids most commonly used for high-level protein expression. These expression plasmids often carry the Col E1 replicon; pACYC184 carries the p15A replicon. The plasmid pHPEX1 (Fig. 3.1 A) was constructed to contain the gene for a heme receptor (*chuA*). The *chuA* gene was inserted into pACYC184 between the *NcoI* and *EcoRI* restriction sites, effectively interrupting the chloramphenicol-resistance gene. The pHPEX1 plasmid imparts tetracycline resistance as do all of the pHPEX plasmids constructed to date. The pHPEX2 plasmid was constructed from pHPEX1 by the addition of the *lacUV5* promoter

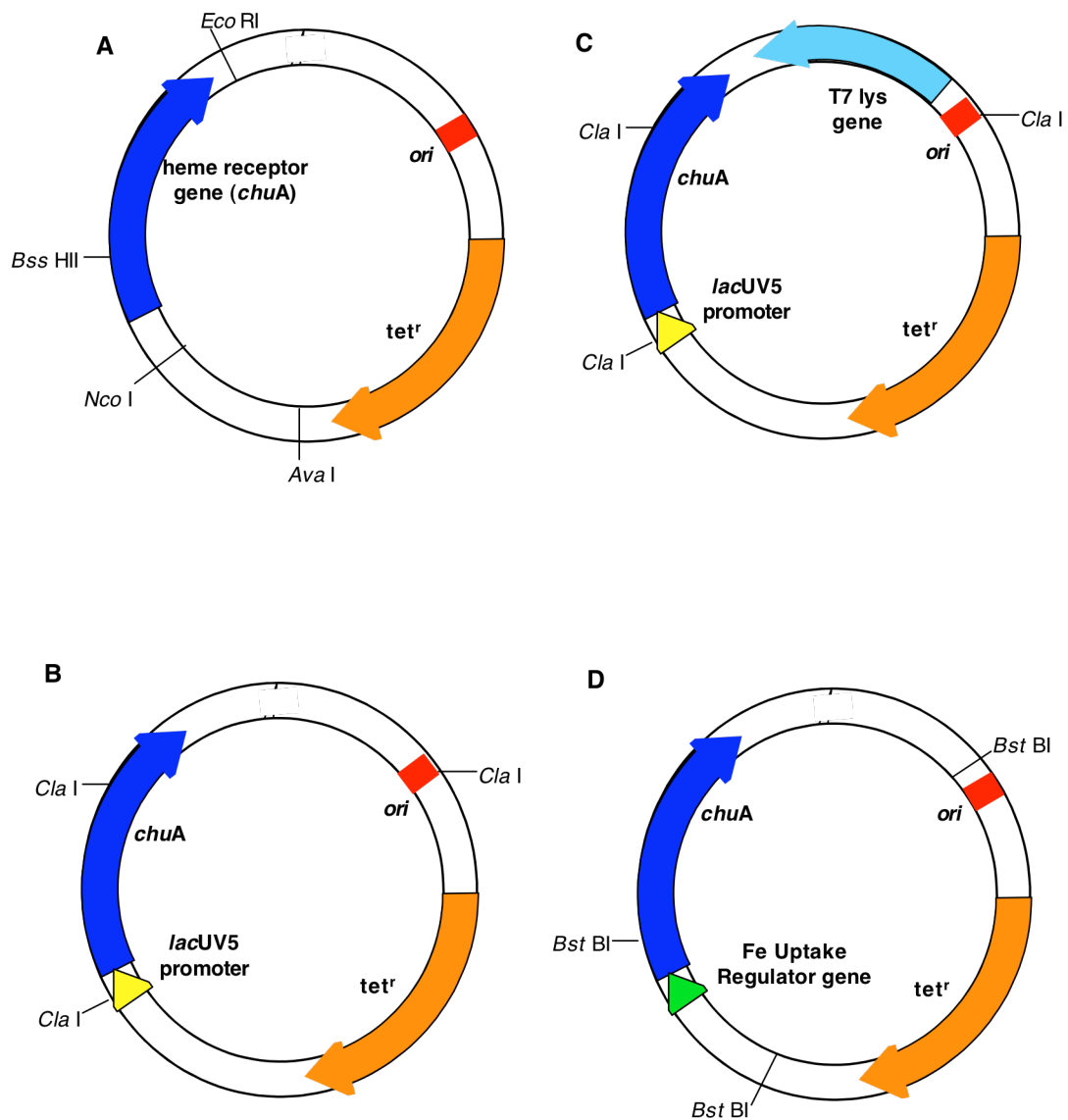


Figure 3.1. Schematic representation of the plasmids pHPEX1 (A), pHPEX2 (B), pHPEX3 (C), and pHPEX-fur (D).

upstream of *chuA* (Fig. 3.1 B), allowing for the control of *chuA* expression levels by the addition of lactose analogs (e.g., IPTG). The pHPEX3 plasmid (Fig. 3.1 C) was constructed by inserting the gene for T7 lysozyme into pHPEX2. The T7-based expression system, which uses T7 RNA polymerase to transcribe genes downstream of the T7 promoter, is commonly used to express recombinant proteins in *E. coli* [162]. The expression of a small amount of T7 lysozyme inhibits low levels of T7 RNA polymerase produced by leakage expression under the *lacUV5* promoter [162]. This prevents the premature expression of the target recombinant protein and is helpful for the T7 RNA polymerase-based expression of proteins otherwise toxic to *E. coli*.

The pHPEX-fur plasmid (Fig. 3.1 D) was also constructed from pHPEX1 by the addition of a iron uptake regulator sequence upstream of *chuA*. The *fur* box allows for the control of *chuA* expression by iron limitation. Diagnostic restriction endonuclease cleavage sites are denoted in the exterior of the plasmids (Fig. 3.1) as is the origin of replication (*ori*) and the position of the tetracycline resistance marker (*tet^r*). Diagnostic restriction digests and DNA sequence analysis confirmed the correct construction of all pHPEX plasmids. The plasmid pHPEX1 was digested with restriction endonuclease *Eco* RI/*Nco* I, *Eco* RI alone, and *Ava* I/*Bss* HII (Fig. 3.2 A). The plasmid pHPEX2 was digested with *Cla* I (Fig. 3.2 B). Plasmid pHPEX3 was digested with *Cla* I, *Ava* I/*Bss* HII, and *Eco* RI (Fig. 3.2 C). Plasmid pHPEX-fur was digested with *Bst* BI (Fig. 3.2 D).

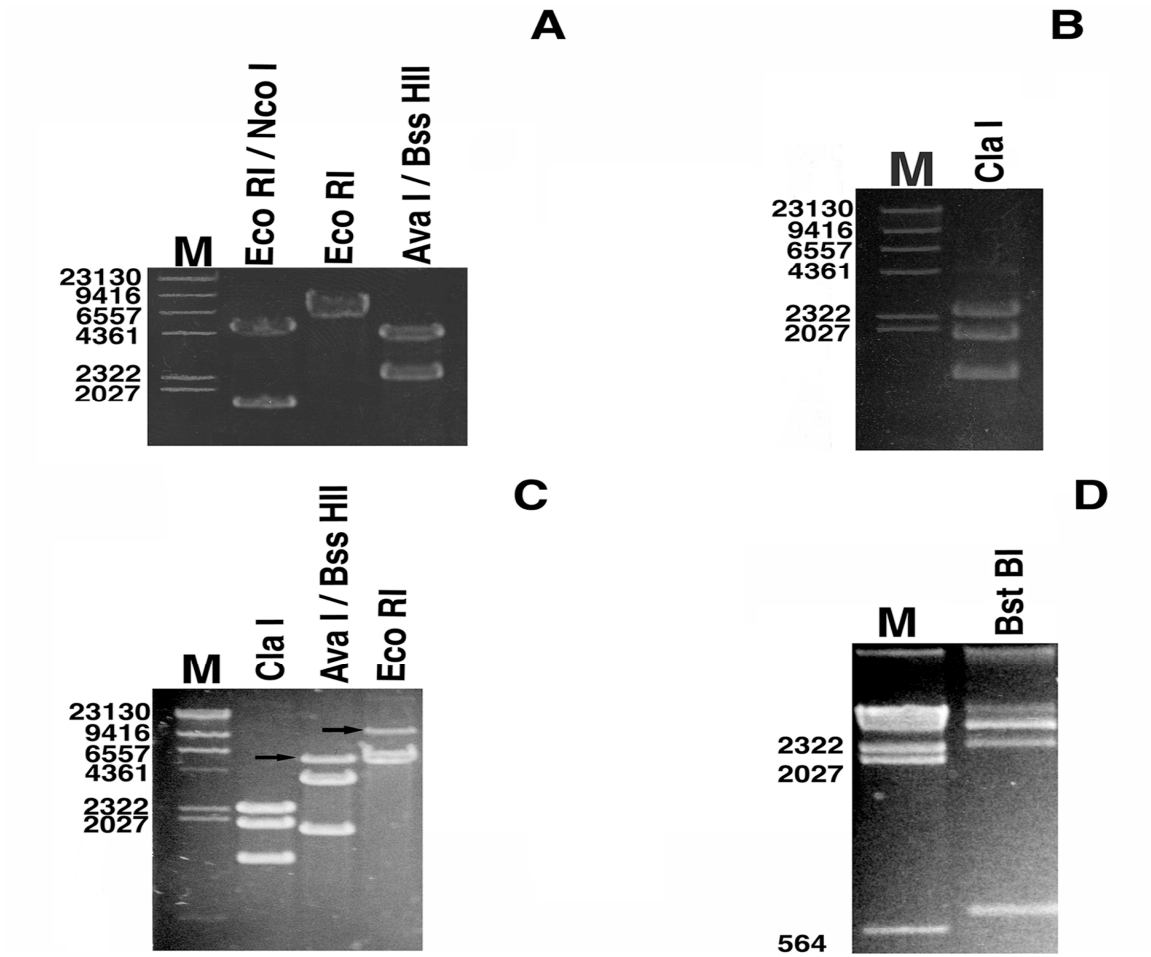


Figure 3.2. Diagnostic restriction digests of pHPEX1 (A), pHPEX2 (B), pHPEX3 (C), and pHPEX-fur (D). Incomplete plasmid digestion products denoted by arrows and marker denoted by M.

Production of ChuA by HPEX Cells

To verify that transformation with an HPEX plasmid led to synthesis of ChuA (the heme receptor), sodium dodecyl sulfate polyacrylamide gel electrophoresis (SDS-PAGE) was used to compare proteins produced by untransformed and pHPEX2-transformed BL-21 (DE3) cells under various culture conditions (Fig. 3.3). A protein corresponding to the monomeric molecular weight of ChuA in crude lysates of BL-21 (DE3) pHPEX2 cells grown in LB supplemented with 0.15 mM 2,2'-bipyridine and 8 μ M hemin was observed (Fig. 3.3, Lane 1). Modest increases in the intensity of this band were observed with the inclusion of IPTG in the culture medium (Fig. 3.3, Lane 2). Conversely, this protein was never detected in the cell lysates of untransformed BL-21 DE3 cells grown in LB supplemented with 0.15 mM 2,2'-bipyridine and 8 μ M hemin, regardless of the addition of 0.2 mM IPTG (Fig. 3.3, Lane 3 and 4).

Function of ChuA by HPEX Cells

To determine if the protein observed by SDS-PAGE was functional as a heme receptor, the abilities of untransformed and pHPEX2-transformed BL-21 (DE3) cells to grow in iron-deficient media supplemented with hemin were compared. BL-21 DE3 was unable to grow in iron-deficient media either in the presence or absence of added hemin (Fig. 3.4). Conversely, addition of hemin to iron-deficient BL-21 (DE3) pHPEX2 cultures resulted in a substantial increase in growth rate, demonstrating the expression

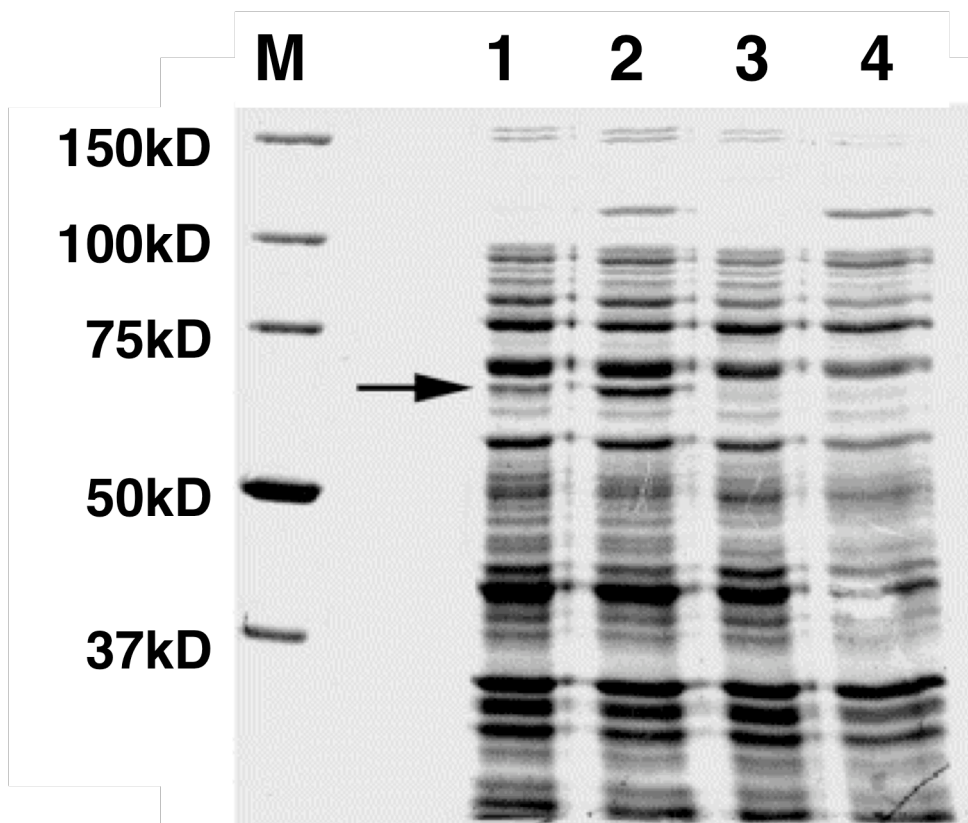


Figure. 3.3. Heme receptor expression by untransformed (lanes 3 and 4) and pHPEX2-transformed (lanes 1 and 2) *E. coli* BL-21 (DE3). Cultures were grown in the presence (lanes 2 and 4) and absence of IPTG (lanes 1 and 3).

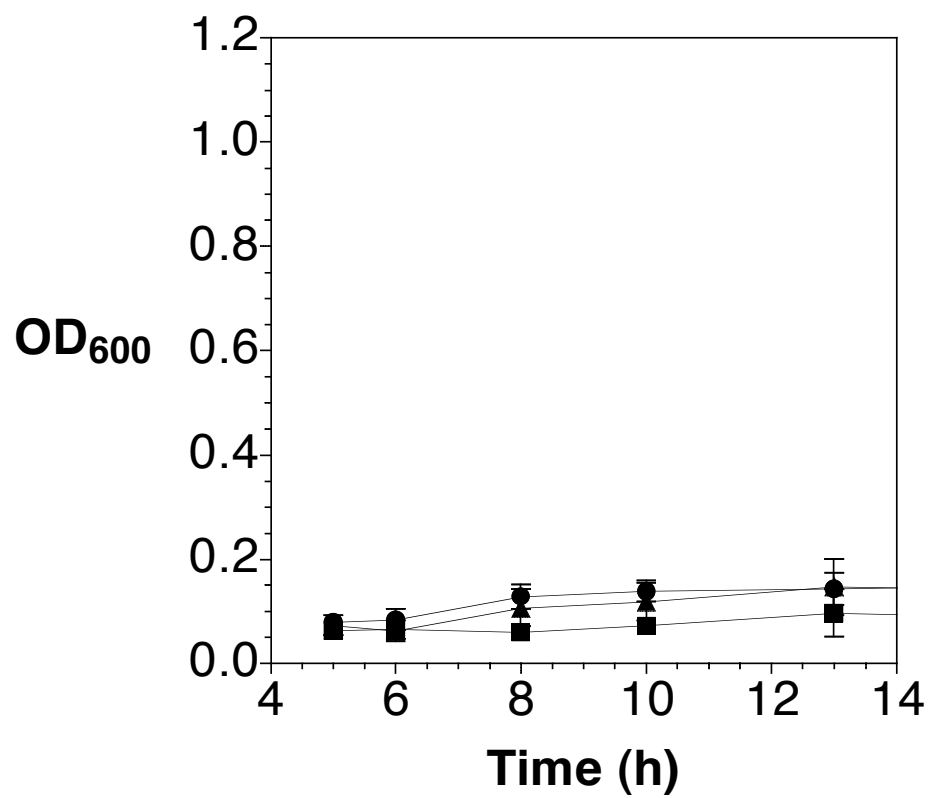


Figure 3.4. Growth of untransformed BL-21 (DE3) cells in minimal media supplemented with 2,2'-bipyridine alone (squares), 2,2'-bipyridine and hemin (circles), 2,2'-bipyridine, hemin, and IPTG (triangles).

of an active ChuA protein (Fig. 3.5). On the other hand, supplementing cultures of BL-21 (DE3) pHPEX2 with IPTG only resulted in slight increases in growth. The results of SDS-PAGE suggest that although addition of IPTG results in modest increases in expression of *chuA*, a substantial quantity of the heme receptor sufficient to support growth is produced in the absence of added inducing agents.

Effect of HPEX System on KatG

In order to evaluate if heme internalized using *chuA* was incorporated into a target recombinant protein, KatG a heme dependent catalase-peroxidase was expressed using the HPEX system. KatG expressed with BL-21 (DE3) pHPEX3 showed a large increase in heme content when heme was added to the medium compared to cultures where heme was withheld from the media as evaluated by UV-Visible absorption spectra (Fig. 3.6). KatG expressed with BL-21 (DE3) pLysS resulted in only a minor increase in heme incorporated (Fig. 3.7).

The effect of expression strain and culture conditions on the catalase activity of isolated KatG was also evaluated. Consistent with the UV-Visible spectra, the highest activity was observed with protein isolated from BL-21 (DE3) pHPEX3 cells where heme was added to culture at the time of induction (Fig. 3.8). Very little activity was observed for KatG isolated from these cells if heme was not added. For KatG isolated from BL-21 (DE3) pLysS, addition of heme at time of induction did result in a modest increase in the active of KatG (Fig. 3.8) commensurate with the observed increase in

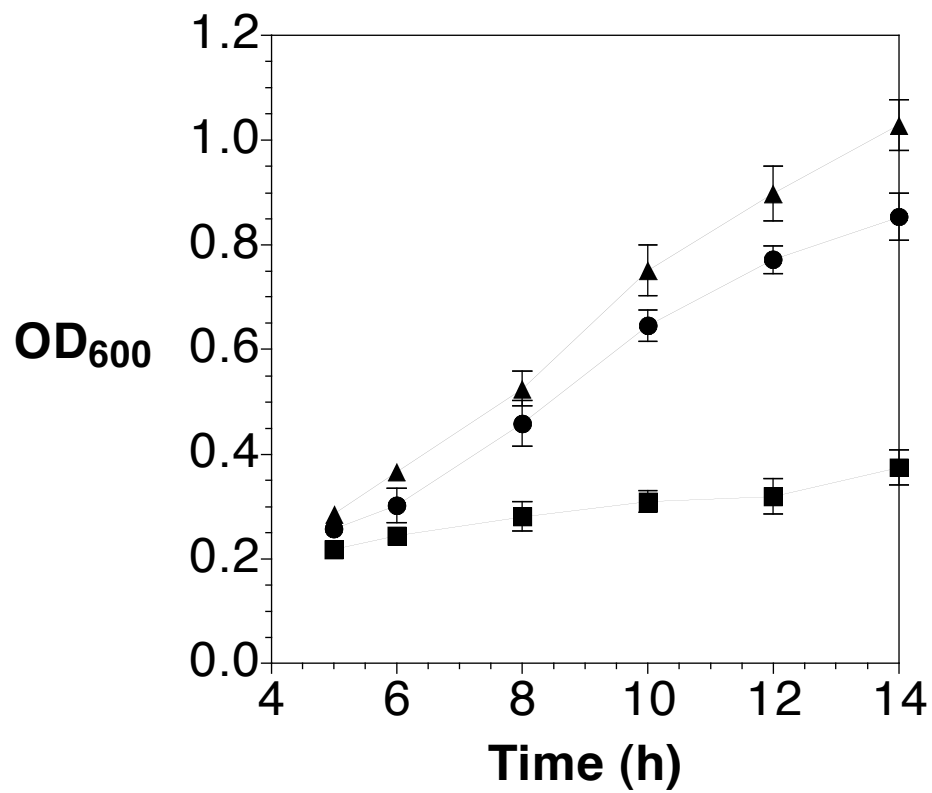


Figure 3.5. Growth of pHPEX2-transformed BL-21 (DE3) cells in minimal media supplemented with 2,2'-bipyridine alone (squares), 2,2'-bipyridine and hemin (circles), 2,2'-bipyridine, hemin, and IPTG (triangles).

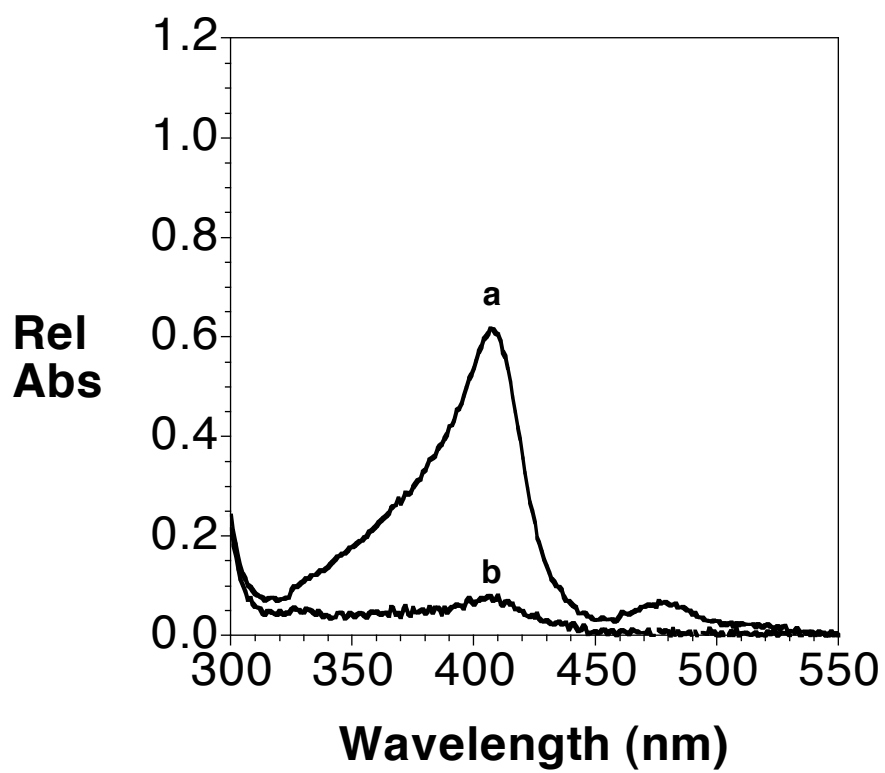


Figure 3.6. UV-Visible absorption spectra of catalase-peroxidase expressed in pHPEX3-transformed cells. Cultures were grown in the presence (a) and absence (b) of hemin.

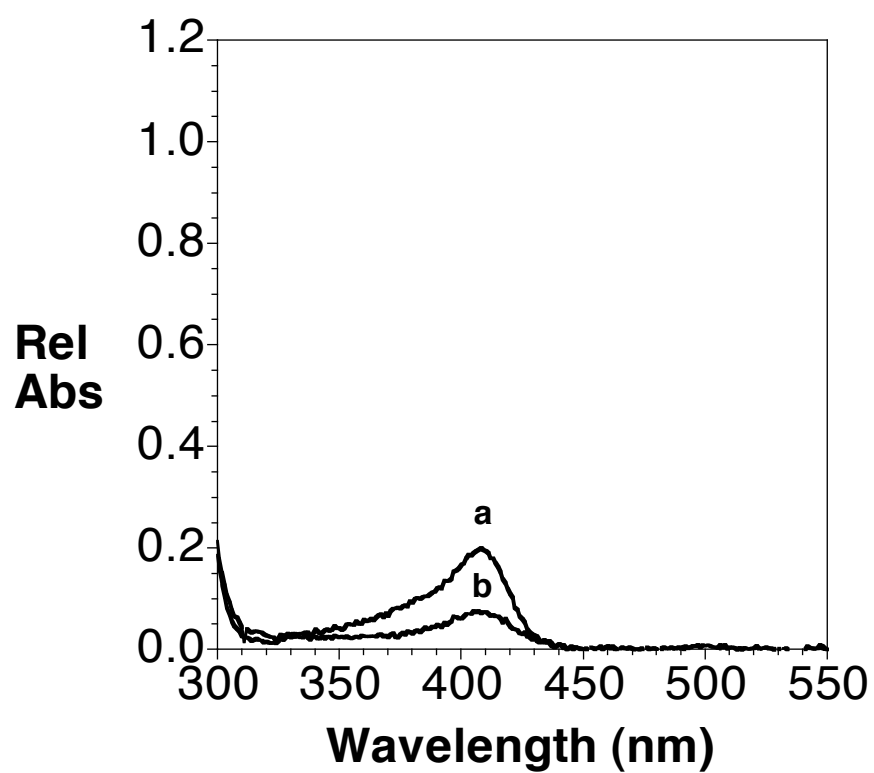


Figure 3.7. UV-Visible absorption spectra of catalase-peroxidase expressed in pLysS-transformed cells. Cultures were grown in the presence (a) and absence (b) of hemin.

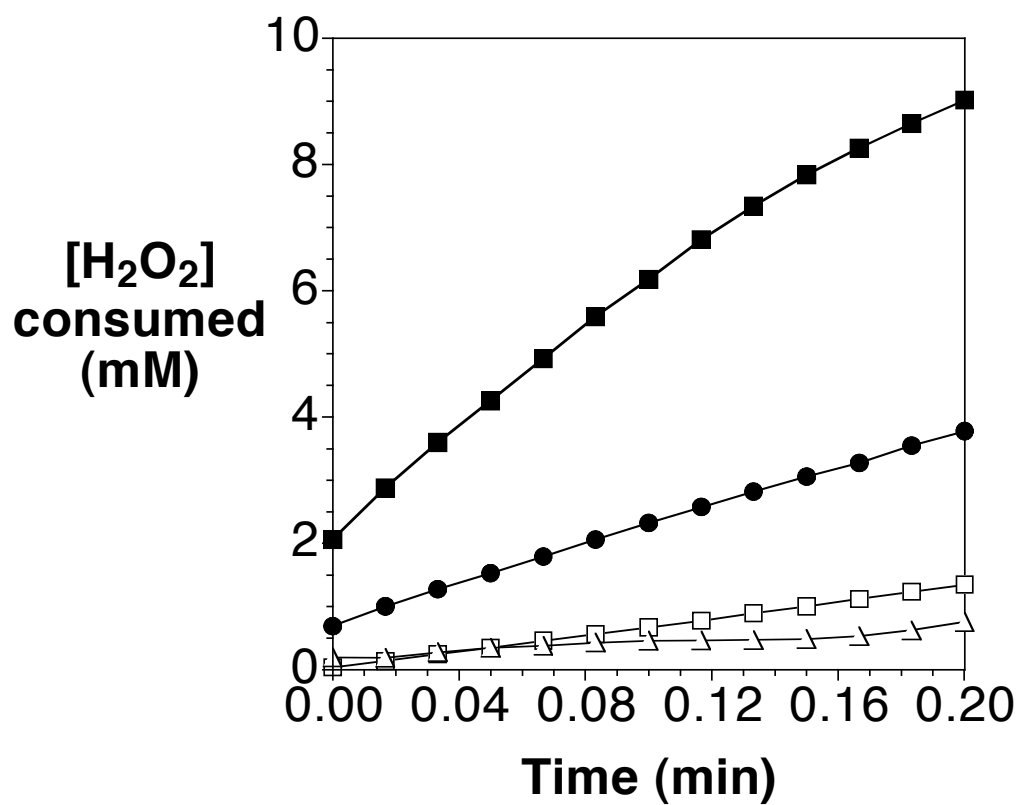


Figure 3.8. Catalase activity of KatG expressed in pLysS- (circles) and pHPEX3-transformed (squares) cells. Cells were grown in the presence (closed symbols) and absence (open symbols) of hemin.

heme content (Fig. 3.7). Without added hemin, very little catalase activity was detected regardless of the strain used for KatG expression.

KatG showed similar k_{cat} values when expressed with both pHPEX3 and pLysS. Likewise, the K_M was comparable for both (Table 3.1). Heme absorption spectra at different iron states was examined to identify differences in KatG expressed with pHPEX3 versus pLysS (Table 3.2). Only very minor differences in absorption characteristics were identified. Similarly, difference spectra (ferric minus ferri-cyano) for KatG from the two expression systems were virtually superimposable (Fig. 3.9). These comparisons were done on a *per-heme* basis to ensure that hemin supplementation produced KatG with the same properties as those obtained when heme was synthesized *de novo* by the expression strain.

Expression of Recombinant Myoglobin using the HPEX System.

Sperm whale myoglobin was expressed with the HPEX system to evaluate the ability of the system for enhancing expression of other recombinant hemoproteins in their holo form. UV-visible absorption spectra for expressed myoglobin with the HPEX system showed a large holomyoglobin as determined from lysed cells (Fig.3.10). In order to insure the heme content was a result of heme incorporation during expression and not adventitious uptake after cells were lysed in the presence of excess heme, UV-visible absorption spectra of whole cells containing expressed myoglobin were performed. Derivatives of the raw UV-visible absorption spectra were performed to

Culture condition	K_M (mM)	k_{cat}/K_M ($M^{-1} s^{-1}$)	Sp. Act. (U/mg)
pHPEX (+ hemin)	6.8	2.6×10^6	2560
pLysS (no hemin)	7.0	2.2×10^6	422

Table 3.1. Catalase kinetic parameters for recombinant KatG from hemin-supplemented cultures of BL-21 (DE3) pHPEX3 and unsupplemented cultures of BL-21 (DE3) pLysS.

Heme State	Cell type	Absorption band maxima (nm)				
		Soret	β	α	CT2	CT1
Ferric	pHPEX	406	—	—	497	640
	pLysS	406	—	—	497	637
Ferric-CN	pHPEX	424	542	—	—	—
	pLysS	424	540	—	—	—
Ferrous	pHPEX	440	560	590	—	—
	pLysS	440	559	590	—	—

Table 3.2. Heme absorption maxima for recombinant KatG from pHPEX3- and pLysS-transformed *E. coli* BL-21 (DE3).

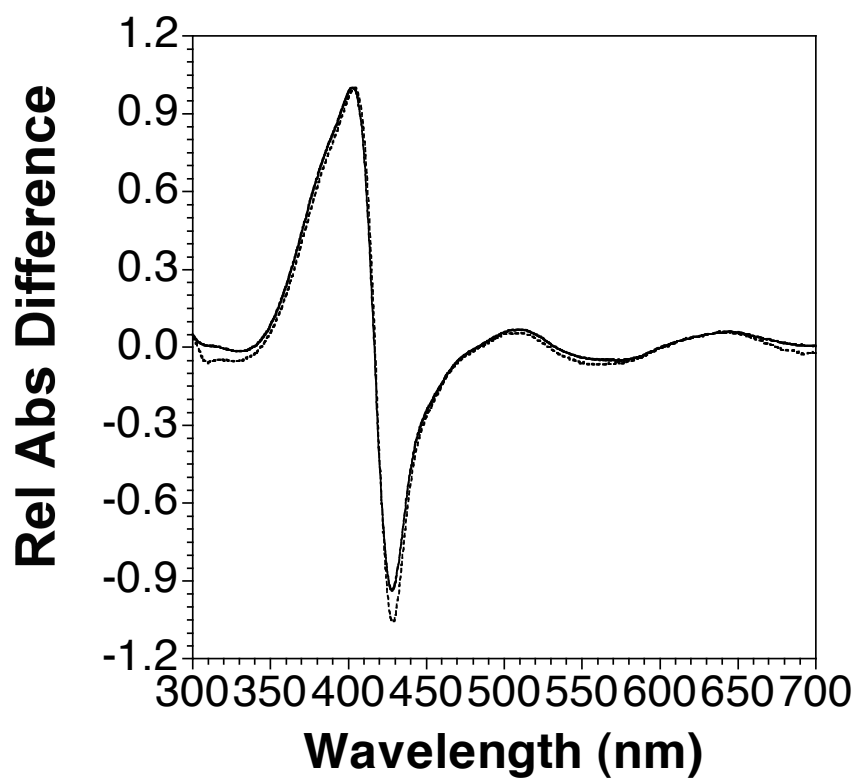


Figure 3.9. Ferric minus ferri-cyano difference spectra for recombinant KatG expressed in pHPEX3- (solid line) and pLysS- (dashed line) transformed systems.

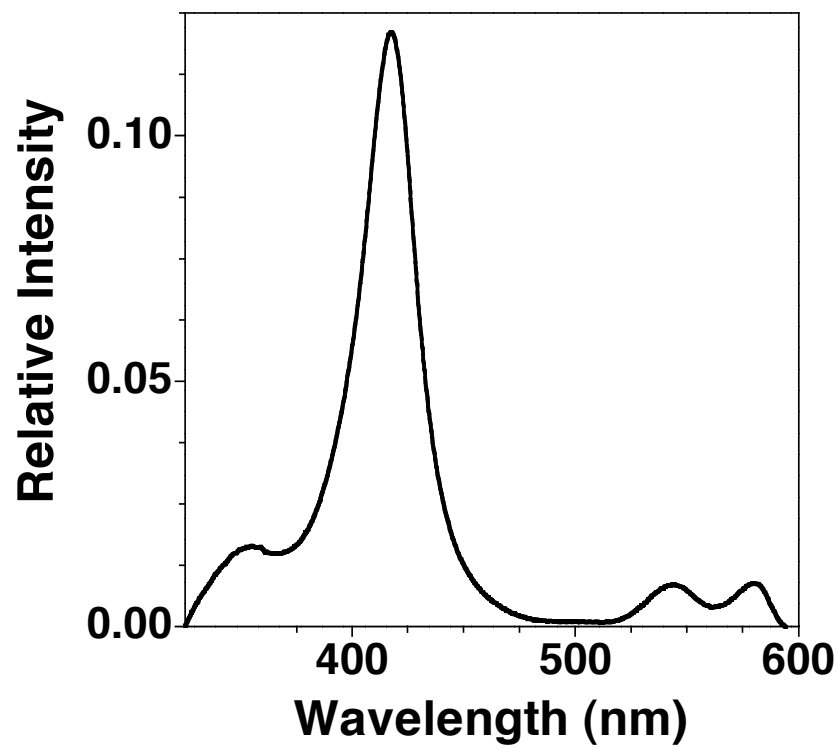


Figure 3.10. UV-Visible absorption spectra for myoglobin expressed in pHPEX3-transformed cells (following lysis).

accent the signals due to holomyoglobin. Myoglobin expressed with BL-21 (DE3) pHPEX3 induced with IPTG showed a strong signal corresponding to holo myoglobin provided that hemin was added to culture medium. If hemin was withheld from the media a much weaker signal was observed (Fig. 3.11). Myoglobin expressed in BL-21 (DE3) pLysS generated little or no holomyoglobin even when hemin was added (Fig. 3.12).

Likewise, the expression of holomyoglobin was enhanced in BL-21 (DE3) pHPEX-fur cells in comparison to a standard *E. coli* expression strain [BL-21 (DE3)] (Fig. 3.13 and Fig. 3.14). Using dipyriddy, to simulate iron-limitation conditions and induce *chuA* expression, and using IPTG to induce expression of myoglobin, the pHPEX-fur-transformed cells showed a strong derivative spectrum corresponding to holo myoglobin when hemin was present in the growth medium. When hemin was excluded from the growth medium, a much weaker derivative spectrum corresponding to holo myoglobin was observed. To insure that the heme signal resulted only from heme incorporated into Mb, spectra of non-induced cultures with hemin added were also compared for each cell line.

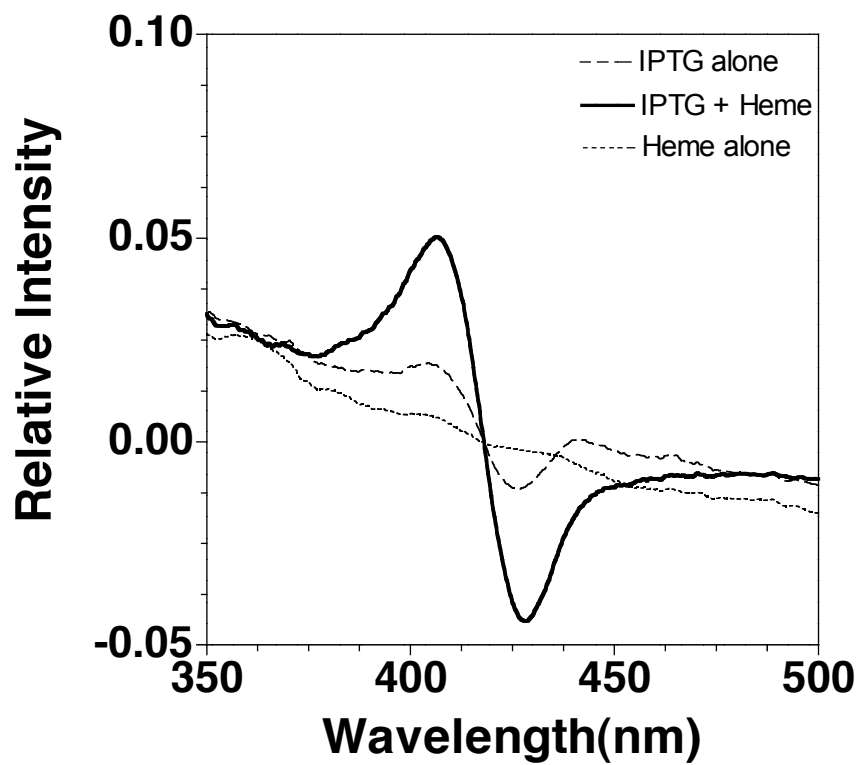


Figure 3.11. Derivative UV-Visible absorption spectra for myoglobin expressed in pHPEX3-transformed cells (whole cells).

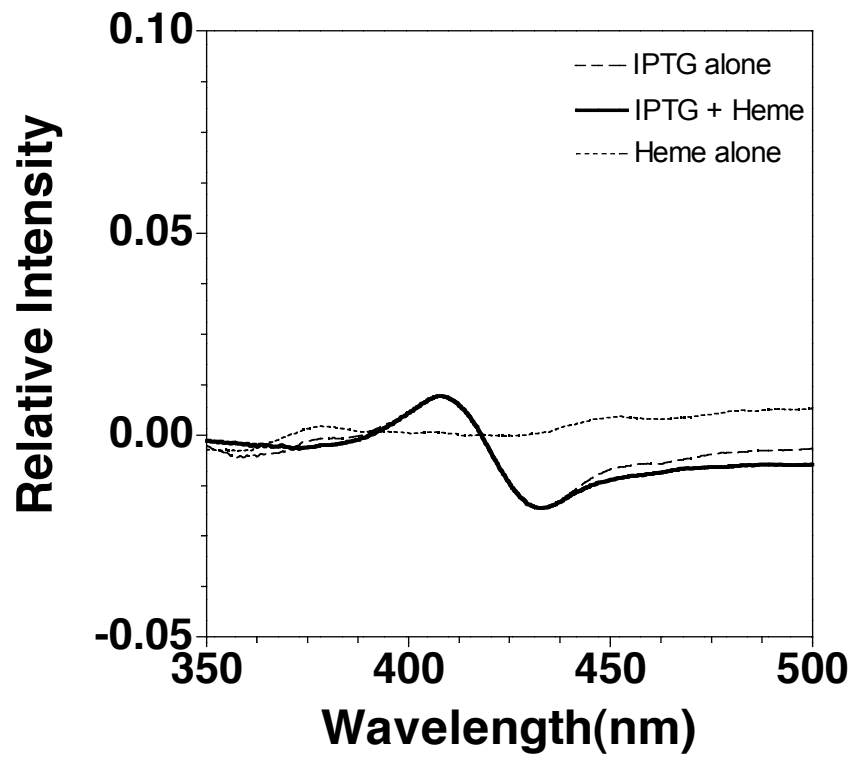


Figure 3.12. Derivative UV-Visible absorption spectra for myoglobin expressed in pLysS-transformed cells (whole cells).

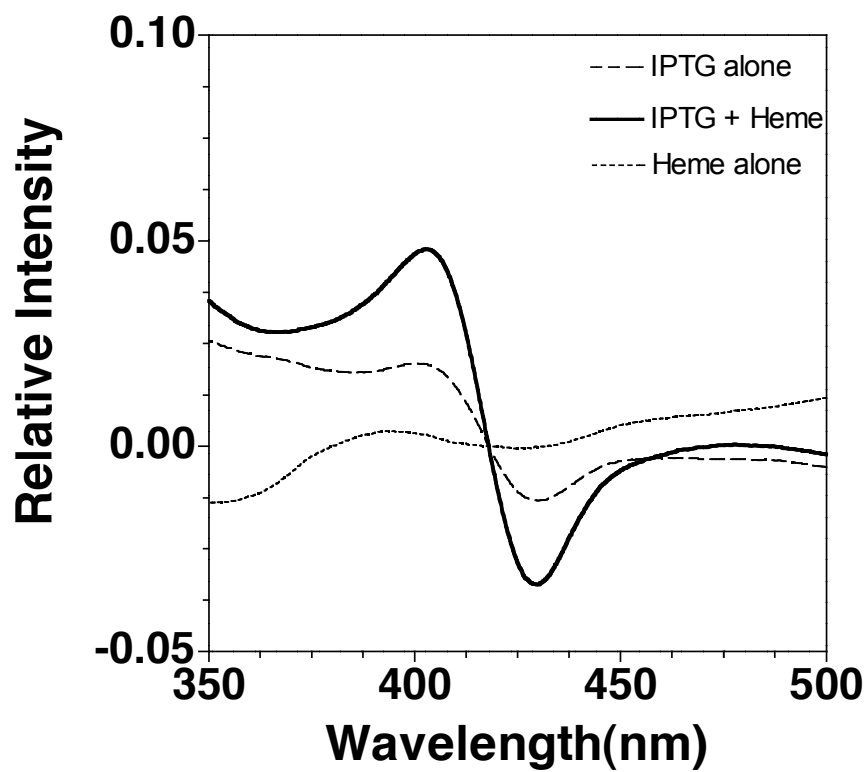


Figure 3.13. Derivative UV-Visible absorption spectra for myoglobin expressed in pHPEX-fur-transformed cells (whole cells).

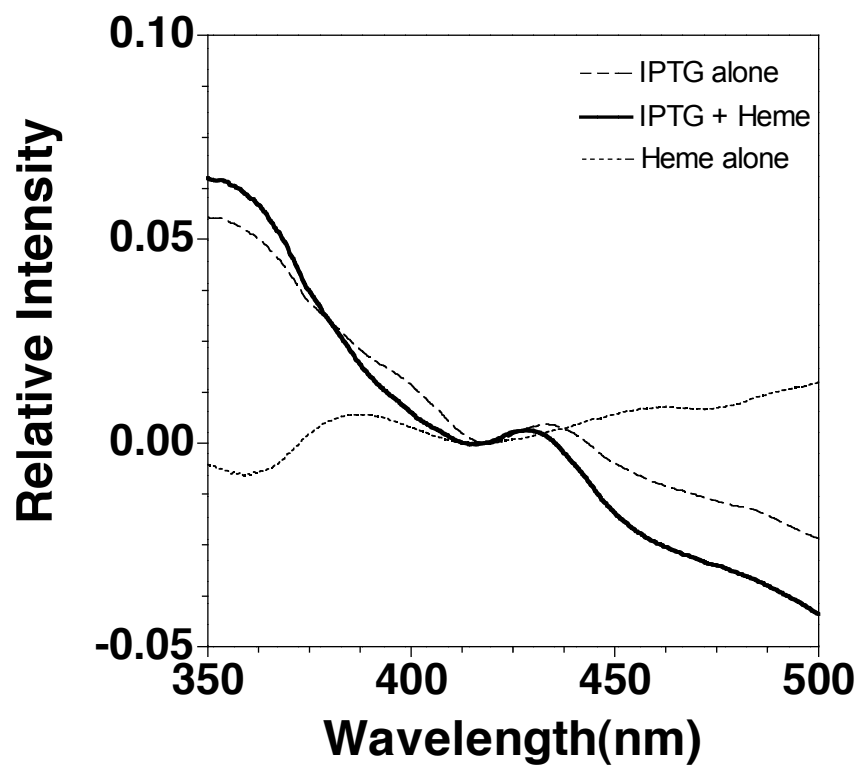


Figure 3.14. Derivative UV-Visible absorption spectra for myoglobin expressed in BL-21(DE3)-transformed cells (whole cells).

KatP

Expression and Purification of KatP

The *katP* gene was cloned into the pET20b(+) vector to produce the pKatP3 expression plasmid, and an *E. coli* expression strain (BL-21 DE3 pLysS) was transformed with the construct as described in Methods. Addition of IPTG to these cells at mid-log phase resulted in the production of a protein at high levels corresponding to the expected molecular weight of mature KatP (Fig. 3.15). However, the expression of another protein was also observed at comparable levels, and the apparent difference in molecular weight between the two was about 3 kDa. Both expression products co-purified when nickel affinity procedures were used, suggesting that both represented some form of recombinant KatP (Fig. 3.15 B, Lane 1). This was confirmed by tryptic digests and mass spectrometric analysis of each band from SDS-PAGE. Each band was determined to be a single protein and each one was identified as KatP.

These initial purification products were subjected to anion exchange FPLC. Catalase activity measurements, UV-Vis absorption spectra, and SDS-PAGE analysis of the fractions from FPLC revealed that heme and catalase activities were associated with the protein of lower apparent molecular weight (Fig. 3.15 B). The complete isolation of KatP corresponding to the lower band was also accomplished using phenyl-Sepharose-based chromatography (Fig.3.15 B, Lane 2).

Our analysis of the amino acid sequence of KatP by SignalP 2.0 and that of another group using a different program suggested the presence of an N-terminal

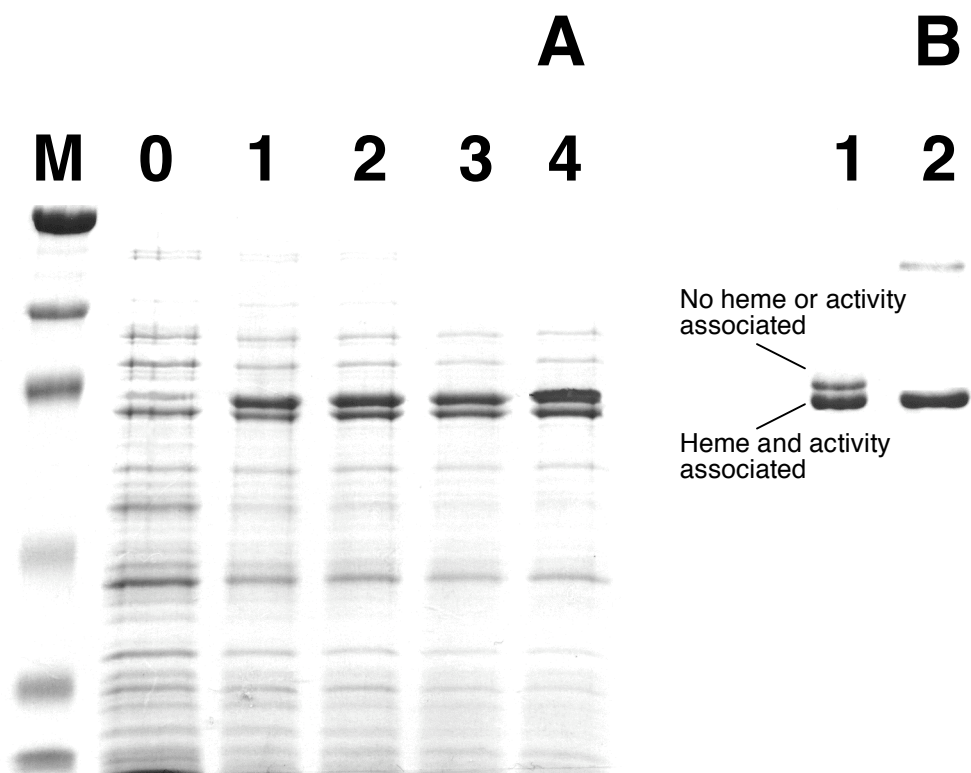


Figure 3.15. SDS-PAGE electrophoretic separation of total cellular protein (A) from BL-21 (DE3)pLysS transformed pKatP3 at time of induction with 1 mM IPTG (lane 0), 1 h post-induction (lane 1), 2 h post-induction (lane 2), 3 h post-induction (lane 3), and 4 h post-induction (lane 4). (B) Purification of KatP by Ni-NTA chromatography (lane 1) and phenyl-Sepharose chromatography (lane 2).

sequence targeting KatP to the periplasmic space [24, 163]. The point of cleavage for the N-terminal signal peptide was predicted to be between residues 23 and 24. N-terminal peptide sequence analysis of our FPLC-isolated KatP was A₂₄D₂₅K₂₆K₂₇E₂₈T₂₉Q₃₀N₃₁F₃₂Y₃₃Y₃₄P₃₅E₃₆T₃₇L₃₈, demonstrating that the signal peptide was cleaved as predicted.

Spectroscopic and Kinetic properties of KatP vs KatG

Absorption spectra recorded for KatP revealed an RZ value of 0.67, consistent with the high aromatic amino acid content of the enzyme. The spectrum for ferric KatP showed a Soret band at 406 nm along with charge transfer transitions at 502 nm and 629 nm indicating a mixture of pentacoordinate and hexacoordinate high-spin heme iron (Fig. 3.16 and 3.17). There was also evidence of minute quantities of hexacoordinate low-spin heme in ferric KatP indicated by a small shoulder at 540 nm. The spectrum for ferrous KatP (Fig. 3.16 and 3.17) suggested predominantly pentacoordinate high-spin heme iron with a Soret band at 439 nm and a β - and α -band at 561 and 581 respectively. Comparisons of the absorption maxima with those of the intracellular *E. coli* catalase–peroxidase (KatG) reveal that the heme environments of the two enzymes are highly similar (Table 3.3). These results and those of others show that *E. coli* KatG has spectral characteristics that are highly similar to those of *Mycobacterium tuberculosis* KatG [37, 164, 165], and *M. tuberculosis* KatG contains a large proportion of hexacoordinate high-spin heme following purification and storage [165].

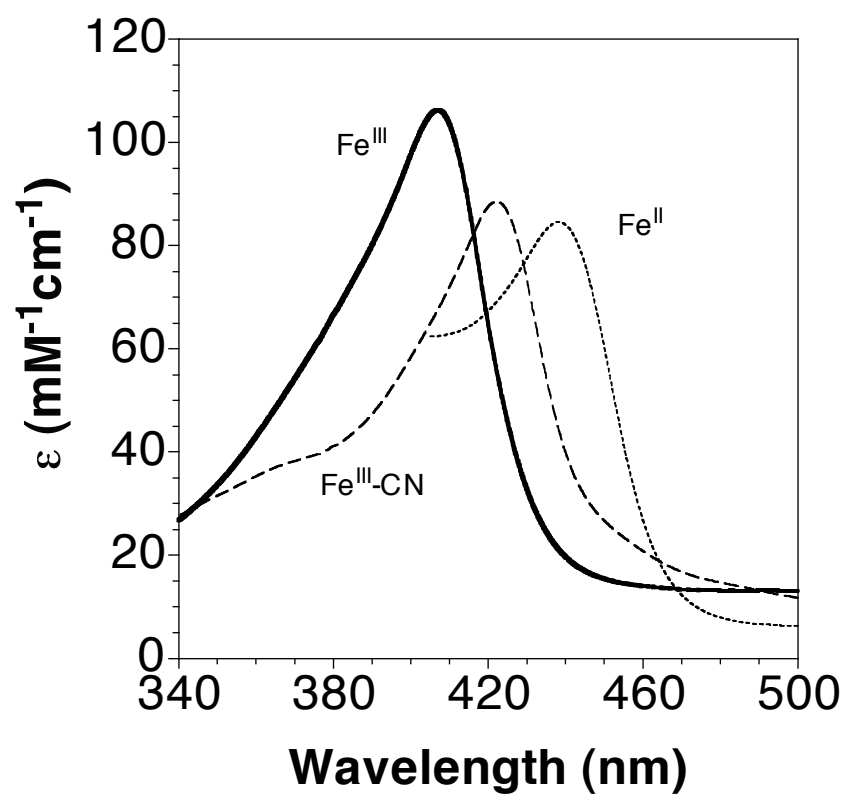


Figure 3.16. Heme absorption spectra for the Soret band of ferric, ferri-cyano, and ferrous forms of KatP.

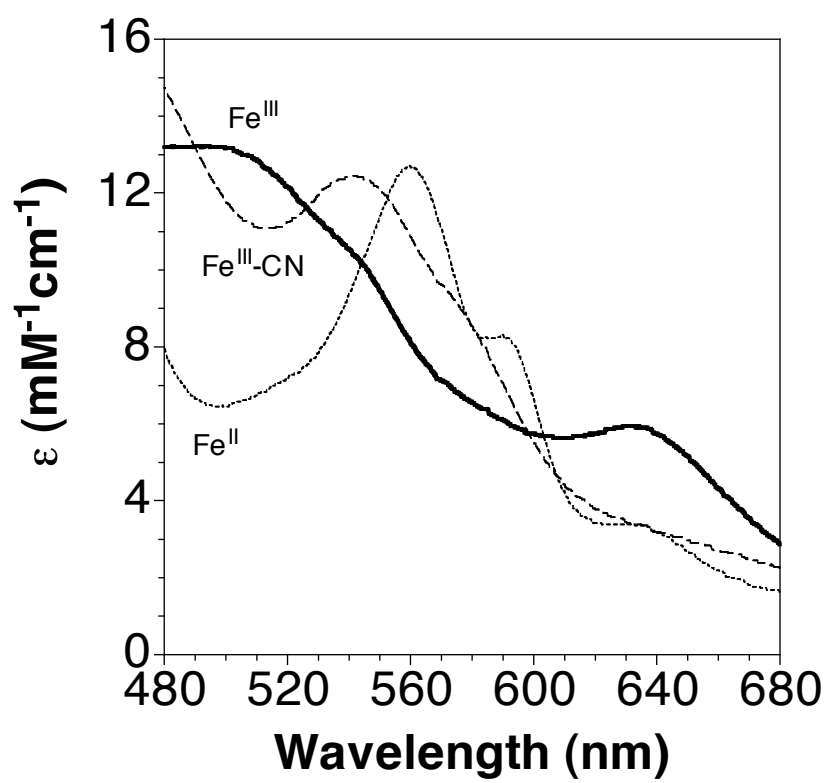


Figure 3.17. Heme absorption spectra for ferric, ferri-cyano, and ferrous forms of KatP (480-680 nm).

Heme State	Protein	Absorption Band Maxima (nm)				
		Soret	β	α	CT2	CT1
Fe ^{III}	KatG	408	–	–	502	629
	KatP	406	–	–	495	634
Fe ^{II} -CN	KatG	423	542	–	N	N
	KatP	422	543	–	N	N
Fe ^{II}	KatG	439	561	581	–	–
	KatP	438	560	590	–	–

Table 3.3. Heme Absorption Maxima for KatP and KatG. Absorption bands that were too weak to make unequivocal assignments of wavelength maxima are indicated by a dash. Transitions that were not expected for a particular species are indicated by N.

The EPR spectrum of KatP is consistent with other catalase-peroxidases in many, but not all, respects [116]. An axial signal [$g = 5.94$ ($A \perp$) and 1.99 ($A \parallel$)] dominates the spectrum of KatP. The very weak rhombic signal [$g = 6.6, 5.06, \text{ and } 1.95$] is also evident (Fig. 3.18). These signals correspond to hexacoordinate and pentacoordinate high-spin hemes, respectively. A spectrum of KatG (intracellular catalase-peroxidase) is also shown for comparison. A larger contribution from rhombic signal in this protein suggests that KatP has a larger proportion of heme in the hexacoordinate high-spin state than other catalase-peroxidases. However, it is important to bear in mind that the presence or absence of the sixth ligand (likely H_2O) is highly sensitive to minute changes in conditions and storage time [166].

KatP showed strong catalase activity consistent with its intracellular relative, *E. coli* KatG (Fig. 3.19). The k_{cat} determined for KatP was modestly higher than that determined for KatG (Table 3.4). However, the apparent K_M for H_2O_2 was considerably higher for KatP than that for KatG (Table 3.4). This contributed to an apparent second-order rate constant for the catalase activity of KatP ($6.4 \times 10^5 \text{ M}^{-1} \text{ s}^{-1}$) that was fivefold lower than KatG ($3.5 \times 10^6 \text{ M}^{-1} \text{ s}^{-1}$).

The peroxidase activities of KatP and KatG were also compared (Fig. 3.20). The apparent k_{cat} value with respect to H_2O_2 for KatP-catalyzed ABTS oxidation was comparable to that observed for KatG (Table 3.4). The peroxidase activity of KatP gave an apparent K_M with respect to H_2O_2 that was threefold higher than that determined for KatG (Table 3.4). The apparent second-order rate constant for the peroxidase activity was about threefold lower for KatP ($2.6 \times 10^4 \text{ M}^{-1} \text{ s}^{-1}$) than for KatG ($7.1 \times 10^4 \text{ M}^{-1} \text{ s}^{-1}$).

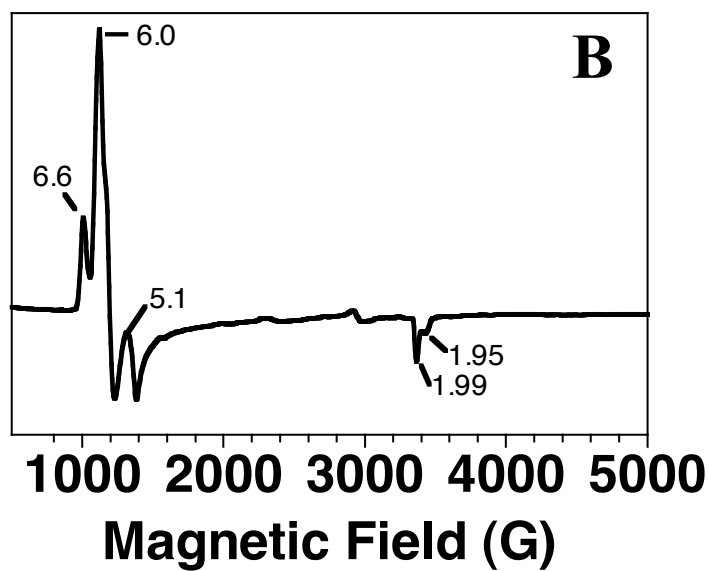
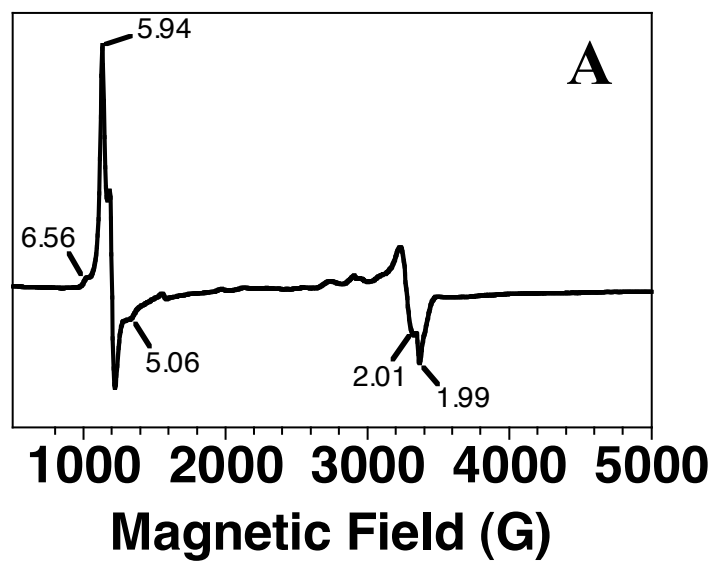


Figure 3.18. EPR Spectrum of ferric KatP (A) and ferric KatG (B).

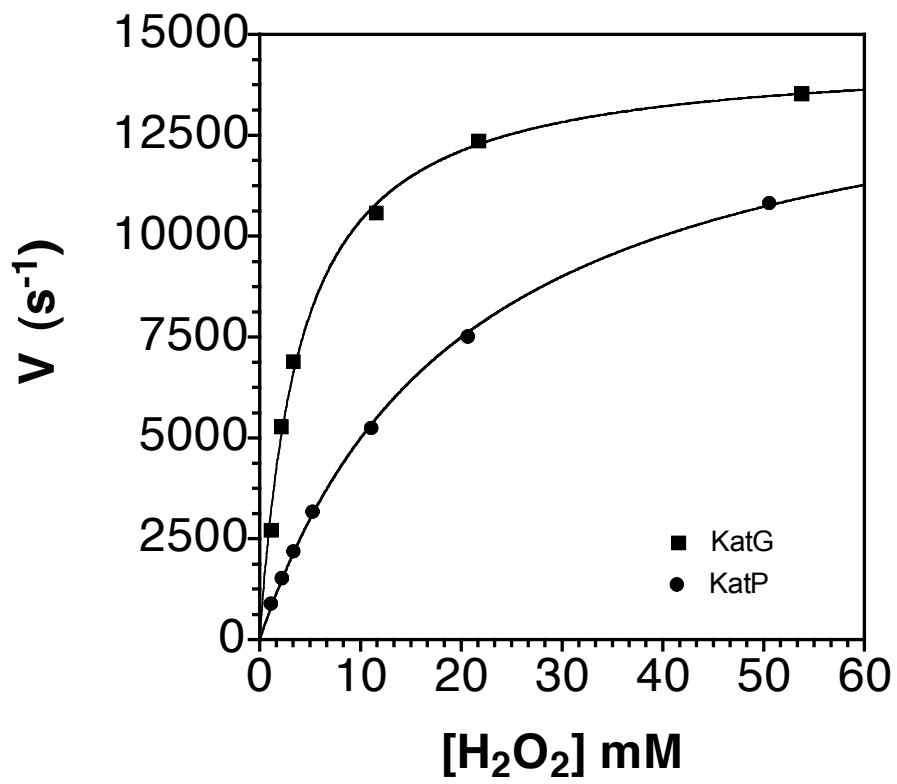


Figure 3.19. Effect of H₂O₂ Concentration on the Catalase Activity of KatG and KatP.

Reaction	Parameter	Enzyme	
		KatG	KatP
Catalase	k_{cat} (s^{-1})	1.4×10^4	1.8×10^4
	K_{M} (mM)	4	27
	K_{app} ($\text{M}^{-1} \text{s}^{-1}$)	3.5×10^6	6.4×10^5
Peroxidase	k_{cat} (s^{-1})	58	77
	K_{M} (mM)	0.83	3.0
	K_{app} ($\text{M}^{-1} \text{s}^{-1}$)	7.1×10^4	2.6×10^4

Table 3.4. Kinetic Parameters for the Catalase and Peroxidase Activities of KatG and KatP

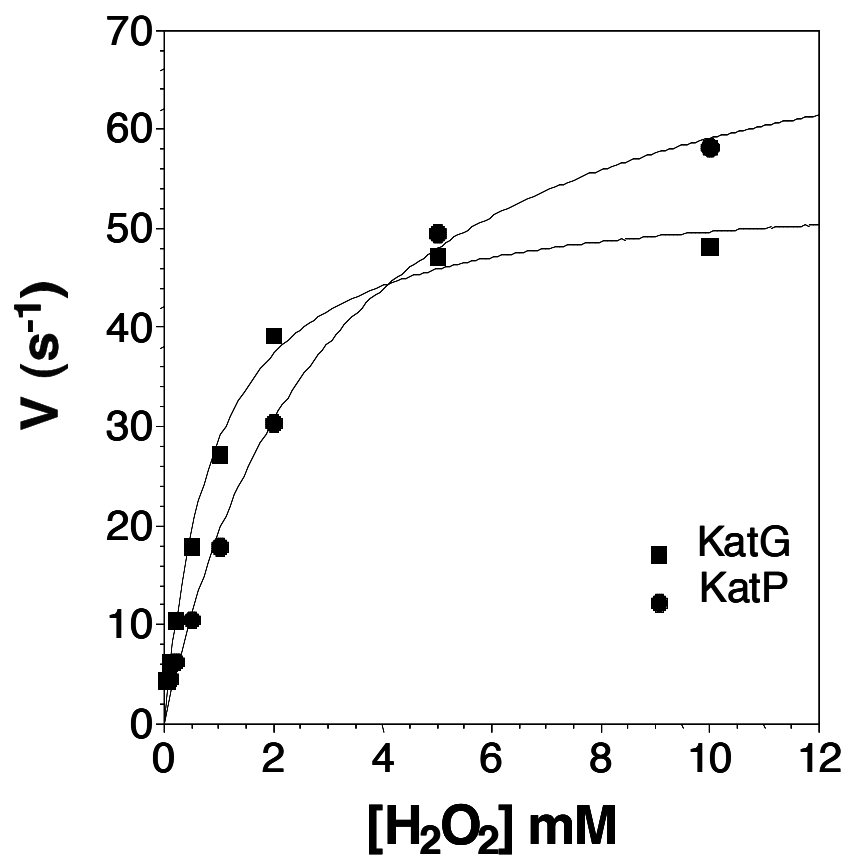


Figure 3.20. Effect of H_2O_2 Concentration on the Peroxidase Activity of KatG and KatP.

Both the catalase and peroxidase activities of KatP showed a sharp pH dependence that is consistent with the family of catalase-peroxidases. Maximal peroxidase activity was observed at a pH of ~ 4.7 and maximal catalase activity was observed at a pH of ~ 7.2 (Fig. 3.21).

Because of the rapid reaction of catalase–peroxidase compound I with H_2O_2 , other hydroperoxides (e.g., peracetic acid) must be used to monitor compound I formation in transient-state kinetic studies (Fig. 3.22). Heme absorption spectral changes were monitored from the reaction between ferric KatP and peracetic acid by a decrease in absorbance at 403 nm and were consistent with the formation of a compound I-like intermediate (Fig. 3.23). Increases in peracetic acid concentration, produced a linear increase in k_{obs} for compound I formation (Fig. 3.24). The apparent second-order rate constant for the reaction was $8.8 \times 10^3 \text{ M}^{-1} \text{ s}^{-1}$. By comparison, the rate constant for the same reaction for KatG from *Synechocystis* PCC 6803 is $3.9 \times 10^4 \text{ M}^{-1} \text{ s}^{-1}$ [35] while that measured for KatG from *M. tuberculosis* is $\sim 6 \times 10^3 \text{ M}^{-1} \text{ s}^{-1}$ [166].

Stopped-flow kinetic analysis of CN^- binding to ferric KatP revealed two-exponential behavior at all cyanide concentrations tested (Fig. 3.25). The exponential for the most rapid reaction accounted for 75% of the signal amplitude and was linearly dependent upon cyanide concentration (Fig. 3.26). From the cyanide concentration apparent second-order rate constant of $3.9 \times 10^5 \text{ M}^{-1} \text{ s}^{-1}$ was determined. This value is very similar to cyanide binding rate constants determined for *E. coli* KatG ($5 \times 10^5 \text{ M}^{-1} \text{ s}^{-1}$), *Synechocystis* PCC 6803 KatG ($4.5 \times 10^5 \text{ M}^{-1} \text{ s}^{-1}$), and monofunctional heme peroxidases [167-169]. The exponential for the second much

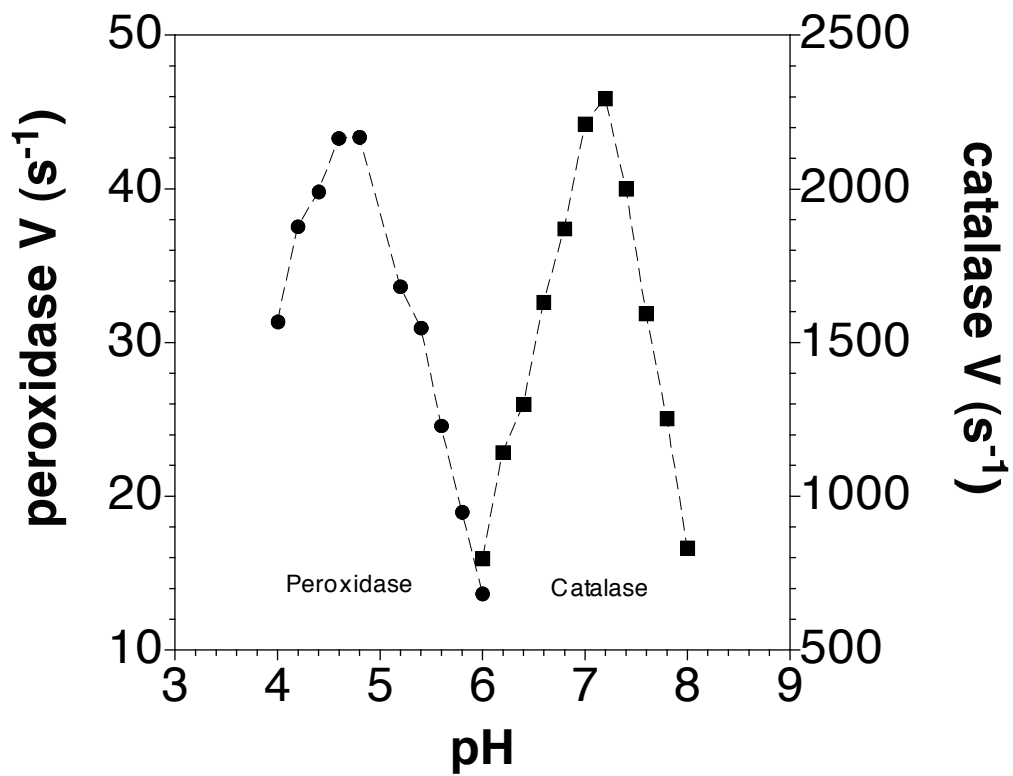


Figure 3.21. Effect of pH on the Catalase and Peroxidase Activity of KatP.

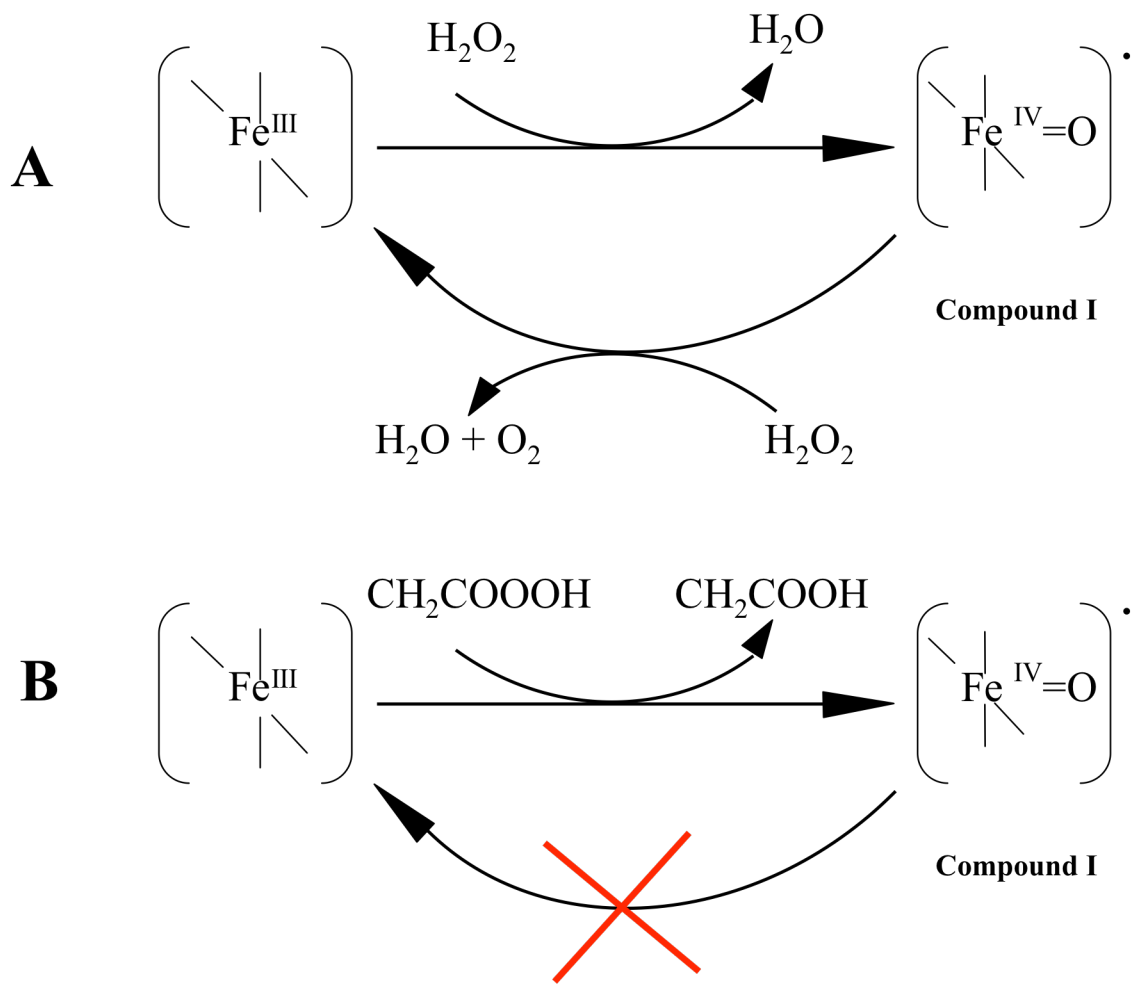


Figure 3.22. KatP Formation of Compound I by Hydrogen Peroxide (A) and Peracetic Acid (B).

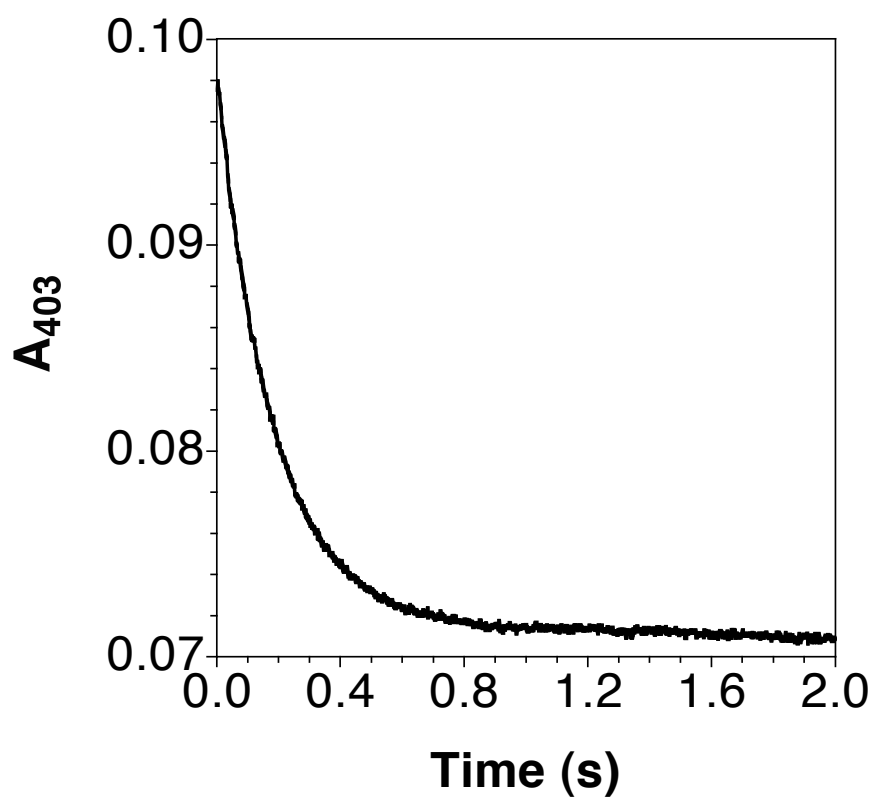


Figure 3.23. Absorption Changes Spectra for KatP Formation of Compound I by Peracetic Acid.

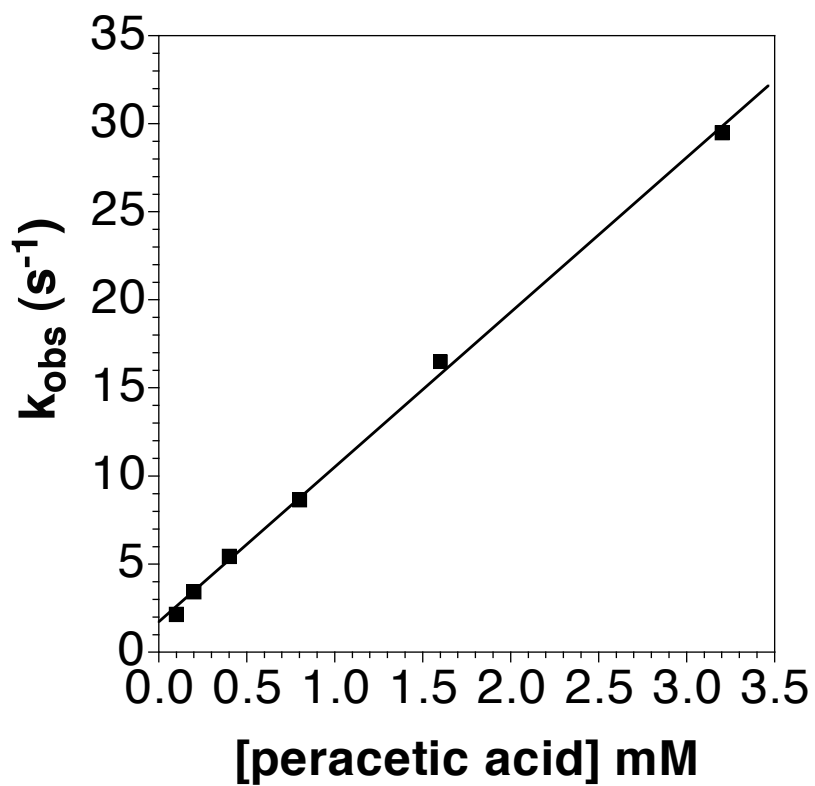


Figure 3.24. Effect of Peracetic Acid Concentration on the Rate of Formation of Compound I.

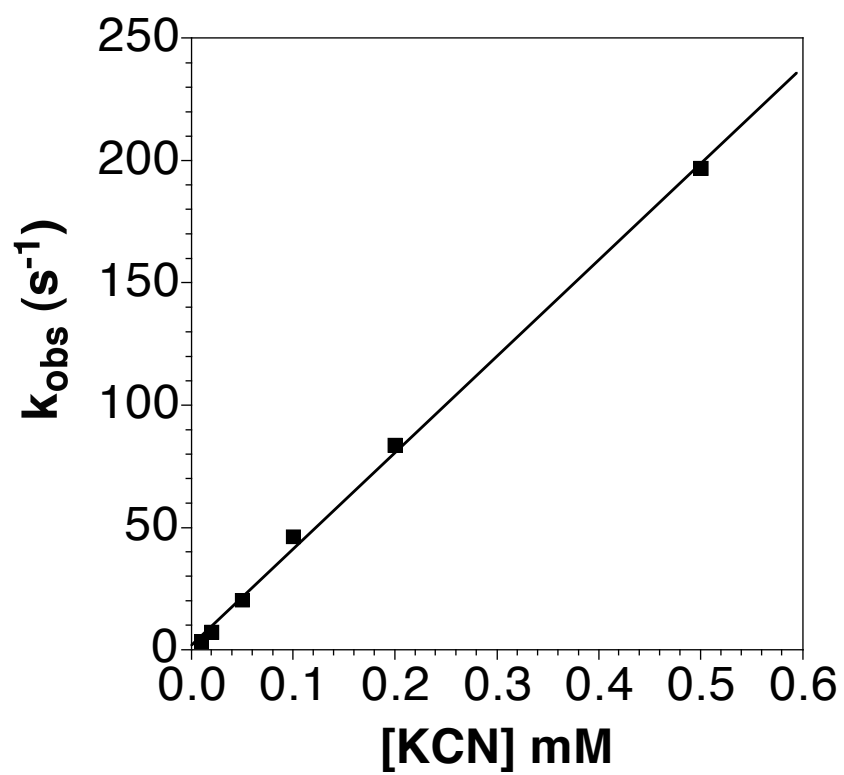


Figure 3.25. Effect of Cyanide Concentration on the Rate of Formation of the Fe^{III}-CN Complex of KatP.

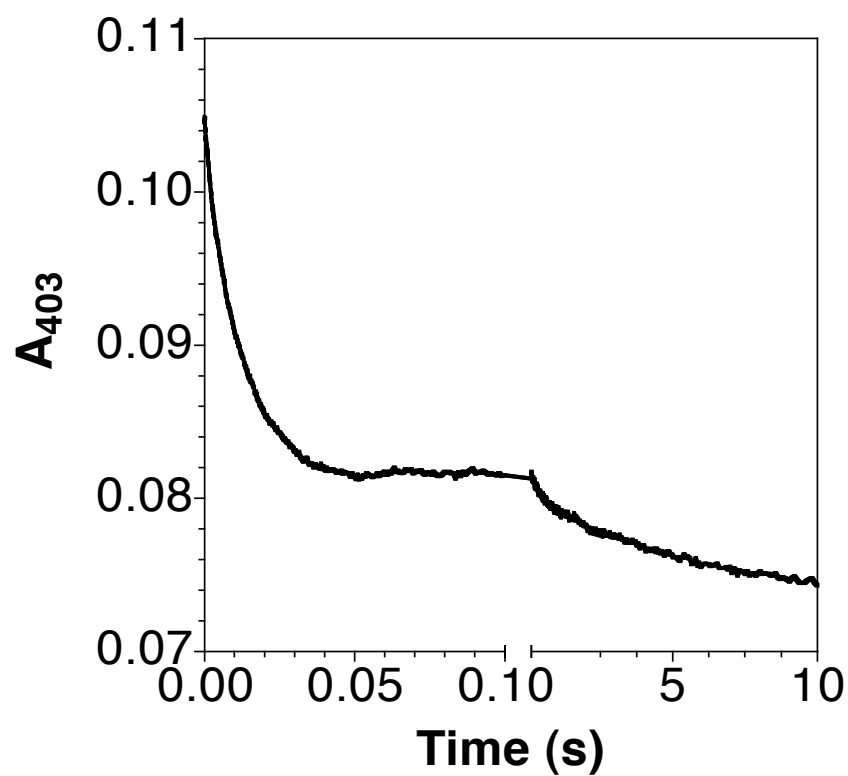


Figure 3.26. Absorption Changes Spectra for KatP Formation of Ferri-cyano Complex.

slower reaction ($\sim 0.3 \text{ s}^{-1}$) accounted for $\sim 25\%$ of the signal amplitude and appeared to be independent of cyanide concentration (Fig 3.26).

Trp-Tyr-Met Covalent Adduct

Covalent Adduct Formation Evaluation by Denaturing Electrophoresis

In our studies of catalase-peroxidases (KatG, KatP and mutants thereof), we have consistently observed the presence of two proteins that are expressed and co-purified. There is also evidence to suggest that others have observed a similar phenomenon [170]. The relative levels of these two proteins in our catalase-peroxidases studies correlate very well with the heme content of the final purified protein. Low heme content correlates with one protein; high heme content correlates with the other. Typical results with KatP provide an excellent example. Following expression and Ni-NTA purification, two bands of roughly equal intensity are observed (Fig. 3.27). Mass spectrometric analysis of the two bands shows that both are KatP. This raised the question: What is the basis for the difference in migration of these two KatP proteins? Our initial hypothesis was that KatP, a protein targeted to the periplasmic space, was expressed more rapidly than it was processed, yielding a larger unprocessed protein and the smaller mature protein. However, repeated attempts to isolate each protein based upon subcellular fractionation techniques were unsuccessful. Furthermore, we produced a construct for the expression of KatP eliminating the codons corresponding to the signal peptide (Ile 2 - Ala 23). This

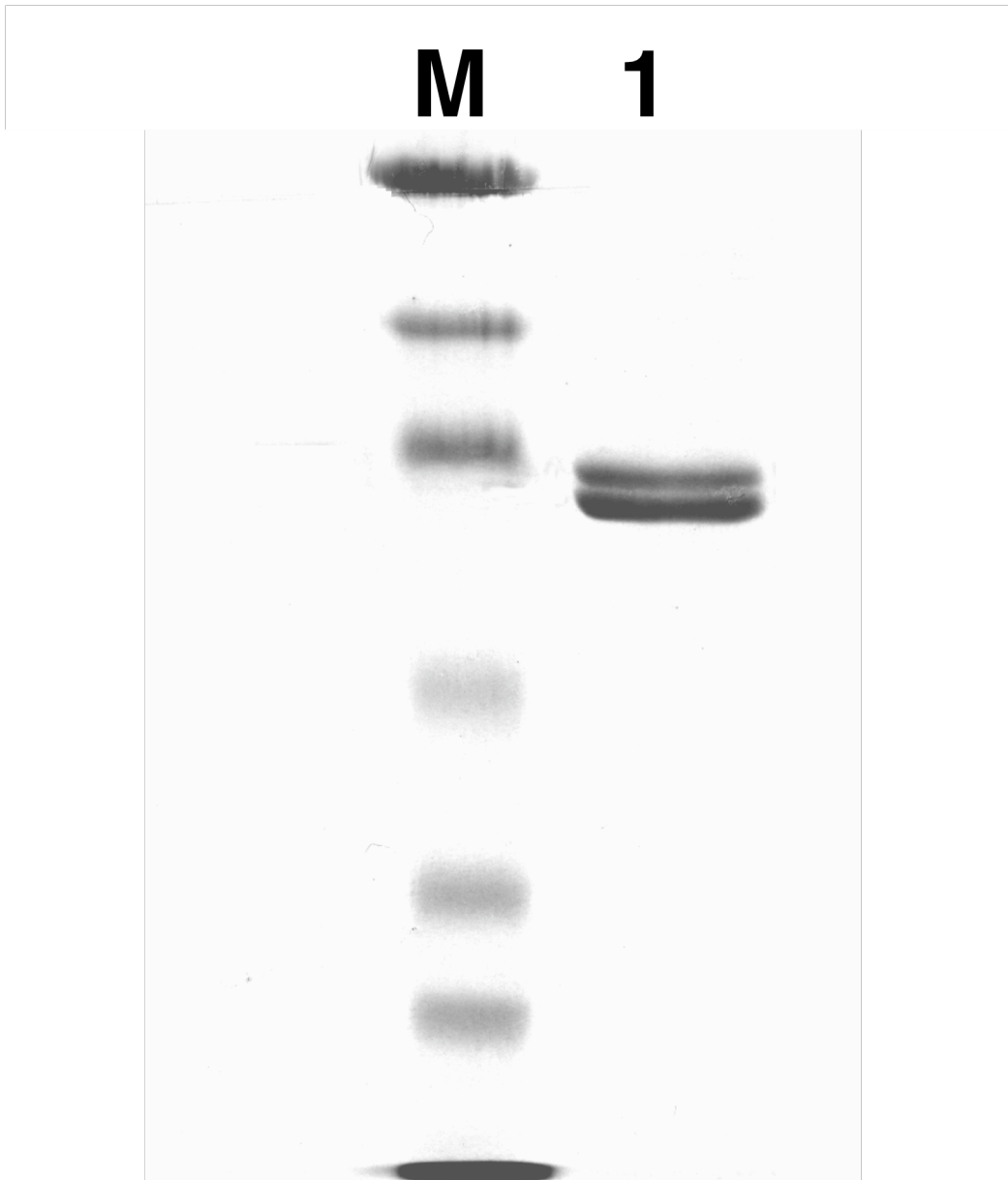


Figure 3.27. SDS-PAGE of Ni-NTA-Purified KatP (lane 1).

construct produced exactly the same results in expression and isolation as observed for the full-length gene. As described previously, the RZ values calculated from absorption spectra of purified KatP revealed that ~50% of the protein produced contained no heme. This correlated to about half the expected activity of the protein. Further separation of the two proteins by FPLC showed that the presence of heme and activity was associated with the protein lower apparent molecular weight.

The crystal structures of catalase-peroxidase from *M. tuberculosis*, *H. marismortui* and *B. pseudomallei* revealed the presence of a three amino acid covalent adduct (Fig. 3.28) [28-30, 171]. The presence of this covalent adduct in catalase-peroxidases might explain this production of the two proteins observed by SDS-PAGE in our typical KatG and KatP preparations. The nature of the covalent adduct is consistent with formation as a result of protein oxidation, and heme is observed in only one of the two proteins.

SDS is an anionic detergent, which binds to and denatures protein. SDS interrupts the protein interaction involved in tertiary folding and places a negative charge on the protein in proportion to the number of amino acids. This uniformity in charge allows the proteins to be separated by mass. The covalent adduct found in catalase-peroxidases should not be disrupted by SDS. The presence of the covalent adduct would inhibit the ability of SDS to completely denature the protein. Protein not completely linearized would be expected to migrate as a more compact structure and at a lower apparent molecular weight as compared to its counterpart. In other words KatG or KatP protein with and without the covalent adduct should migrate with two different apparent molecular weights. Protein that was expressed containing heme would be expected to

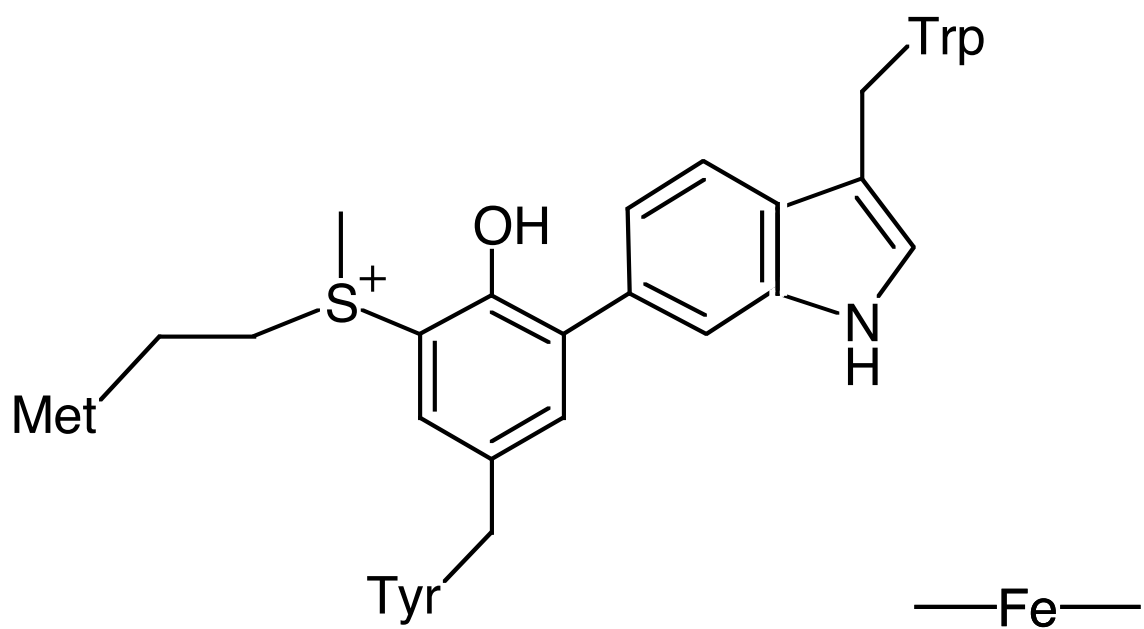


Figure 3.28. Trp-Tyr-Met Covalent Adduct of Catalase-Peroxidases.

migrate as a lower molecular weight protein while protein that never contained heme would migrate at the expected molecular weight. Therefore, the next important step was to determine if the addition of heme to catalase-peroxidase lacking the covalent adduct may result in its formation. Given the discussion above, SDS-PAGE presents a good system to evaluate the role of heme in the formation of the covalent adduct.

In our lab, expression of KatG typically results in the production of a large amount of apo-KatG. KatG expressed in this manner can be reconstituted with heme to produce an enzyme with full catalase and peroxidase activities [120]. If the covalent adduct is essential for catalase activity, then reconstitution would seem to allow for adduct formation. Taken together, this makes KatG ideal for evaluating the need for heme in the formation of the covalent adduct found in all catalase-peroxidases.

The KatG protein was produced in *E. coli* as previously described in the methods section. The RZ values calculated from absorption spectra recorded for purified KatG showed that ~95% of the protein produced contained no heme (Fig. 3.29). As with KatP, SDS-PAGE analysis showed the production of two KatG proteins, but the band of higher apparent weight dominated over that with a lower apparent molecular weight (Fig. 3.30). To evaluate the affect of heme on the formation of the covalent adduct hemin was added to KatG and its migration by SDS-PAGE was compared to apo-KatG. Upon the addition of 1 eq. of hemin, a migration shift for KatG was observed (Fig. 3.30, lane 2). This migration shift indicated that ~50% of the protein had undergone covalent adduct formation. As mentioned above, the structure of the covalent adduct suggests formation by oxidative chemistry. It is consistent with the catalytic abilities of peroxidases to suggest that such chemistry could be supported by an Fe-containing porphyrin. To

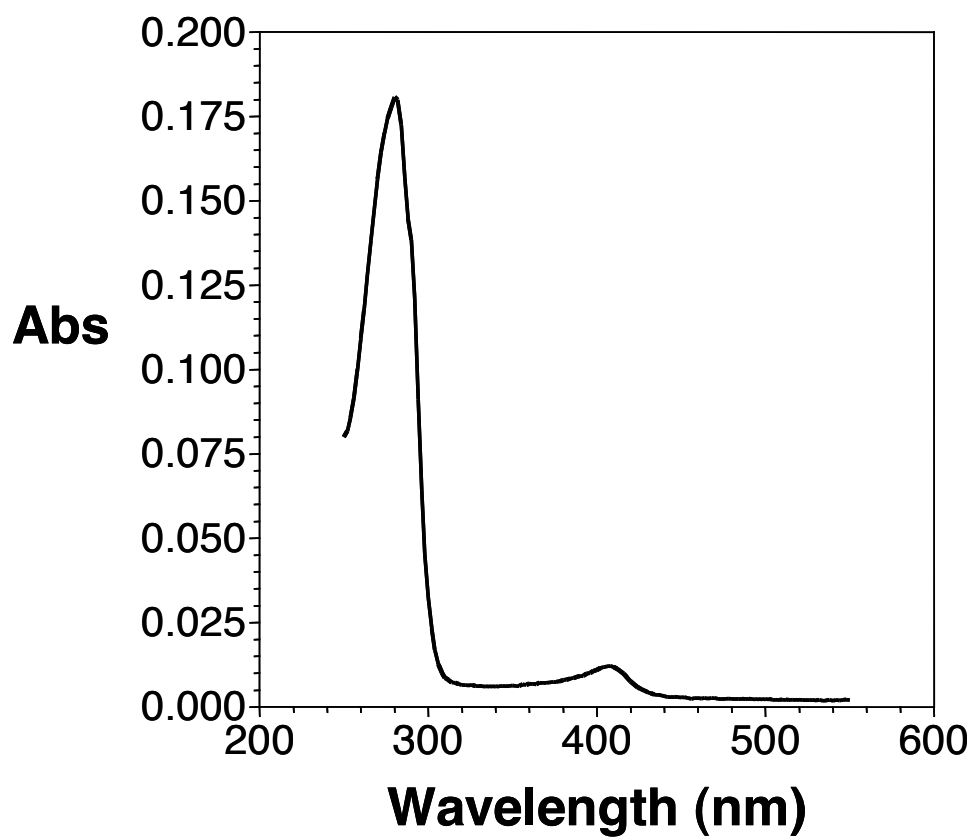


Figure 3.29. Absorption Spectrum of KatG purified from cultures with no supplementation of δ -ALA of ferrous ammonium sulfate.

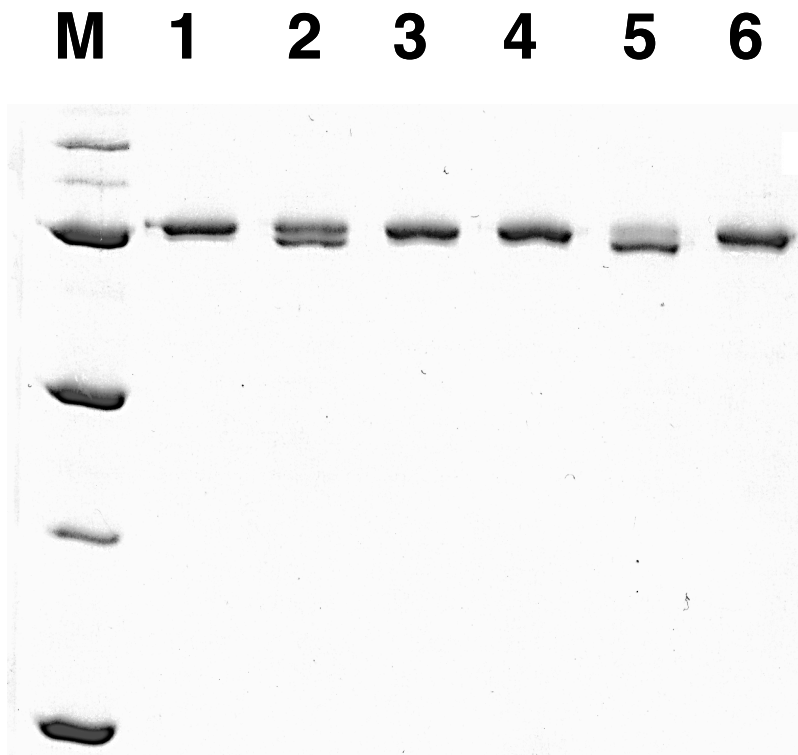


Figure 3.30. Effect of Heme and Peroxide on Migration of apo-KatG by SDS-PAGE. Apo-KatG (lane 1) with heme (lanes 2 and 5), Zn-PPIX (lanes 3 and 6), and peracetic acid (lanes 4-6) added.

explore this further, apo KatG was reconstituted with the redox-inactive porphyrin, Zn-protoporphyrin IX. Upon the addition of Zn-protoporphyrin IX, no migration shift was observed (Fig. 3.30, lane 3). An oxidant may also be required in addition to the heme group. Bacteria are constantly exposed to oxidants like H₂O₂ and other hydroperoxides (i.e., misfires in aerobic metabolism, etc). The presence of contaminating oxidants could explain why the covalent adduct could form with only the addition of heme. To further examine the need of an oxidant with heme on the formation of the covalent adduct, peracetic acid (2 eq) was added to KatG along with hemin. SDS-PAGE revealed a near complete migration shift of KatG protein (Fig. 3.30, lane 5). This shift indicated the formation of the covalent adduct in ~90-95% of KatG. However, the presence of peracetic acid alone or with Zn- protoporphyrin IX and KatG resulted in no migration shift (Fig. 3.30, lane 4 and lane 6). The formation of this adduct also requires a redox active protoporphyrin.

Mass Spectrometry

Mass spectrometry (MS) has long been used to identify the mass of chemical compounds, and relies on successful ionization of the compound to be analyzed. The ionized compounds will travel at a certain velocity through an electrostatic field in accordance with their mass-to-charge ratios (m/Z). Consequently, the time of flight of these ions will be reflective of their mass. However, problems arise when trying to get large molecules into the gas phase. The development of the Matrix-Assisted Laser

Desorption-Ionization (MALDI) mass spectrometry (MS) is a highly effective approach and has become one of the leading tools used to accurately determine the mass of large molecules (e.g., proteins, peptides). With MALDI, the molecules are diluted into a matrix. Using a short intense laser pulse, the matrix is excited, leading to the desorption and ionization of the target molecules (Fig. 3.31). Because the typical mass of the matrix is much less than the molecules to be evaluated, their time of flight are dramatically different, making it relatively easy to ignore signals due to the matrix itself.

Covalent Adduct Evaluation by MALDI

The presence of a Met-Tyr-Trp covalent adduct in KatG was evaluated by MALDI-MS. The presence of a three amino acid covalent adduct was first discovered with the publication of the first crystal structures of catalase-peroxidase in *M. tuberculosis*, *H. marismortui* and *B. pseudomallei* [28-30, 171, 172]. This was later confirmed by mass spectrometry of tryptic digest products of catalase-peroxidases [33, 173]. Catalase-peroxidases is expected to be cut into various peptide fragments by trypsin. However, trypsin does not cleave the covalent bonds of the Met-Tyr-Trp adduct. This will alter the expected fragments obtained from tryptic digests of these proteins.

In gel digestion using trypsin was preformed on co-purified KatG containing both proteins with and without the covalent adduct. Monoisotopic masses of peptides from SDS-PAGE extracted and digested protein were identified by MALDI-MS. Fragment masses were run through a sequence database to predict fragment sequence using Biotool

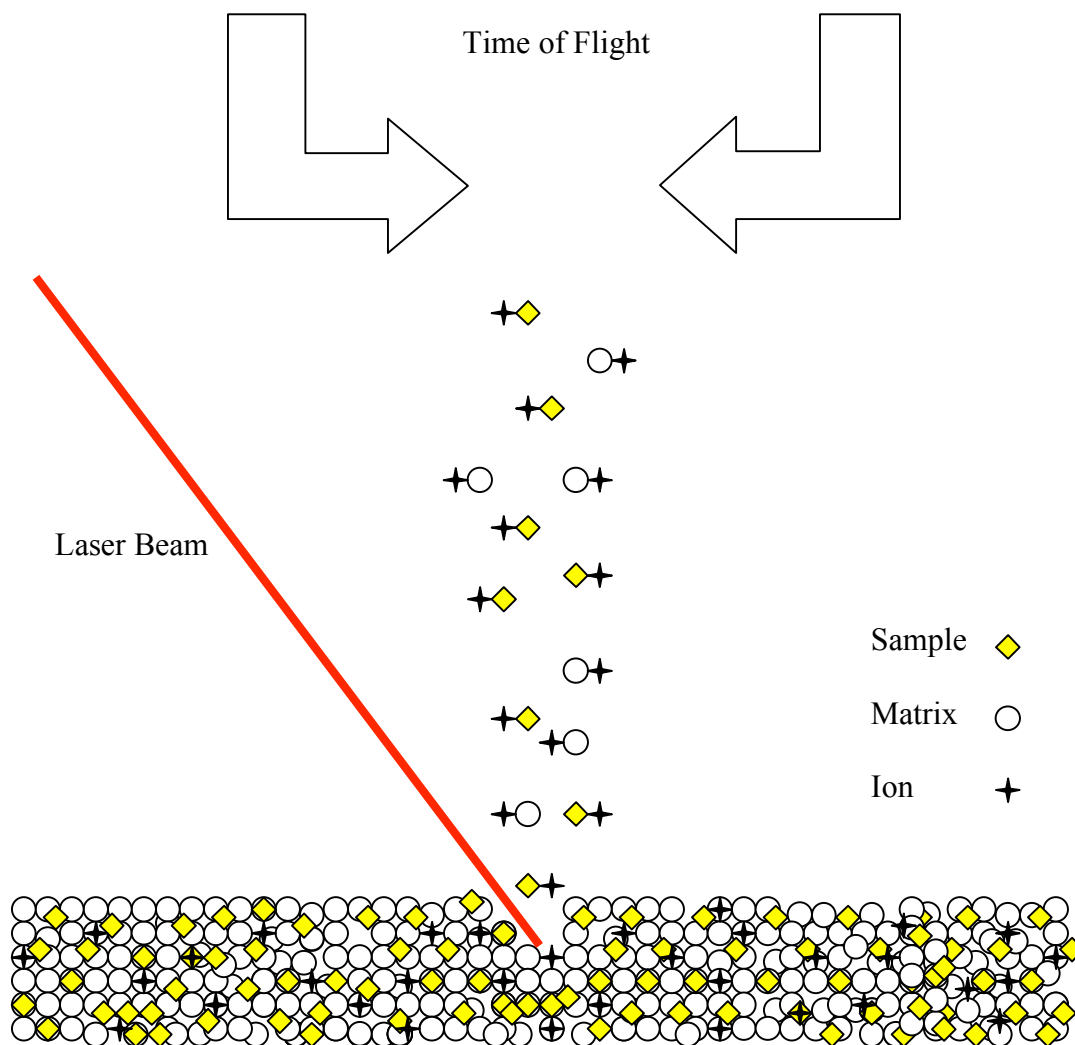


Figure 3.31. Matrix-Assisted Laser Desorption-Ionization Mass Spectrometry Schematic.

Mascot Sequence Identifier. Digestion of KatG without the covalent adduct resulted in three separated peptide fragment peaks corresponding to each of the three peptides containing a residue involved in the covalent adduct (Fig. 3.32). However, digestion of KatG already containing the covalent adduct lacked the corresponding individual peptide fragments (Fig. 3.33), indicating that the three fragments were linked together.

Effects of Y226F on KatG

In order to interrupt formation of the three amino acid adduct, site-specific substitution of the Tyr participant (Tyr 226 in KatG) with Phe was carried out. This Tyr is conserved in all catalase-peroxidases. The mutation of Tyr 226 to Phe would prevent the coupling of radicals between Trp and Tyr and should stop the formation of the covalent adduct in KatG. Expression of KatG^{Y226F} resulted in the production of one protein band as evaluated by SDS-PAGE (Fig. 3.34). The molecular weight of this band corresponded to wtKatG lacking the covalent adduct.

Catalase and peroxidase activities of KatG^{Y226F} were compared to wtKatG. Catalase activity for KatG^{Y226F} was essentially eliminated (Fig. 3.35). Conversely, KatG^{Y226F} showed an increase in peroxidase activity relative to wtKatG at low concentrations of hydrogen peroxide (Fig. 3.36). However, at high concentrations of hydrogen peroxide, a loss of peroxidase activity was observed. This loss of activity may be due to inactivation of peroxidase by hydrogen peroxide. This phenomenon is commonly observed in monofunctional peroxidases (e.g., horseradish peroxidase)

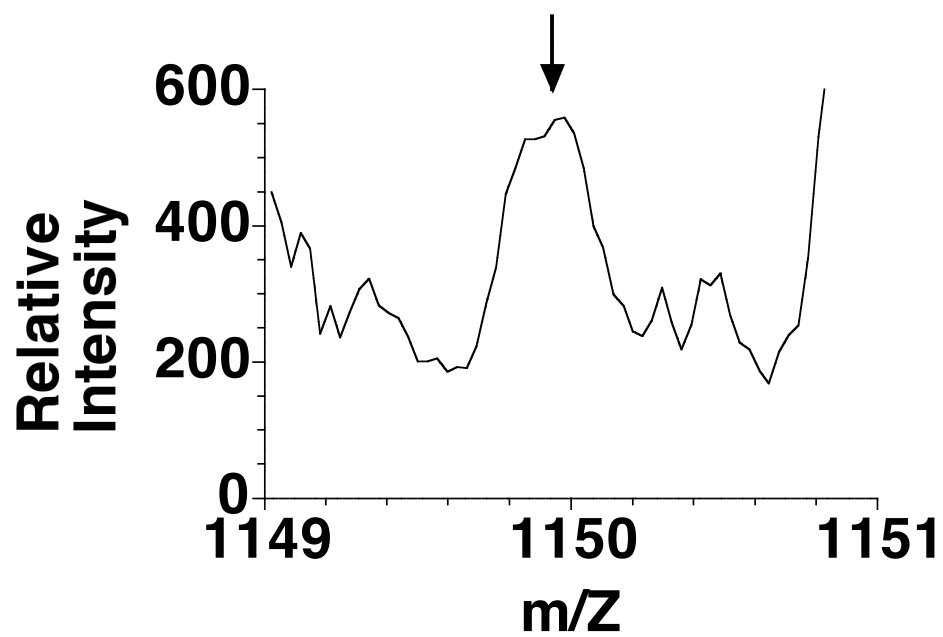


Figure 3.32. MALDI Spectrum of Tryptic Digest of KatG without Covalent Adduct. Trp peptide fragment designated by arrow.

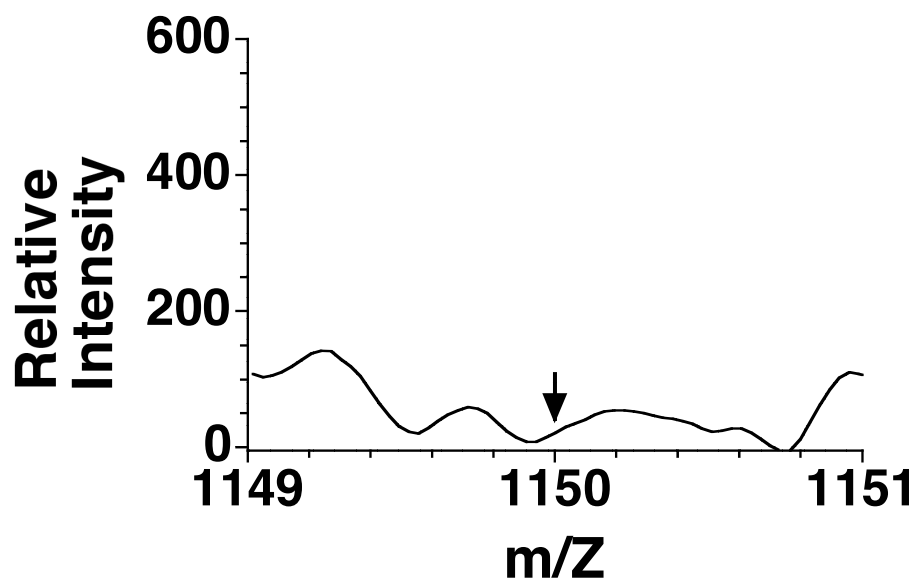


Figure 3.33. MALDI Spectrum of Tryptic Digest of KatG with Covalent Adduct. Trp peptide fragment designated by arrow.

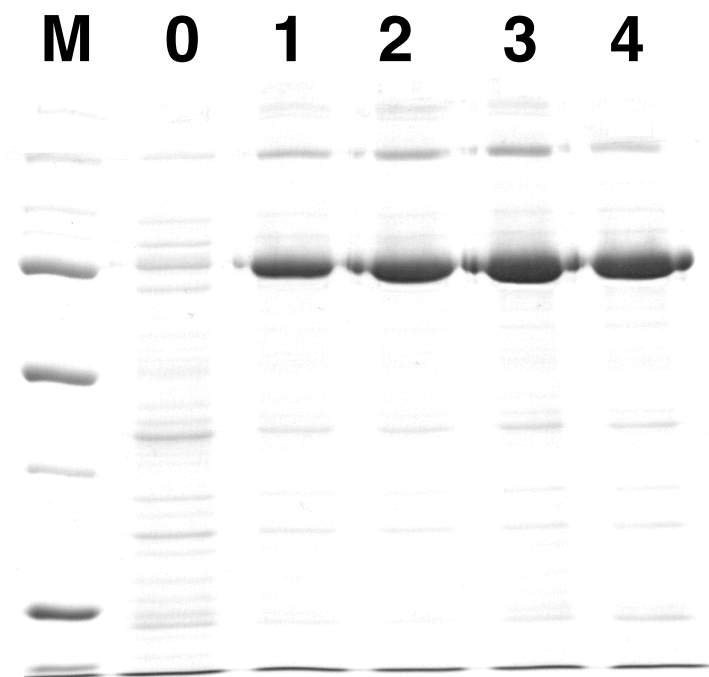


Figure 3.34. SDS electrophoretic separation of total cellular protein from BL-21 (DE3)pLysS transformed pKatG^{Y226F} at time of induction with 1 mM IPTG (lane 0), 1 h post-induction (lane 1), 2 h post-induction (lane 2), 3 h post-induction (lane 3), and 4 h post-induction (lane 4).

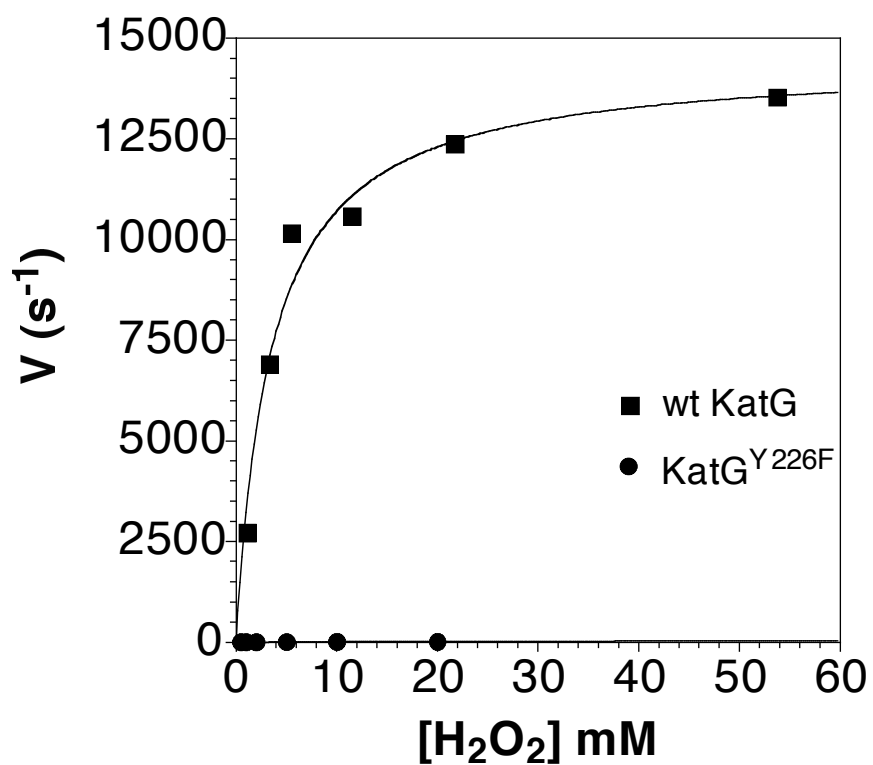


Figure 3.35. Effect of H_2O_2 Concentration on the Catalase Activity of wtKatG and KatG^{Y226F}.

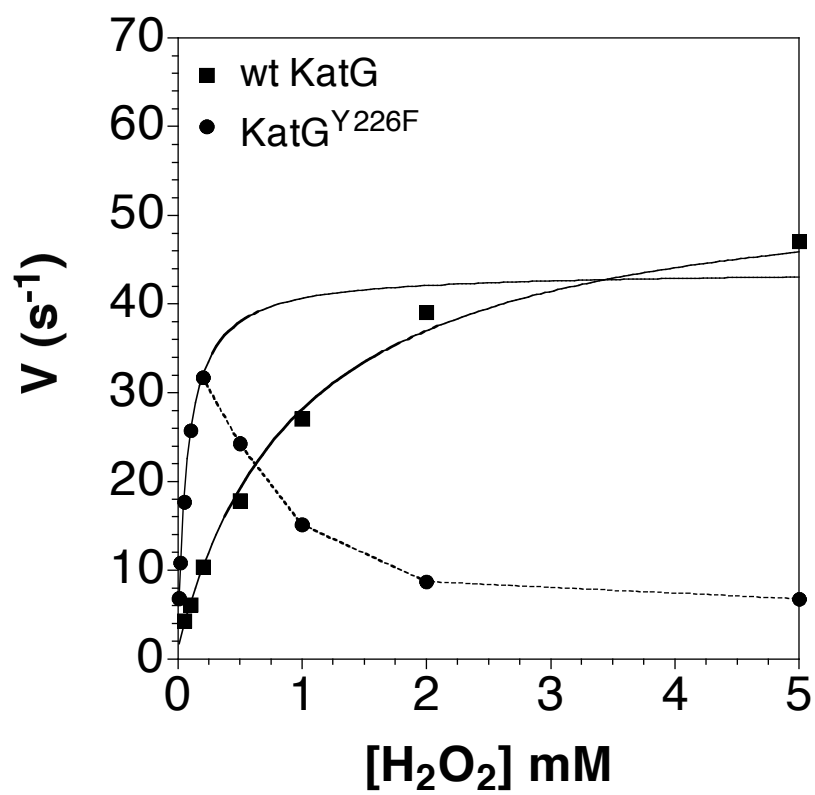


Figure 3.36. Effect of H_2O_2 Concentration on the Peroxidase Activity of wtKatG and KatG^{Y226F}.

[174-177]. In catalase-peroxidases, the loss of catalase activity makes it susceptible to inactivation by hydrogen peroxide [178]. In the peroxidase catalytic cycle, the reduction of Compound II is the rate-limiting step. The accumulation of Compound II allows it to react with excess hydrogen peroxide to produce compound III (reaction 12). Compound III is an inactive form of the enzyme and results in the loss of activity.

These results and those of others indicate that the covalent adduct appears to be vital for catalase activity. Conversely, this adduct is not required for peroxidase activity [31, 33, 34, 173]. SDS-PAGE was also used to evaluate the formation of the covalent adduct in KatG^{Y226F} as with wtKatG (above). In order to evaluate the effect of heme on the formation of covalent adduct in KatG^{Y226F}, hemin was added to KatG^{Y226F} and compared to apo-KatG^{Y226F}. The addition of 1 eq. of hemin resulted in no apparent migration shift of KatG^{Y226F} (Fig. 3.37, lane 2). This indicated that none of the protein had formed the covalent adduct and the substitution of Tyr with Phe disrupted its formation. The need of an oxidant in the formation of the covalent adduct in KatG^{Y226F} was also evaluated. Upon the addition of 2 eq. of peracetic acid to KatG^{Y226F} along with hemin, there was no apparent migration shift (Fig. 3.37, lane 5). This further indicated the complete disruption of the covalent adduct formation. As with wtKatG, peracetic acid alone did not result in a migration shift (Fig. 3.37, lane 4). The non-redox active Zn-PPIX also did not have any effect on the protein migration with or without the presence of peracetic acid (Fig. 3.37, lane 3 and lane 6).

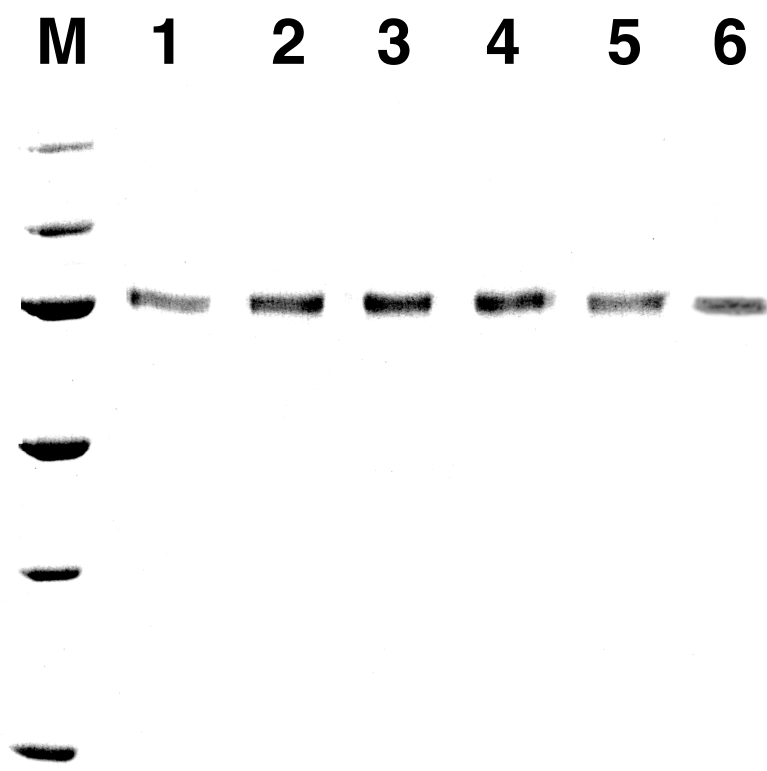


Figure 3.37. Effect of Heme and Peroxide on Migration of KatG^{Y226F} by SDS-PAGE. Hemin (lanes 2 and 5), Zn-PPIX (lanes 3 and 6), and peracetic acid (lanes 4-6) were added to Apo-KatG^{Y226F} (lane1)

CHAPTER FOUR

DISCUSSION

Hemoproteins are a widely distributed in nature and compose an important class of biologically important metalloproteins that have a common active site cofactor, an iron-porphyrin complex also called heme. These proteins are involved in a wide range of functions such as the transportation of dioxygen (hemoglobin and myoglobin), catalysis of the disproportionation and reduction of hydrogen peroxide (catalases and peroxidase), oxidation of organic substrates (cytochrome P450), production of reactive oxygen species (NADPH oxidase and myeloperoxidase), and electron transport (cytochrome oxidase). Each hemoprotein, unique in its function, differs in the specific form of the heme complex, which undergoes different transformations in the oxidation state, ligands, and spin states controlled by the protein. This diversity of function makes hemoproteins a robust model for studying the important relationship between the structure of proteins and their functions.

The research in this dissertation addresses hemoprotein structure and function in three ways. It addresses a long-standing impediment to progress in hemoprotein

structure/function studies. That is, the difficulty of expressing large quantities of these enzymes and proteins in their holo state. Secondly, it is the first to give a complete description of the spectral and catalytic properties of a periplasmic catalase-peroxidase uniquely produced by highly virulent pathogenic bacteria. The catalase-peroxidases provide an excellent opportunity to address a poorly understood aspect of the structure/function equation. That is, mechanisms by which distant structural components fine tune an active site for a specific catalytic purpose. Along these lines, the research described in this dissertation has addresses the requirement for formation of a unique Trp-Tyr-Met covalent adduct and its role in catalase-peroxidase catalysis.

Expression of Recombinant Hemoproteins

A commonly observed problem in the expression of recombinant hemoproteins is that large quantities of the protein are expressed but very little of it actually contains heme. A major goal of the research described in this dissertation was to develop an expression system that resolves this problem. The idea was to produce an *E. coli* strain for hemoprotein expression that could draw exogenously added heme directly from its growth medium to incorporate into the target protein as it was expressed. The development of the HPEX system accomplishes this by giving *E. coli* strains a heme receptor. The HPEX plasmid (e.g., pHPEX2) containing the heme receptor gene, *chuaA*, was transformed into *E. coli* expression strain BL-21 (DE3) and expressed. This produced a protein corresponding to the molecular weight of ChuA. While ChuA seemed

to be expressed with the HPEX plasmids, the question of its ability to function as a heme transporter remained unclear. The function of ChuA was evaluated by the ability of HPEX-transformed cells to grow in iron-deficient media using exogenous heme as the only iron source. *E. coli* cells transformed with pHPEX2 were able to use exogenous heme for growth in iron-deficient media. This indicated that ChuA was functional and could be used to draw in heme into the *E. coli* cells from the media. The question about whether or not heme brought in by ChuA would be incorporated into target hemoproteins was also examined. The expression of KatG in *E. coli* cells transformed with pHPEX3, showed a 10 fold increase in heme content. Thus, KatG exhibited full activity. The HPEX system was shown to give standard *E. coli* expression strains the ability to produce a functional heme receptor, which, as we have demonstrated, can be used to give recombinant hemoproteins a full capacity of heme.

The benefits to be realized from enhancing expression of recombinant hemoproteins in their holo state are far-reaching. These benefits can be divided into two broad categories: 1) therapeutic application of hemoproteins and 2) advancing the study of hemoprotein structure/function relationships. This dissertation demonstrates that the HPEX system is likely to be useful in both.

Application for Therapeutic use of Hemoproteins

Due to the constant occurrence of medical emergencies, a significant population with congenital blood diseases like hemophilia, and the ever-present danger of natural

disasters, there is always a high demand for stored blood to use for life-saving transfusions. The short supply of stored blood is exacerbated by several challenges. These challenges have fueled interest in the development of effective blood substitutes. One of the most promising possibilities is cell-free hemoglobin. Where blood, even under refrigeration, has a short shelf-life (30-45 days), hemoglobin can be stored at room temperature for months and even years [179]. This opens the possibility for transportation and immediate use by emergency personnel at the scene of need. Blood cells, due to their antigenic properties, must be typed and cross-matched to ensure safe transfusion. Cell-free hemoglobin is not antigenic, allowing for the elimination of these time consuming procedures.

In spite of the many advantages for using cell-free hemoglobin as a blood substitute, there are two major drawbacks that prevent its application in this role. The first is that Hb is a potent scavenger of NO. NO binds to Hb 8000 times faster than O₂ [180]. One important role of NO is the mediation of smooth muscle relaxation. The uptake of NO by extracellular Hb causes vasoconstriction and increase in blood pressure [180, 181]. Substitution of amino acids in the distal pocket of the globin proteins with large aromatic or aliphatic amino acid has been shown to inhibit the non-covalent capture of NO [182]. The substitution of Leu in the α subunit and Val in the β subunit of hemoglobin with Trp decrease NO binding and inhibits NO dioxygenation reaction. This resolves the hypertensive effect of extracellular hemoglobin as a blood substitute. The second problem with using cell-free hemoglobin as a blood substitute is that the hemoglobin tetramer is susceptible to dissociation into α/β dimers in an extracellular environment. In this form, the protein becomes much more susceptible to autoxidation

leading to greater oxidative stress [179]. Furthermore, kidney function is interrupted by these dissociated α/β dimers. This is resolved by generating cross-linked or polymeric forms of hemoglobin on one hand, or by generating a fusion construct to express two α subunits in tandem with a glycine linker [182]. The latter, of course, requires manipulation of the hemoglobin gene by molecular cloning techniques.

Interestingly, the resolution of both of these major problems by molecular cloning techniques (i.e., by producing unnatural hemoglobins) makes the use of natural sources of hemoglobin as blood substitutes impossible. They must be produced through the expression of recombinant forms. In terms of expression levels, cost of materials, ease of use, and ease of manipulation, *E. coli* expression systems are by far the most advantageous for producing large quantities of recombinant proteins.

Unfortunately, with it comes to the expression of recombinant hemoproteins in *E. coli*, a major drawback is the fact that a vast majority of the protein lacks the heme prosthetic group essential for activity. Clearly, hemoglobin without heme is useless as a blood substitute, even if it is produced at very high levels. Part of the research described in this dissertation involved the development of a hemoprotein expression (HPEX) system designed to increase the heme content of recombinant hemoproteins expressed in *E. coli*. The HPEX strains described express a heme receptor, increasing their capacity to withdraw hemin directly from the extracellular environment. This system eliminates the need to supplement media with relatively high concentrations of heme precursors (e.g., 0.5 mM δ -ALA) instead only requiring supplementation with low-hemin concentrations (e.g., 8 μ M). The data presented in this dissertation strongly suggest that

the HPEX system will be useful for the expression of recombinant hemoglobin to be used as a blood substitute.

Hemoglobin and myoglobin are allies in the transport and storage of oxygen. The α and β subunits of hemoglobins are analogous to myoglobin. Here myoglobin is used as a model for hemoglobin. The globins are an ideal group to use with the HPEX system. The expression of sperm whale myoglobin with the HPEX system confirmed the production of a functional heme receptor. Mb expressed with BL-21 (DE3) pHPEX3 and BL-21 (DE3) pHPEX-fur cells showed an increase in heme content when hemin was added to the cultures at the time of induction. When hemin was excluded from the culture medium, absorption derivative spectra of whole cells showed a low heme content. When Mb was expressed with BL-21 (DE3) and BL-21 (DE3) pLysS cells, absorption derivative spectra showed no increase in heme content even if hemin was added to the culture medium.

Application to Studies of Heme Enzyme Structure and Function

The wide range of biochemical processes mediated by hemoproteins is nothing short of astonishing. The fact that these proteins all use essentially the same iron porphyrin cofactor to accomplish these tasks makes the diversity even more impressive. Clearly, the structure of the protein around the heme cofactor is the factor that dictates the function of one hemoprotein in comparison to another. Indeed, hemoproteins are a robust

group for studying the relationship between the structure of a protein and its catalytic abilities.

The study of structure/function relationships in hemoproteins requires large amounts of active protein and the ability to produce large quantities of variants (produced by site-directed or other mutagenesis procedures). Indeed, techniques like stopped-flow kinetic analysis, EPR, NMR, X-ray crystallography, magnetic circular dichroism, etc. are very protein intensive. Almost always, high-level expression of recombinant forms is required, and as mentioned previously, *E. coli* expression systems are the most productive, least expensive, and least complicated. Unfortunately, it is also very common that a significant portion of the expressed protein lacks heme. Indeed, the purified enzymes often contain less than 10% of the heme expected. Addition of heme biosynthetic precursors such as δ -ALA and ferrous ammonium sulfate alleviates this problem to some degree. However, large quantities of these materials must be added (0.5 mM).

Catalase-peroxidases are ideal enzymes to examine a poorly understood aspect of hemoprotein structure and function. They utilize a single active site to catalyze at least two different reactions. Interestingly, this active site is almost identical to active sites found in monofunctional peroxidases. As the name implies, monofunctional peroxidases have virtually no catalase activity. Given their nearly identical active sites, it appears that unique structures external to the catalase-peroxidase active site modulate its catalytic properties even from distances of 30 Å and more. There are very few systems so ideally set up to evaluate long-range influences on active site structure and function.

Although, expression of catalase-peroxidases in standard *E. coli* strains results in large quantities of protein, it is almost all in its apo-state. Even addition of δ -ALA and ferrous ammonium sulfate do little to improve expression of the holoenzyme. These enzymes would appear to be the perfect candidates for the HPEX system. In our laboratory, we use the T7-RNA polymerase-based pET system for the expression of catalase-peroxidases. The best results has been observed using BL-21 (DE3) pLysS. Consequently, BL-21 (DE3) pHPEX3 strain was the most appropriate strain to use as a basis for comparison.

Using BL-21 (DE3) pHPEX3 cells, KatG was expressed at levels comparable to those observed in the pLysS-transformed system. When hemin was excluded from the culture medium, absorption spectra of the partially purified protein showed a very low-heme content. Addition of hemin to the culture at the time of induction resulted in the same yield of isolated KatG protein, but the enzyme had a 10-fold greater heme content. Conversely, when BL-21 (DE3) pLysS was used in place of our pHPEX3-transformed strain, addition of hemin to the culture at induction resulted in only a 3.5-fold increase in heme content. The expression of KatG with the HPEX system allowed for substantial improvement in its heme content by simply adding hemin to the growth medium at time of induction.

The moderate increase in heme content and activity of KatG expressed in BL-21 (DE3) pLysS cultures containing hemin is noteworthy. Many *E. coli* strains (including this one) are apparently unable to use extracellular heme as an iron source for growth only because they lack a heme receptor [8-10]. Nevertheless, addition of hemin to expression cultures can improve the heme content of recombinant hemoproteins [167].

Our mechanism by which this might occur is the transmembrane movement of hemin through the membrane bilayer [183]. The rate-determining step in this process is almost certainly “heme flipping” whereby the propionate groups go from an orientation into the extracellular environment to pointing into the periplasmic space. As expected, this process is slow and not sufficient to supply the demands of over-expressed hemoproteins [184, 185].

The spectral and kinetic properties of KatG expressed in BL-21 (DE3) pHPEX3 grown in hemin-supplemented media were compared to those of KatG expressed in BL-21 (DE3) pLysS grown in unsupplemented media. Spectrally, the absorption maxima for the ferric, ferri-cyano, and ferrous forms of KatG derived from each system were consistent with one another and other catalase–peroxidases [35, 37, 165, 167]. Indeed, the ferric minus ferri-cyano difference spectra were nearly identical to one another (Fig. 3.9). Kinetically, the K_M of KatG for H_2O_2 was unchanged by expression conditions and was consistent with values reported for KatG [37, 186] and other catalase–peroxidases [167]. Likewise, *on a per-heme basis*, k_{cat}/K_M values for KatG obtained from either expression system were consistent with one another and with values reported for other catalase–peroxidases [37, 167]. On the other hand, on the basis of protein concentration (i.e., specific activity), KatG isolated from hemin-supplemented BL-21 (DE3) pHPEX3 cultures had much greater activity than unsupplemented BL-21 (DE3) pLysS cultures. This indicates that holo KatG expressed in the HPEX system has the same properties as holo KatG produced by other means. However, the yield of holo KatG is much greater in the HPEX system than other *E. coli* expression strains.

The study suggests that the HPEX system will be a *versatile* system for hemoprotein expression. As already noted, it has enhanced Mb expression as well as KatG, two completely different proteins. It has also enhanced the expression of variants of KatG, such as KatG^{ΔFG}, KatG^{Y226F}, KatG^{R117A}, and KatG^{D597A}. A potential benefit derived from using a receptor-based heme scavenging system is that other sources of heme or heme derivatives could be used in place of hemin. The outer membrane-bound heme receptors like ChuA produced by Gram-negative pathogens allow for heme uptake from hemoproteins like hemoglobin or myoglobin [9, 10]. Likewise, these receptors have also been shown to support uptake of tetrapyrroles other than hemin. Substitutions of the metal (e.g., zincprotoporphyrin IX) as well as substitutions of the side chains on the macrocycle (e.g., ferriporphyrin) are well accommodated by these heme receptors [187]. Consequently, it is possible that the HPEX system may be used to express recombinant hemoproteins bearing unusual natural heme derivatives or even unnatural synthetic hemes. One limitation seen thus far with the HPEX system is that it has not been able to resolve the expression of some hemoproteins in inclusion bodies. However, it is feasible that the HPEX system may be used in conjunction with other systems (e.g., chaperones) to resolve this issue. The chaperone GroEL, which is responsible for assisting the correct folding of many different proteins, has been shown to increase expression of correctly folded cytochrome P450 when expressed with the enzyme [188]. It is likely that the presence of heme is also required for the correct folding. The HPEX system may be ideal for increasing the production of the correctly folded cytochrome P450 along with GroEL.

Periplasmic Catalase-Peroxidase

Escherichia coli O157:H7 is a highly virulent and deadly food-borne pathogen. Indeed, O157:H7 is recognized as one of the most virulent even among the shiga-toxin-producing *E. coli* strains [12, 20]. This strain produces several factors that are absent from less pathogenic or non-pathogenic *E. coli*. Among these is a unique periplasm-targeted catalase-peroxidase (KatP). KatP along with KatA (from *L. pneumophila*) and KatY (from *Y. pestis*) are part of a unique subgroup among the family of the bifunctional catalase–peroxidases. This is evident from available sequence data showing these enzymes to be more closely related to one another than they are to their cytoplasmic counterparts [189, 190]. For example, KatP shares greater sequence identity with KatY and KatA than it does with KatG, the intracellular catalase–peroxidase common to all *E. coli* strains [189, 190]. Indeed, it has been suggested that these periplasmic catalase–peroxidases were the result of lateral gene transfer from an archaeon [17]. Analysis of numerous new catalase–peroxidase gene sequences (recently available due to intensive genome sequencing efforts) has cast doubt on this origin for the periplasmic catalase–peroxidases [28]. However, it is clear that the periplasmic enzymes form a cluster that is distinct from other catalase–peroxidases [28]. Interestingly, it has been suggested that KatP represents one of the most recently acquired virulence factors by *E. coli* O157:H7 [191]. Clearly, the routes by which such organisms acquire new potential virulence factors is an important problem whose solution will be aided by additional genomic and proteomic information.

Among the periplasmic catalase–peroxidases, KatA, KatY, and KatP are produced by highly virulent bacterial pathogens but not by their less pathogenic or non-pathogenic relatives, suggesting that these enzymes may be used as virulence factors. This hypothesis is supported by the fact that expression of KatY by pathogenic *Yersinia* species corresponds with a shift from 26 to 37 °C, a feature that coincides with transfer of the bacterium from the flea to the mammalian host [25, 26]. Similarly, in *L. pneumophila*, KatA has been shown to impart characteristics that support its survival within the macrophage host [23, 192]. Despite the potential role of these enzymes in the virulence of these pathogens, only one has been previously isolated [31] and none of the three has received a careful evaluation of its spectral or kinetic properties. The cloning, expression, isolation, and characterization of KatP, a periplasmic catalase–peroxidase recently identified in highly virulent *E. coli* O157:H7 is described in this dissertation.

KatP was post-translationally processed according to the putative periplasm-targeting sequence on its N-terminal end. The mature enzyme displayed heme content consistent with other catalase–peroxidases as judged by its 0.67 RZ value. Absorption spectra of ferric and ferrous KatP are suggestive of a mixed population of high-spin hexacoordinate and pentacoordinate hemes, as well as some of the hexacoordinate low-spin complex. EPR spectra confirm the dominance of the high-spin species and suggest a higher than usual proportion of hexacoordinate high-spin heme.

Consistent with its heme content, KatP displays strong catalase and peroxidase activities. The k_{cat} values calculated for each activity are comparable to, if not greater than, those determined for the cytosolic catalase–peroxidases (Table 4). KatP shows

sharp pH dependence in both catalase and peroxidase activities. The optima for catalase ~pH 7 and peroxidase ~ pH 5 are similar to catalase–peroxidases.

One striking difference between KatP and other catalase–peroxidases evaluated to date is the relatively high K_M for H_2O_2 . At 27 mM, the K_M of KatP for H_2O_2 as determined from its catalase activity is the highest yet reported for any of the bifunctional enzymes by at least fivefold [167, 193]. The K_M for H_2O_2 as determined from the peroxidase activity of KatP (3 mM) is also larger than that determined for KatG (0.83 mM). Though the same kinetic treatment has not been undertaken for the other periplasmic enzymes, it has been reported that KatY has a low-catalase activity [25, 26]. Supposing that low concentrations of H_2O_2 (i.e., $0.05 \times K_M$) were used in these studies, a low apparent catalase activity would be expected. One possible explanation for this observation is the presence of a sixth ligand (probably H_2O) in the resting form of the enzyme. The EPR spectrum indicates a greater proportion of hexacoordinate high-spin heme. An inflated K_M for H_2O_2 would be an expected outcome if the displacement of this sixth ligand was more difficult in KatP than in other catalase–peroxidases. On the other hand, rate constants determined for the reactions of KatP with other hydroperoxides (e.g., peracetic acid) and heme ligands (e.g., CN^-) are well within the range of those determined for other catalase–peroxidases. Together these data suggest that high apparent K_M values of KatP for H_2O_2 are due to quite subtle differences in its active site compared with other catalase–peroxidases.

Though the periplasmic catalase–peroxidases have been implicated as virulence factors, the mechanisms by which they contribute to the growth and survival of these pathogens have not been elucidated. It has been suggested that the primary benefit to

these pathogens for producing a second catalase–peroxidase is derived from the cellular location of the enzyme [27]. By placing a highly active H₂O₂ decomposition catalyst within the periplasmic space, the ability to remove H₂O₂ before it is allowed to damage critical inner-membrane components is realized. Indeed, there is precedent for strong periplasmic catalase activity (from monofunctional catalases) in *Brucella abortus* (a mammalian pathogen) [194, 195], *Vibrio fischeri* (a light-generating symbiont of *Euprymna scolopes*) [196, 197], and *Pseudomonas syringae* (a plant pathogen) [198, 199]. All of these organisms appear to use catalase to fend off host responses that involve production of abundant reactive oxygen species and oxidants derived from them (e.g., HOCl). In a similar manner, the organisms that produce these unique periplasmic bifunctional catalase–peroxidases encounter similar host responses. *Y. pestis* and *L. pneumophila* are both intracellular pathogens, and *E. coli* O157:H7 induces the migration of neutrophils to the site of infection in the intestinal lumen [200].

The peroxidase activity of the periplasmic catalase–peroxidases may provide another essential function by reducing reactive peroxides likely to be produced as a result of the immune response, including peroxynitrite (ONOO⁻) and its conjugate peroxynitrous acid (ONOOH). Catalase-peroxidases also have peroxynitritase activity to decompose ONOO⁻ generated by macrophages (Fig. 4.1). KatG in *M. tuberculosis* has been shown to decompose ONOO⁻ at a similar rate to myeloperoxidase, 10⁵ M⁻¹s⁻¹ and 10⁶ M⁻¹s⁻¹ respectively [151]. In our laboratory, we have observed that ONOO⁻ reacts rapidly with KatP to form compound I as seen by a decrease in absorbance at 404nm (Fig. 4.2). Following this, the slow conversion of compound I to compound II is also observed indicated by the increase in absorbance 420nm (Fig. 4.3). It is important to bear

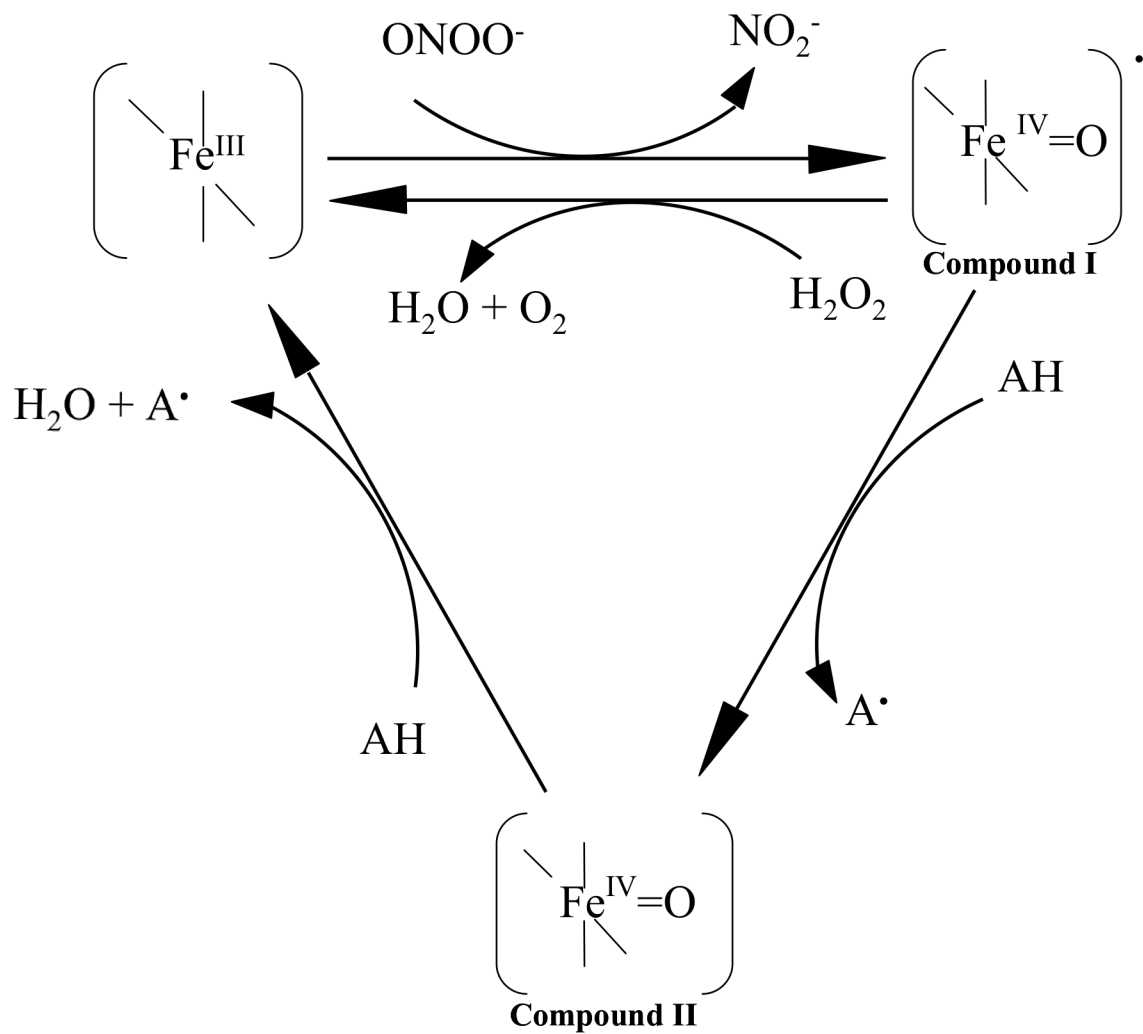


Figure 4.1 Incorporation of Peroxynitrite in the Catalytic Cycle of Catalase-peroxidase.

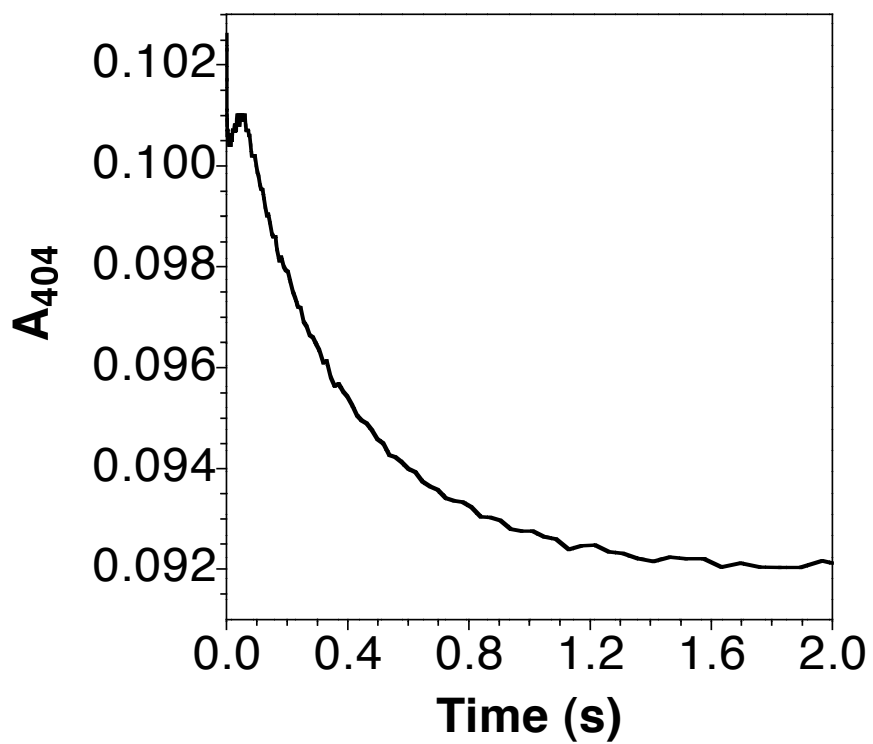


Figure 4.2. KatP Compound I Formation in the present of 200 μ m Peroxynitrite.

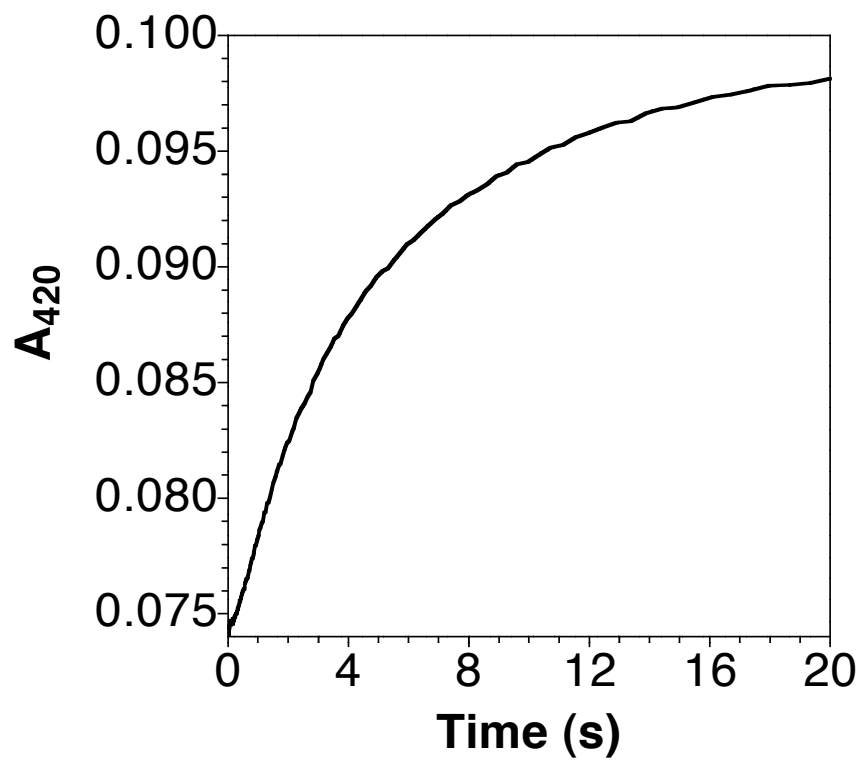


Figure 4.3. KatP Compound I Conversion to Compound II in the present of Peroxynitrite.

in mind that compound I can also be reduced back to the ferric state by H_2O_2 (Fig. 4.1), another peroxide generated at high levels by macrophages and neutrophils. The ability of catalase-peroxidases to simultaneously decompose ONOO^- and H_2O_2 would be expected to greatly enhance bacterial ability to survive.

In the face of agents such as ONOO^- , the advantages for producing a periplasmic peroxide decomposition catalyst become even more pronounced. The pK_a for peroxynitrite is around 7, thus, under physiological circumstances a significant proportion of peroxynitrite is expected to exist in its ionized form, and thus, be unable to cross the inner-membrane where it might be dealt with by cytosolic catalases and catalase-peroxidase. The presence of a periplasmic catalase-peroxidase might be particularly effective for preventing such host-derived damage. It has also been suggested that the peroxidase activity may serve additional functions contributing to virulence. Indeed, others have observed that the *katA* gene is essential for the survival of *L. pneumophila* in the stationary phase, and they suggest that this benefit most likely results from the peroxidase activity of KatA rather than its catalase activity [32].

Role of Trp-Tyr-Met Covalent Adduct

Since the publication of the crystal structure of catalase-peroxidases, more insight has been given to the function of this enzyme. The crystal structures of KatG from *M. tuberculosis*, *H. marismortui* and *B. pseudomallei* reveals an active site almost identical to class I peroxidases (e.g., cytochrome c peroxidase). However, the electron density

maps do suggest the presence of a Trp-Tyr-Met covalent adduct peripheral to the active site (Fig. 4.4) [30, 171]. All three amino acids found in this adduct are conserved in all catalase-peroxidases.

The expression of recombinant hemoproteins results in the vast majority of the protein lacking the heme prosthetic group [1-6]. This comes as a consequence of the expression of the protein outpacing the production of the heme prosthetic group. SDS-PAGE evaluation of recombinant KatP shows two proteins with molecular weights around that of KatP. Mass spectrometric analysis revealed both proteins to be KatP. Characterization of both showed one to have heme and activity while the other had neither. The discovery of the Trp-Tyr-Met covalent adduct in catalase-peroxidases may help to explain this phenomenon. The lack of heme in a similar system (e.g., cytochrome c peroxidase) results in protein without the covalent adduct which requires the presence of heme in the active site for its formation [201]. The presence of heme in catalase-peroxidases would yield a protein unable to be completely denatured by SDS as a result of its inability to disrupt the covalent adduct. Incompletely denatured catalase-peroxidases would migrate at a different apparent molecular weight than their completely denatured counterparts. The ability to distinguish KatP with and without this covalent adduct by SDS-PAGE makes it a good way to monitor the presence of the cross-link in catalase-peroxidases. The expression of KatG results in ~ 95 % of apo-protein, and is ideal for monitoring cross-link formation. The addition of heme to purified apo-KatG showed a migration shift of ~ 50% of the protein indicating the formation of the covalent adduct. In similar systems, the presence of heme has also been shown to be required in the active site for the formation of this covalent adduct [201]. An interesting aspect about

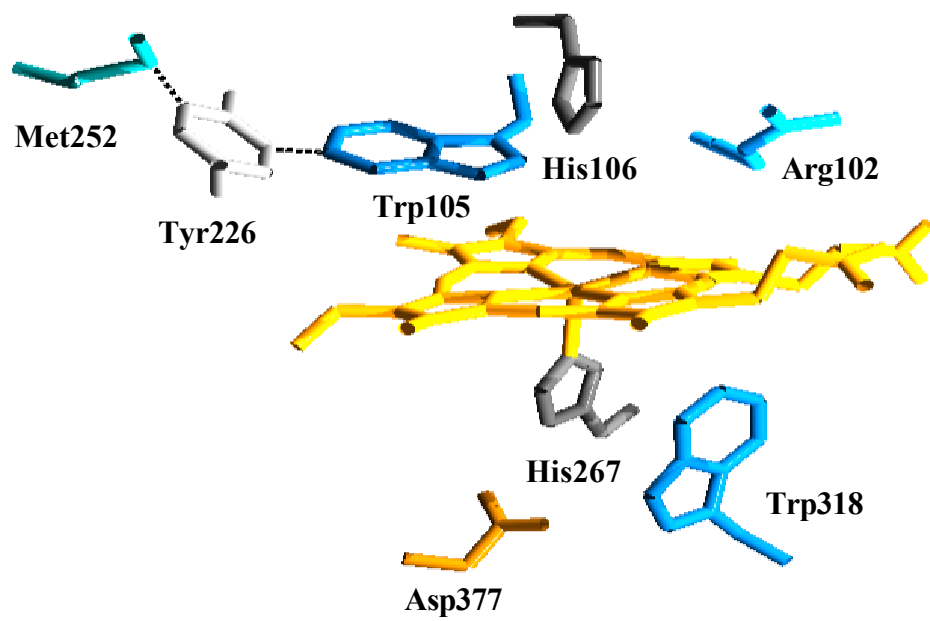


Figure 4.4. Active Site Representation of *E. coli* Catalase-Peroxidase [29].

the formation of this covalent adduct is that it appears to involve some redox chemistry. This was confirmed when the non-redox active Zn-protoporphyrin IX was added to apo-KatG, no formation of cross-link was observed. The formation of the covalent adduct in only half of KatG protein indicated that heme alone was not sufficient enough to facilitate the cross-link. The redox chemistry of the cross-link formation implicated perhaps the need of an exogenous oxidant. The addition of peracetic acid along with heme to apo-KatG showed formation of the covalent adduct in nearly 100% of the protein. Others have also shown that the formation of the covalent adduct involves a redox-linked reaction and requires the presence of peroxide or other oxidants alone with heme in the active site [201, 202]. The substitution of the central amino acid, Tyr to Phe, results in the disruption of the covalent adduct revealed by SDS-PAGE. The addition of heme or peroxide to KatG^{Y226F} showed no migration shift indicating no formation of covalent adduct.

This adduct appears to be essential for the full function of the enzyme. Indeed, substitution of either the tyrosine or the tryptophan residue with phenylalanine has been shown to interrupt the formation of the adduct and completely eliminate catalase activity [203, 204]. Interestingly, peroxidase activity is retained or even enhanced in these variants. On the other hand, mutation of methionine does not interrupt the cross-link between tyrosine and tryptophan [202]. Like the Trp and Tyr substitutions, mutation of Met also eliminates catalase activity but maintains peroxidase activity. This indicates that the formation of the Trp-Tyr link is the first step in adduct formation and suggests that Trp-Tyr cross-linking is not sufficient to generate catalase activity.

The formation of the Trp-Tyr-Met adduct is proposed by Ortiz de Montellano to be an autocatalytic process that uses compound I as the oxidizing species (Fig. 4.5) [202]. Formation of compound I leads to oxidation of both Trp and Tyr (Fig. 4.5a-b). Coupling of the two radicals results in the formation of the Trp-Tyr link (c). Formation of a second compound I intermediate further oxidizes the Trp-Tyr link (d-e). A nucleophilic attack of the sulfur atom of Met results in the formation of the Tyr-Met link, yielding the Trp-Tyr-Met adduct (f-g). The role this covalent adduct plays in catalase-peroxidases activity is not fully understood. The Trp-Tyr-Met covalent adduct may help provide the correct architecture of the active site. It also may be involved in the electron tunneling that is essential for catalysis. What is obvious is that this covalent adduct is required for the two-electron reduction of compound I involved in catalase activity but does not seem to be required for the two-electron reduction for peroxidase activity.

Summary

The activation of dioxygen is important to life in an aerobic environment. Transition metals are the key to this activation. However, active oxygen is highly reactive and can react with most macromolecules with damaging even life-threatening consequences. The control of this double-edged sword is essential. Nature has developed ways to control active oxygen by controlling the environment in which oxygen is activated. The control of iron during transport and storage and its placement in structures like porphyrins to generate a prosthetic group is part of the control of oxygen

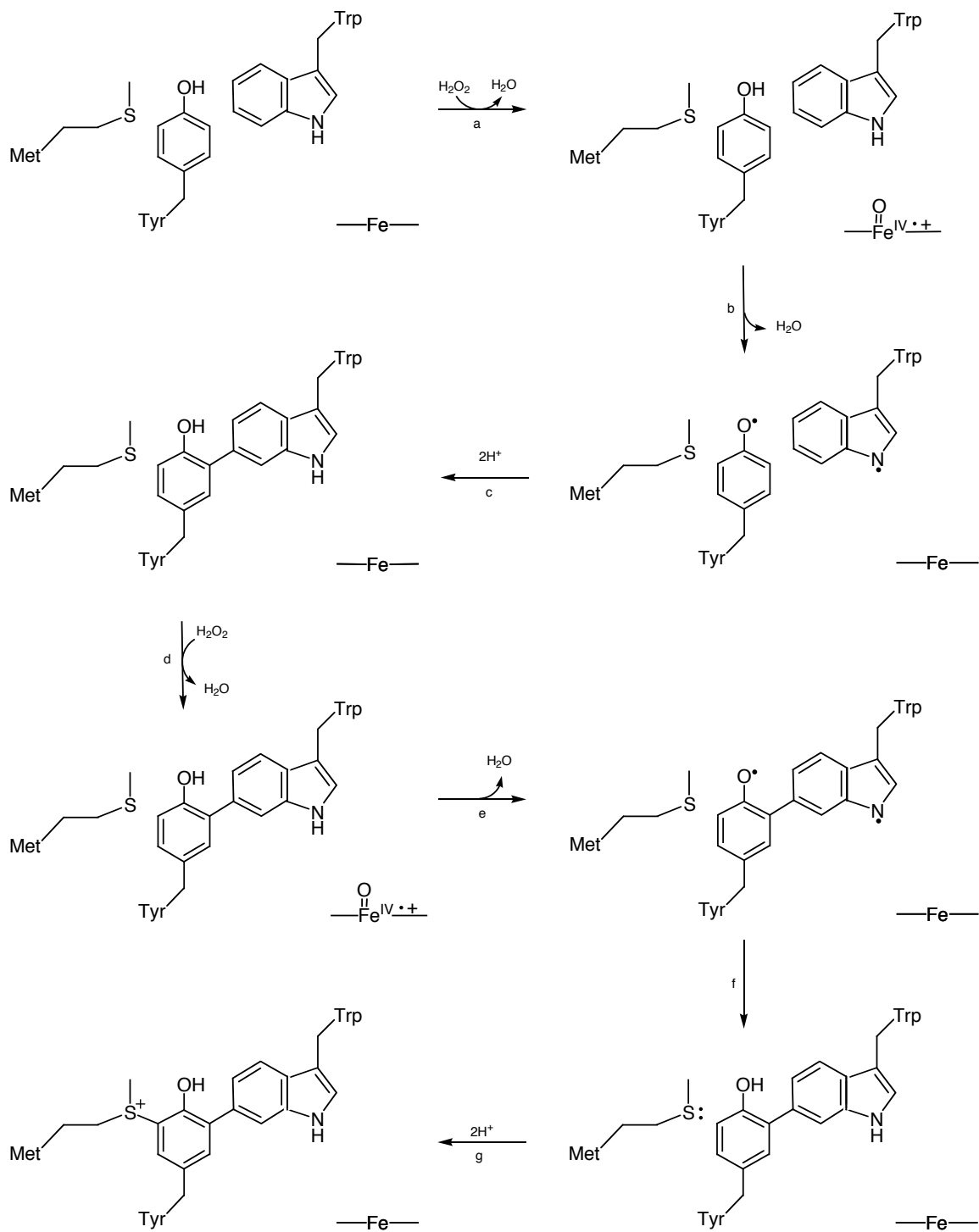


Figure 4.5. Proposed Mechanism for Formation of the Trp-Tyr-Met Adduct of Catalase-peroxidase.

activation. This alone is not sufficient. The protein environment around the prosthetic group (e.g., heme) must provide pinpoint control in order to achieve the desired function. Furthermore, there must be mechanisms in place to dispose of reactive oxygen species when they are unintentionally released.

In both respects, hemoproteins are an intriguing group of proteins. They demonstrate exquisite catalytic control, and some of them are used for rapid removal of reactive oxygen species. The versatility of function demonstrated by proteins that all use the same prosthetic group is ensured by the structure of the protein itself. This, of course, occurs at many levels. The first being the ligand(s) to the heme iron which are usually supplied by the protein. The second being the immediate environment of the heme and its ligand, and the third being the global protein structure, which may include features some distance from the active site. A complete understanding of how protein structure dictates heme function at all levels will have invaluable benefits to science and medicine. This dissertation describes the development and testing of a protein expression system that alleviates a common difficulty in successful production of hemoproteins in their holo state.

This HPEX system is designed to increase heme content of a protein of interest by simply supplementing the expression medium with hemin. The HPEX system was shown to express a functional heme receptor. The system has been shown to enhance expression of very different proteins in their holo state. The catalase-peroxidases are heme-containing enzymes that provide a unique opportunity to evaluate how protein structures distant from the active site actually serve to fine-tune its catalytic capabilities.

Interestingly, there is a set of periplasmic catalase-peroxidases which are only produced by highly pathogenic bacteria. These periplasmic enzymes may be virulence factors. This dissertation describes the first complete characterization of one of these enzymes, KatP from *E. coli* O157:H7. Absorption and EPR spectra of KatP were consistent with other catalase-peroxidase in that they indicated a dominance of high-spin heme. However, KatP showed a greater proportion of the hexacoordinate high-spin state. Apparent k_{cat} values for both catalase and peroxidase were somewhat higher consistent with most other catalase-peroxidases. On the other hand, K_M values were higher for KatP. KatP formation of compound I and CN^- binding were also consistent with other catalase-peroxidase. Along with its location in the periplasm, KatP reacts with peroxyxynitrite to form compound I. This may make KatP ideally suited to address the reactive species produced by the immune response to invading bacteria.

The presence of a Trp-Tyr-Met covalent adduct was shown to affect the migration of KatG protein by SDS-PAGE. The formation of the covalent adduct required the presence of the heme. The non-redox active Zn-protoporphyrin IX did not result in the formation of the covalent adduct, indicating that redox activity was required. The formation of the covalent adduct was enhanced by a peroxide only if a redox active porphyrin was also present. The covalent adduct was required for catalase activity but not peroxidase activity. Interestingly, KatG became more sensitive to higher concentrations of hydrogen peroxide if it was unable to establish the covalent adduct. This is typical of monofunctional peroxidases, which also lack catalase activity.

REFERENCES

- [1] Chouchane, S., Lippai, I., and Magliozzo, R. S., Catalase-peroxidase (mycobacterium tuberculosis katg) catalysis and isoniazid activation, *Biochemistry* 39 (2000) 9975-9983.
- [2] Nie, G., Reading, N. S., and Aust, S. D., Expression of the lignin peroxidase h2 gene from phanerochaete chrysosporium in escherichia coli, *Biochemical and Biophysical Research Communications* 249 (1998) 146-150.
- [3] Nishimoto, M., Clark, J. E., and Masters, B. S., Cytochrome p450 4a4: Expression in escherichia coli, purification, and characterization of catalytic properties, *Biochemistry* 32 (1993) 8863-8870.
- [4] Smith, M. A., Napier, J. A., Stymne, S., Tatham, A. S., Shewry, P. R., and Stobart, A. K., Expression of a biologically active plant cytochrome b5 in escherichia coli, *Biochemical Journal* 303 (1994) 73-79.
- [5] Sinha, N., and Ferguson, S. J., An escherichia coli ccm (cytochrome c maturation) deletion strain substantially expresses hydrogenobacter thermophilus cytochrome c552 in the cytoplasm: Availability of haem influences cytochrome c552 maturation, *FEMS Microbiology Letters* 161 (1998) 1-6.
- [6] Jung, Y., Kwak, J., and Lee, Y., High-level production of heme-containing holoproteins in escherichia coli, *Applied Microbiology and Biotechnology* 55 (2001) 187-191.

- [7] Woodard S. I., and Dailey H. A., Regulation of heme biosynthesis in *escherichia coli*, *Archives of Biochemistry and Biophysics* 316 (1995) 110-115.
- [8] Mills, M., and Payne, S. M., Genetics and regulation of heme iron transport in *shigella dysenteriae* and detection of an analogous system in *escherichia coli* o157:H7, *Journal of Bacteriology* 177 (1995) 3004-3009.
- [9] Wandersman, C., and Stojiljkovic, I., Bacterial heme sources: The role of heme, hemoprotein receptors and hemophores, *Current Opinion in Microbiology* 3 (2000) 215-220.
- [10] Bracken, C. S., Baer, M. T., Abdur-Rashid, A., Helms, W., and Stojiljkovic, I., Use of heme-protein complexes by the *yersinia enterocolitica* hemr receptor: Histidine residues are essential for receptor function, *Journal of Bacteriology* 181 (1999) 6063-6072.
- [11] Torres, A. G., and Payne, S. M., Haem iron-transport system in enterohaemorrhagic *escherichia coli* o157:H7, *Molecular Microbiology* 23 (1997) 825-833.
- [12] Law, D., Virulence factors of *escherichia coli* o157 and other shiga toxin- producing *e. coli*, *Journal of Applied Microbiology* 88 (2000) 729-745.
- [13] Law, D., and Kelly, J., Use of heme and hemoglobin by *escherichia coli* o157 and other shiga-like- toxin-producing *e. coli* serogroups, *Infection and Immunity* 63 (1995) 700-702.
- [14] Mills, M., and Payne, S., Identification of *shua*, the gene encoding the heme receptor of *shigella dysenteriae*, and analysis of invasion and intracellular multiplication of a *shua* mutant, *Infect. Immun.* 65 (1997) 5358-5363.

- [15] Thompson, J. M., Jones, H. A., and Perry, R. D., Molecular characterization of the hemin uptake locus (hmu) from *yersinia pestis* and analysis of hmu mutants for hemin and hemoprotein utilization, *Infection and Immunity* 67 (1999) 3879-3892.
- [16] Schryvers, A. B., and Stojiljkovic, I., Iron acquisition systems in the pathogenic *neisseria*, *Molecular Microbiology* 32 (1999) 1117-1123.
- [17] Litwin, C. M., and Byrne, B. L., Cloning and characterization of an outer membrane protein of *vibrio vulnificus* required for heme utilization: Regulation of expression and determination of the gene sequence, *Infection and Immunity* 66 (1998) 3134-3141.
- [18] Stojiljkovic, I., Larson, J., Hwa, V., Anic, S., and So, M., Hmbr outer membrane receptors of pathogenic *neisseria* spp.: Iron-regulated, hemoglobin-binding proteins with a high level of primary structure conservation, *Journal of Bacteriology* 178 (1996) 4670-4678.
- [19] Stojiljkovic, I., and Hantke, K., Transport of haemin across the cytoplasmic membrane through a haemin-specific periplasmic binding-protein-dependent transport system in *yersinia enterocolitica*, *Mol. Microbiol.* 13 (1994) 719-732.
- [20] Law, D., and Kelly, J., Use of heme and hemoglobin by *escherichia-coli* o157 and other shiga-like-toxin-producing *escherichia-coli* serogroups, *Infection and Immunity* 63 (1995) 700-702.
- [21] Hillar, A., Van Caesele, L., and Loewen, P. C., Intracellular location of catalase-peroxidase hydroperoxidase i of *escherichia coli*, *FEMS Microbiology Letters* 170 (1999) 307-312.

- [22] Bandyopadhyay, P., and Steinman, H. M., Legionella pneumophila catalase-
peroxidases: Cloning of the katb gene and studies of katb function, Journal of
Bacteriology 180 (1998) 5369-5374.
- [23] Bandyopadhyay, P., and Steinman, H. M., Catalase-peroxidases of legionella
pneumophila: Cloning of the kata gene and studies of kata function, Journal of
Bacteriology 182 (2000) 6679-6686.
- [24] Brunder, W., Schmidt, H., and Karch, H., Katp, a novel catalase-peroxidase encoded
by the large plasmid of enterohaemorrhagic escherichia coli o157:H7, Microbiology 142
(1996) 3305-3315.
- [25] Garcia, E., Nedialkov, Y. A., Elliott, J., Motin, V. L., and Brubaker, R. R.,
Molecular characterization of katy (antigen 5), a thermoregulated chromosomally
encoded catalase-peroxidase of yersinia pestis, Journal of Bacteriology 181 (1999) 3114-
3122.
- [26] Mehigh, R. J., and Brubaker, R. R., Major stable peptides of yersinia pestis
synthesized during the low- calcium response, Infection and Immunity 61 (1993) 13-22.
- [27] Amemura-Maekawa, J., Mishima-Abe, S., Kura, F., Takahashi, T., and Watanabe,
H., Identification of a novel periplasmic catalase-peroxidase kata of legionella
pneumophila, FEMS Microbiology Letters 176 (1999) 339-344.
- [28] Bertrand, T., Eady, N. A. J., Jones, J. N., Nagy, J. M., Jamart-Gregoire, B., Raven,
E. L., and Brown, K. A., Crystal structure of mycobacterium tuberculosis catalase-
peroxidase, Journal of Biological Chemistry 279 (2004) 38991-38999.

- [29] Yamada, Y., Fujiwara, T., Sato, T., Igarashi, N., and Tanaka, N., The 2.0 angstrom crystal structure of catalase-peroxidase from *haloarcula marismortui*, *Nature Structural Biology* 9 (2002) 691-695.
- [30] Carpena, X., Loprasert, S., Mongkolsuk, S., Switala, J., Loewen, P. C., and Fita, I., Catalase-peroxidase katg of *burkholderia pseudomallei* at 1.7 a resolution, *Journal of Molecular Biology* 327 (2003) 475-489.
- [31] Yu, S., Giroto, S., Zhao, X., and Magliozzo, R. S., Rapid formation of compound ii and a tyrosyl radical in the y229f mutant of *mycobacterium tuberculosis* catalase-peroxidase disrupts catalase but not peroxidase function, *J. Biol. Chem.* 278 (2003) 44121-44127.
- [32] Santoni, E., Jakopitsch, C., Obinger, C., and Smulevich, G., Manipulating the covalent link between distal side tryptophan, tyrosine, and methionine in catalase-peroxidases: An electronic absorption and resonance raman study, *Biopolymers* 74 (2004) 46-50.
- [33] Jakopitsch, C., Kolarich, D., Petutschnig, G., Furtmuller, P. G., and Obinger, C., Distal side tryptophan, tyrosine and methionine in catalase-peroxidases are covalently linked in solution, *FEBS Letters* 552 (2003) 135-140.
- [34] Jakopitsch, C., Auer, M., Ivancich, A., Ruker, F., Furtmuller, P. G., and Obinger, C., Total conversion of bifunctional catalase-peroxidase (katg) to monofunctional peroxidase by exchange of a conserved distal side tyrosine, *J. Biol. Chem.* 278 (2003) 20185-20191.
- [35] Regelsberger, G., Jakopitsch, C., Ruker, F., Krois, D., Peschek, G. A., and Obinger, C., Effect of distal cavity mutations on the formation of compound i in catalase-peroxidases, *Journal of Biological Chemistry* 275 (2000) 22854-22861.

- [36] Regelsberger, G., Jakopitsch, C., Furtmuller, P. G., Rueker, F., Switala, J., Loewen, P. C., and Obinger, C., The role of distal tryptophan in the bifunctional activity of catalase-peroxidases., *Biochemical Society Transactions* 29 (2001) 99-105.
- [37] Hillar, A., Peters, B., Pauls, R., Loboda, A., Zhang, H., Mauk, A. G., and Loewen, P. C., Modulation of the activities of catalase-peroxidase hpi of escherichia coli by site-directed mutagenesis, *Biochemistry* 39 (2000) 5868-5875.
- [38] Halliwell, B., and Gutteridge, J. M. C., Oxygen-toxicity, oxygen radicals, transition-metals and disease, *Biochemical Journal* 219 (1984) 1-14.
- [39] Koppenol, W. H., Thermodynamics of reactions involving oxyradicals and hydrogen-peroxide, *Bioelectrochemistry and Bioenergetics* 18 (1987) 3-11.
- [40] Wood, P. M., The potential diagram for oxygen at ph-7, *Biochemical Journal* 253 (1988) 287-289.
- [41] Miller, D. M., Buettner, G. R., and Aust, S. D., Transition-metals as catalysts of autoxidation reactions, *Free Radical Biology and Medicine* 8 (1990) 95-108.
- [42] Surdhar, P. S., and Armstrong, D. A., Redox potentials of some sulfur-containing radicals, *Journal of Physical Chemistry* 90 (1986) 5915-5917.
- [43] Buettner, G. R., The pecking order of free-radicals and antioxidants - lipid-peroxidation, alpha-tocopherol, and ascorbate, *Archives of Biochemistry and Biophysics* 300 (1993) 535-543.
- [44] Devries, S., Berden, J. A., and Slater, E. C., Properties of a semi-quinone anion located in the qh2-cytochrome-c oxidoreductase segment of the mitochondrial respiratory-chain, *Febs Letters* 122 (1980) 143-148.

- [45] Anderson, R. F., Energetics of the one-electron reduction steps of riboflavin, *fmn* and *fad* to their fully reduced forms, *Biochimica Et Biophysica Acta* 722 (1983) 158-162.
- [46] Harris, D. C., Rinehart, A. L., Hereld, D., Schwartz, R. W., Burke, F. P., and Salvador, A. P., Reduction potential of iron in transferrin, *Biochimica Et Biophysica Acta* 838 (1985) 295-301.
- [47] Klotz, I. M., and Kurtz, D. M., Metal-dioxygen complexes - a perspective, *Chemical Reviews* 94 (1994) 567-568.
- [48] Toyokuni, S., Iron and carcinogenesis: From fenton reaction to target genes, *Redox Report* 7 (2002) 189-197.
- [49] Lloyd, R. V., Hanna, P. M., and Mason, R. P., The origin of the hydroxyl radical oxygen in the fenton reaction, *Free Radical Biology and Medicine* 22 (1997) 885-888.
- [50] Raleigh, J. A., and Shum, F. Y., Hydroxyl radical scavengers and membrane damage - supplementary role for alpha-tocopherol in scavenging secondary radicals, *Radiation Research* 94 (1983) 664-665.
- [51] Anbar, M., Meyerste.D, and Neta, P., Reactivity of aliphatic compounds towards hydroxyl radicals, *Journal of the Chemical Society B-Physical Organic* (1966) 742.
- [52] Pryor, W. A., Why is the hydroxyl radical the only radical that commonly adds to DNA? Hypothesis: It has a rare combination of high electrophilicity, high thermochemical reactivity, and a mode of production that can occur near DNA, *Free Radical Biology and Medicine* 4 (1988) 219-223.
- [53] Jaruga, P. W., Rodriguez, H., and Dizdaroglu, M., Measurement of 8-hydroxy-2'-deoxyadenosine in DNA by liquid chromatography/mass spectrometry, *Free Radical Biology and Medicine* 31 (2001) 336-344.

- [54] Zastawny, T. H., Altman, S. A., Randerseichhorn, L., Madurawe, R., Lumpkin, J. A., Dizdaroglu, M., and Rao, G., DNA-base modifications and membrane damage in cultured-mammalian-cells treated with iron ions, *Free Radical Biology and Medicine* 18 (1995) 1013-1022.
- [55] Kumar, S., and Bandyopadhyay, U., Free heme toxicity and its detoxification systems in human, *Toxicology Letters* 157 (2005) 175-188.
- [56] O'Brian, M., Heme synthesis in the rhizobium-legume symbiosis: A palette for bacterial and eukaryotic pigments, *J. Bacteriol.* 178 (1996) 2471-2478.
- [57] Ryter, S. W., and Tyrrell, R. M., The heme synthesis and degradation pathways: Role in oxidant sensitivity - heme oxygenase has both pro- and antioxidant properties, *Free Radical Biology and Medicine* 28 (2000) 289-309.
- [58] Shifman, J. M., Gibney, B. R., Sharp, R. E., and Dutton, P. L., Heme redox potential control in de novo designed four-alpha-helix bundle proteins, *Biochemistry* 39 (2000) 14813-14821.
- [59] Caughey, W. S., Smythe, G. A., Okeeffe, D. H., Maskasky, J. E., and Smith, M. L., Heme-a of cytochrome-c oxidase - structure and properties - comparisons with heme-b, heme-c and heme-s and derivatives, *Journal of Biological Chemistry* 250 (1975) 7602-7622.
- [60] Allen, J. W. A., Leach, N., and Ferguson, S. J., The histidine of the c-type cytochrome cxxch haem-binding motif essential for haem attachment by the escherichia coli cytochrome maturation (ccm) apparatus, *Biochemical Journal* 389 (2005) 587-592.
- [61] Tomlinson, E. J., and Ferguson, S. J., Conversion of a c type cytochrome to a b type that spontaneously forms in vitro from apo protein and heme: Implications for c type

cytochrome biogenesis and folding, *Proceedings of the National Academy of Sciences of the United States of America* 97 (2000) 5156-5160.

[62] Antonini, E., and Brunori, M., in, 1971, North-Holland, Amsterdam.

[63] White, R. E., and Coon, M. J., Oxygen activation by cytochrome-p-450, *Annual Review of Biochemistry* 49 (1980) 315-356.

[64] Adachi, S., Nagano, S., Ishimori, K., Watanabe, Y., Morishima, I., Egawa, T., Kitagawa, T., and Makino, R., Roles of proximal ligand in heme-proteins - replacement of proximal histidine of human myoglobin with cysteine and tyrosine by site-directed mutagenesis as models for p-450, chloroperoxidase, and catalase, *Biochemistry* 32 (1993) 241-252.

[65] Quillin, M. L., Arduini, R. M., Olson, J. S., and Phillips, G. N., High-resolution crystal-structures of distal histidine mutants of sperm whale myoglobin, *Journal of Molecular Biology* 234 (1993) 140-155.

[66] Krzywda, S., Murshudov, G. N., Brzozowski, A. M., Jaskolski, M., Scott, E. E., Klizas, S. A., Gibson, Q. H., Olson, J. S., and Wilkinson, A. J., Stabilizing bound o-2 in myoglobin by valine(68) (e11) to asparagine substitution, *Biochemistry* 37 (1998) 15896-15907.

[67] Perutz, M. F., Rossmann, M. G., Cullis, A. F., Muirhead, H., Will, G., and North, A. C. T., Structure of hemoglobin. A three-dimensional fourier synthesis at 5.5- \AA . Resolution, obtained by x-ray analysis, *Nature* 185 (1960) 416-422.

[68] Kendrew, J. C. D., R. E.; Strandberg, B. E.; Hart, R. G.; Davies, D. R.; Phillips, D. C.; Shore, V. C., Structure of myoglobin. Three-dimensional fourier synthesis at 2 \AA . Resolution, *Nature* 185 (1960) 422-427.

- [69] Collman, J. P., Boulatov, R., Sunderland, C. J., and Fu, L., Functional analogues of cytochrome c oxidase, myoglobin, and hemoglobin, *Chemical Reviews* 104 (2004) 561-588.
- [70] Theorell, H., Crystalline myoglobin. V. Oxygen-binding curve of myoglobin, *Biochemische Zeitschrift* 268 (1934) 73-82.
- [71] Finch, J. T., Perutz, M. F., Bertles, J. F., and Doebler, J., Structure of sickled erythrocytes and of sickle-cell hemoglobin fibers, *Proceedings of the National Academy of Sciences of the United States of America* 70 (1973) 718-722.
- [72] Gelin, B. R., Lee, A. W. M., and Karplus, M., Hemoglobin tertiary structural-change on ligand-binding - its role in the co-operative mechanism, *Journal of Molecular Biology* 171 (1983) 489-559.
- [73] Klingenberg, M., Pigments of rat liver microsomes, *Archives of Biochemistry and Biophysics* 75 (1958) 376-386.
- [74] Sono, M., Roach, M. P., Coulter, E. D., and Dawson, J. H., Heme-containing oxygenases, *Chemical Reviews* 96 (1996) 2841-2887.
- [75] Lemberg, M. R., Cytochrome oxidase, *Physiological Reviews* 49 (1969) 48.
- [76] Wikstrom, M., Krab, K., and Saraste, M., *Cytochrome oxidase a synthesis*, ed., Academic Press Inc., New York 1981.
- [77] Iwata, S., Ostermeier, C., Ludwig, B., and Michel, H., Structure at 2.8-angstrom resolution of cytochrome-c-oxidase from *paracoccus-denitrificans*, *Nature* 376 (1995) 660-669.

- [78] Antalík, M., Jancura, D., Palmer, G., and Fabian, M., A role for the protein in internal electron transfer to the catalytic center of cytochrome c oxidase, *Biochemistry* 44 (2005) 14881-14889.
- [79] Varotsis, C., Zhang, Y., Appelman, E. H., and Babcock, G. T., Resolution of the reaction sequence during the reduction of O₂ by cytochrome-oxidase, *Proceedings of the National Academy of Sciences of the United States of America* 90 (1993) 237-241.
- [80] Chance, B., and Erecinsk.M, Flow flash kinetics of cytochrome a₃-oxygen reaction in coupled and uncoupled mitochondria using liquid dye laser, *Archives of Biochemistry and Biophysics* 143 (1971) 675.
- [81] Gibson, Q. H., and Greenwood, C., Reactions of cytochrome oxidase with oxygen and carbon monoxide, *Biochemical Journal* 86 (1963) 541.
- [82] Turrens, J. F., Mitochondrial formation of reactive oxygen species, *Journal of Physiology-London* 552 (2003) 335-344.
- [83] Welinder, K. G., Superfamily of plant, fungal and bacterial peroxidases, *Current Opinion in Structural Biology* 2 (1992) 388-393.
- [84] Schuller, D. J., Ban, N., vanHuystee, R. B., McPherson, A., and Poulos, T. L., The crystal structure of peanut peroxidase, *Structure* 4 (1996) 311-321.
- [85] Boerjan, W., Ralph, J., and Baucher, M., Lignin biosynthesis, *Annual Review of Plant Biology* 54 (2003) 519-546.
- [86] Hilden, K. S., Makela, M. R., Hakala, T. K., Hatakka, A., and Lundell, T., Expression on wood, molecular cloning and characterization of three lignin peroxidase (lip) encoding genes of the white rot fungus *Phlebia radiata*, *Current Genetics* 49 (2006) 97-105.

- [87] Loew, G., Structure, spectra, and function of heme sites, *International Journal of Quantum Chemistry* 77 (2000) 54-70.
- [88] Wang, J. M., Mauro, J. M., Edwards, S. L., Oatley, S. J., Fishel, L. A., Ashford, V. A., Xuong, N. H., and Kraut, J., X-ray structures of recombinant yeast cytochrome-c peroxidase and 3 heme-cleft mutants prepared by site-directed mutagenesis, *Biochemistry* 29 (1990) 7160-7173.
- [89] Pennerhahn, J. E., Eble, K. S., McMurry, T. J., Renner, M., Balch, A. L., Groves, J. T., Dawson, J. H., and Hodgson, K. O., Structural characterization of horseradish-peroxidase using exafs spectroscopy - evidence for fe=O ligation in compound-i and compound-ii, *Journal of the American Chemical Society* 108 (1986) 7819-7825.
- [90] Moss, T. H., Ehrenber.A, and Bearden, A. J., Mossbauer spectroscopic evidence for electronic configuration of iron in horseradish peroxidase and its peroxide derivatives, *Biochemistry* 8 (1969) 4159.
- [91] Houseman, A. L. P., Doan, P. E., Goodin, D. B., and Hoffman, B. M., Comprehensive explanation of the anomalous epr-spectra of wild-type and mutant cytochrome-c peroxidase compound-es, *Biochemistry* 32 (1993) 4430-4443.
- [92] Wittenbe, J. B., Noble, R. W., Wittenbe.Ba, Antonini, E., Brunori, M., and Wyman, J., Studies on equilibria and kinetics of reactions of peroxidase with ligands .2. Reaction of ferropoxidase with oxygen, *Journal of Biological Chemistry* 242 (1967) 626.
- [93] Adediran, S. A., Kinetics of the formation of p-670 and of the decay of compound iii of horseradish peroxidase, *Archives of Biochemistry and Biophysics* 327 (1996) 279-284.
- [94] Yamazaki, I., and Piette, L. H., The mechanism of aerobic oxidase reaction catalyzed by peroxidase, *Biochimica Et Biophysica Acta* 77 (1963) 47-64.

- [95] Nakajima, R., and Yamazaki, I., The mechanism of oxypoxidase formation from ferryl peroxidase and hydrogen-peroxide, *Journal of Biological Chemistry* 262 (1987) 2576-2581.
- [96] Arnao, M. B., Acosta, M., Delrio, J. A., and Garcíacanoas, F., Inactivation of peroxidase by hydrogen-peroxide and its protection by a reductant agent, *Biochimica Et Biophysica Acta* 1038 (1990) 85-89.
- [97] Warburg, O., Versuche und uberledbeudem carcinomgewebe (methoden). *Biochem Z.* 142 (1923) 317-333.
- [98] Stern, K. G., The constitution of the prosthetic group of catalase, *J. Biol. Chem.* 112 (1936) 661-669.
- [99] Fita, I., and Rossmann, M. G., The active center of catalase, *Journal of Molecular Biology* 185 (1985) 21-37.
- [100] Zamocky, M., and Koller, F., Understanding the structure and function of catalases: Clues from molecular evolution and in vitro mutagenesis, *Progress in Biophysics & Molecular Biology* 72 (1999) 19-66.
- [101] Chelikani, P., Fita, I., and Loewen, P. C., Diversity of structures and properties among catalases, *Cellular and Molecular Life Sciences* 61 (2004) 192-208.
- [102] Melik-Adamyán, W. R., Barynin, V. V., Vagin, A. A., Borisov, V. V., Vainshtein, B. K., Fita, I., Murthy, M. R. N., and Rossmann, M. G., Comparison of beef liver and penicillium vitale catalases,, *Journal of Molecular Biology* 188 (1986) 63-72.
- [103] Chaga, G. S., Medin, A. S., Chaga, S. G., and Porath, J. O., Isolation and characterization of catalase from penicillium-chrysogenum, *Journal of Chromatography* 604 (1992) 177-183.

- [104] Murshudov, G. N., Grebenko, A. I., Barynin, V., Dauter, Z., Wilson, K. S., Vainshtein, B. K., MelikAdamyanyan, W., Bravo, J., Ferran, J. M., Ferrer, J. C., Switala, J., Loewen, P. C., and Fita, I., Structure of the heme d of penicillium vitale and escherichia coli catalases, *Journal of Biological Chemistry* 271 (1996) 8863-8868.
- [105] Paoli, M., Marles-Wright, J., and Smith, A., Structure-function relationships in heme-proteins, *DNA and Cell Biology* 21 (2002) 271-280.
- [106] Vainshtein, B. K., Melikadamyanyan, W. R., Barynin, V. V., Vagin, A. A., and Grebenko, A. I., 3-dimensional structure of the enzyme catalase, *Nature* 293 (1981) 411-412.
- [107] Bravo, J., Mate, M. J., Schneider, T., Switala, J., Wilson, K., Loewen, P. C., and Fita, I., Structure of catalase hpii from escherichia coli at 1.9 angstrom resolution, *Proteins-Structure Function and Genetics* 34 (1999) 155-166.
- [108] Nicholis, P., Fita, I., and Loewen, P. C., Enzymology and structure of catalase, in *Advances in inorganic chemistry*, in Sykes, A., (Ed.), Academic Press, San Diego, 2001, pp. 51-106.
- [109] Kirkman, H., Galiano, S., and Gaetani, G., The function of catalase-bound nadph, *J. Biol. Chem.* 262 (1987) 660-666.
- [110] Ng, V. H., Cox, J. S., Sousa, A. O., MacMicking, J. D., and McKinney, J. D., Role of katg catalase-peroxidase in mycobacterial pathogenesis: Countering the phagocyte oxidative burst, *Molecular Microbiology* 52 (2004) 1291-1302.
- [111] Triggsraine, B. L., Doble, B. W., Mulvey, M. R., Sorby, P. A., and Loewen, P. C., Nucleotide-sequence of katg, encoding catalase hpi of escherichia-coli, *Journal of Bacteriology* 170 (1988) 4415-4419.

- [112] Claiborne, A., and Fridovich, I., Purification of the ortho-dianisidine peroxidase from *Escherichia coli* - physicochemical characterization and analysis of its dual catalytic and peroxidatic activities, *Journal of Biological Chemistry* 254 (1979) 4245-4252.
- [113] Cannac-Caffrey, V., Hudry-Clergeon, G., Petillot, Y., Gagnon, J., Zaccari, G., and Franzetti, B., The protein sequence of an archaeal catalase-peroxidase, *Biochimie* 80 (1998) 1003-1011.
- [114] Welinder, K. G., Bacterial catalase-peroxidases are gene duplicated members of the plant peroxidase superfamily, *Biochimica Et Biophysica Acta* 1080 (1991) 215-220.
- [115] Patterson, W. R., and Poulos, T. L., Crystal-structure of recombinant pea cytosolic ascorbate peroxidase, *Biochemistry* 34 (1995) 4331-4341.
- [116] Baker, R. D., Cook, C. O., and Goodwin, D. C., Properties of catalase-peroxidase lacking its c-terminal domain, *Biochemical and Biophysical Research Communications* 320 (2004) 833-839.
- [117] Sundaramoorthy, M., Kishi, K., Gold, M. H., and Poulos, T. L., The crystal structure of manganese peroxidase from *Phanerochaete chrysosporium* at 2.06-Å resolution, *Journal of Biological Chemistry* 269 (1994) 32759-32767.
- [118] Sutherland, G. R. J., and Aust, S. D., Thermodynamics of binding of the distal calcium to manganese peroxidase, *Biochemistry* 36 (1997) 8567-8573.
- [119] Zamocky, M., Regelsberger, G., Jakopitsch, C., and Obinger, C., The molecular peculiarities of catalase-peroxidases, *FEBS Letters* 492 (2001) 177-182.
- [120] Li, Y., in *Chemistry and Biochemistry*, 2005 p. 190 Auburn University, Auburn, AL.

- [121] Li, Y. J., and Goodwin, D. C., Vital roles of an interhelical insertion in catalase-peroxidase bifunctionality, *Biochemical and Biophysical Research Communications* 318 (2004) 970-976.
- [122] Murray, C. J. L., World tuberculosis burden, *Lancet* 335 (1990) 1043-1044.
- [123] Bernstein, J., Lott, W. A., Steinberg, B. A., and Yale, H. L., Chemotherapy of experimental tuberculosis .5. Isonicotinic acid hydrazide (nydrazid) and related compounds, *American Review of Tuberculosis* 65 (1952) 357-364.
- [124] Zhang, Y., Heym, B., Allen, B., Young, D., and Cole, S., The catalase peroxidase gene and isoniazid resistance of mycobacterium-tuberculosis, *Nature* 358 (1992) 591-593.
- [125] Shikama, K., A controversy on the mechanism of autoxidation of oxymyoglobin and oxyhemoglobin - oxidation, dissociation, or displacement, *Biochemical Journal* 223 (1984) 279-280.
- [126] Shikama, K., The molecular mechanism of autoxidation for myoglobin and hemoglobin: A venerable puzzle, *Chemical Reviews* 98 (1998) 1357-1373.
- [127] Wallace, W. J., Houtchens, R. A., Maxwell, J. C., and Caughey, W. S., Mechanism of autoxidation for hemoglobins and myoglobins - promotion of superoxide production by protons and anions, *Journal of Biological Chemistry* 257 (1982) 4966-4977.
- [128] Brantley, R. E., Smerdon, S. J., Wilkinson, A. J., Singleton, E. W., and Olson, J. S., The mechanism of autoxidation of myoglobin, *Journal of Biological Chemistry* 268 (1993) 6995-7010.
- [129] George, P., and Stratmann, C. J., The oxidation of myoglobin to metmyoglobin by oxygen .3. Kinetic studies in the presence of carbon monoxide, and at different hydrogen-

- ion concentrations with considerations regarding the stability of oxymyoglobin, *Biochemical Journal* 57 (1954) 568-573.
- [130] Weiss, J. J., Nature of iron-oxygen bond in oxyhaemoglobin, *Nature* 202 (1964) 83.
- [131] Sugawara, Y., Matsuoka, A., Kaino, A., and Shikama, K., Role of globin moiety in the autoxidation reaction of oxymyoglobin - effect of 8 m urea, *Biophysical Journal* 69 (1995) 583-592.
- [132] Tsubamoto, Y., Matsuoka, A., Yusa, K., and Shikama, K., Protozoan myoglobin from *paramecium-caudatum* - its autoxidation reaction and hemichrome formation, *European Journal of Biochemistry* 193 (1990) 55-59.
- [133] Gorsky, L., Koop, D., and Coon, M., On the stoichiometry of the oxidase and monooxygenase reactions catalyzed by liver microsomal cytochrome p-450. Products of oxygen reduction, *J. Biol. Chem.* 259 (1984) 6812-6817.
- [134] Zangar, R. C., Davydov, D. R., and Verma, S., Mechanisms that regulate production of reactive oxygen species by cytochrome p450, *Toxicology and Applied Pharmacology* 199 (2004) 316-331.
- [135] Nordblom, G. D., and Coon, M. J., Hydrogen-peroxide formation and stoichiometry of hydroxylation reactions catalyzed by highly purified liver microsomal cytochrome-p-450, *Archives of Biochemistry and Biophysics* 180 (1977) 343-347.
- [136] Hlavica, P., and Lewis, D. F. V., Allosteric phenomena in cytochrome p450-catalyzed monooxygenations, *European Journal of Biochemistry* 268 (2001) 4817-4832.
- [137] Gruenke, L. D., Konopka, K., Cadieu, M., and Waskell, L., The stoichiometry of the cytochrome p-450-catalyzed metabolism of methoxyflurane and benzphetamine in the

- presence and absence of cytochrome b(5), *Journal of Biological Chemistry* 270 (1995) 24707-24718.
- [138] Mehigh, R. J., and Brubaker, R. R., Major stable peptides of yersinia-pestis synthesized during the low-calcium response, *Infection and Immunity* 61 (1993) 13-22.
- [139] Demircay, Z., Eksioglu-Demiralp, E., Ergunt, T., and Akoglut, T., Phagocytosis and oxidative burst by neutrophils in patients with recurrent furunculosis, *British Journal of Dermatology* 138 (1998) 1036-1038.
- [140] Bolwell, G. P., and Wojtaszek, P., Mechanisms for the generation of reactive oxygen species in plant defence - a broad perspective, *Physiological and Molecular Plant Pathology* 51 (1997) 347-366.
- [141] Babior, B. M., Nadph oxidase, *Current Opinion in Immunology* 16 (2004) 42-47.
- [142] Jesaitis, A. J., Structure of human phagocyte cytochrome-b and its relationship to microbicidal superoxide production, *Journal of Immunology* 155 (1995) 3286-3288.
- [143] Cross, A. R., Rae, J., and Curnutte, J. T., Cytochrome-b(-245) of the neutrophil superoxide-generating system contains 2 nonidentical hemes - potentiometric studies of a mutant form of gp91(phox), *Journal of Biological Chemistry* 270 (1995) 17075-17077.
- [144] Fujii, H., Finnegan, M. G., Miki, T., Crouse, B. R., Kakinuma, K., and Johnson, M. K., Spectroscopic identification of the heme axial ligation of cytochrome b(558) in the nadph oxidase of porcine neutrophils, *Febs Letters* 377 (1995) 345-348.
- [145] Fujii, H., Finnegan, M. G., and Johnson, M. K., The active form of the ferric heme in neutrophil cytochrome b(558) is low-spin in the reconstituted cell-free system in the presence of amphophil, *Journal of Biochemistry* 126 (1999) 708-714.

- [146] Cross, A. R., Parkinson, J. F., and Jones, O. T. G., Mechanism of the superoxide-producing oxidase of neutrophils - o-2 is necessary for the fast reduction of cytochrome b-245 by nadph, *Biochemical Journal* 226 (1985) 881-884.
- [147] Rotrosen, D., Yeung, C. L., Leto, T. L., Malech, H. L., and Kwong, C. H., Cytochrome-b558 - the flavin-binding component of the phagocyte nadph oxidase, *Science* 256 (1992) 1459-1462.
- [148] Babior, B. M., Nadph oxidase: An update, *Blood* 93 (1999) 1464-1476.
- [149] Rosen, H., and Klebanoff, S. J., Bactericidal activity of a superoxide anion-generating system - model for the polymorphonuclear leukocyte, *Journal of Experimental Medicine* 149 (1979) 27-39.
- [150] Eberhardt, M. K., Reactive oxygen metabolites, ed., CRC Press LLC, Boca Raton, FL 2001.
- [151] Wengenack, N. L., Jensen, M. P., Rusnak, F., and Stern, M. K., Mycobacterium tuberculosis katg is a peroxynitritase, *Biochemical and Biophysical Research Communications* 256 (1999) 485-487.
- [152] Beckman, J. S., -oONO: Rebounding from nitric oxide, *Circ Res* 89 (2001) 295-297.
- [153] Brunelli, L., Crow, J. P., and Beckman, J. S., The comparative toxicity of nitric-oxide and peroxynitrite to escherichia-coli, *Archives of Biochemistry and Biophysics* 316 (1995) 327-334.
- [154] Goodwin, D. C., Landino, L. M., and Marnett, L. J., Reactions of prostaglandin endoperoxide synthase with nitric oxide and peroxynitrite, *Drug Metabolism Reviews* 31 (1999) 273-294.

- [155] Sambrook, J., Maniatis, T., and Fritsch, E. F., *Molecular cloning: A laboratory manual*, ed., Cold Spring Harbor 1989.
- [156] Gill, S. C., and von Hippel, P. H., Calculation of protein extinction coefficients from amino acid sequence data, *Analytical Biochemistry* 182 (1989) 319-326.
- [157] Falk., J. E., *Porphyrins and metalloporphyrins*, ed., Elsevier Publishing, New York 1964.
- [158] Nelson, D. P., and Kiesow, L. A., Enthalpy of decomposition of hydrogen-peroxide by catalase at 25 °c (with molar extinction coefficients of H_2O_2 solutions in uv), *Analytical Biochemistry* 49 (1972) 474.
- [159] S.L. Scott, W.-J. C., A. Bakac and J.H. Espenson, *J. Phys. Chem.* 97 (1993) 6710–6714.
- [160] Hellman U., Wernstedt C., Gonez J., and Heldin C. H., Improvement of an in-gel digestion procedure for the micropreparation of internal protein fragments for amino acid sequencing, *Analytical Biochemistry* 224 (1995) 451-455.
- [161] Rosenfeld, J., Capdevielle, J., Guillemot, J. C., and Ferrara, P., In-gel digestion of proteins for internal sequence analysis after one- or two-dimensional gel electrophoresis, *Analytical Biochemistry* 203 (1992) 173-179.
- [162] Studier, F. W., Use of bacteriophage t7 lysozyme to improve an inducible t7 expression system, *Journal of Molecular Biology* 219 (1991) 37-44.
- [163] Nielsen, H., Engelbrecht, J., Brunak, S., and Von Heijne, G., Identification of prokaryotic and eukaryotic signal peptides and prediction of their cleavage sites, *Protein Engineering* 10 (1997) 1-6.

- [164] Hillar, A., and Loewen, P. C., Comparison of isoniazid oxidation catalyzed by bacterial catalase-peroxidases and horseradish peroxidase, *Archives of Biochemistry and Biophysics* 323 (1995) 438-446.
- [165] Chouchane, S., Girotto, S., Kapetanaki, S., Schelvis, J. P. M., Yu, S., and Magliozzo, R. S., Analysis of heme structural heterogeneity in mycobacterium tuberculosis catalase-peroxidase (katg), *Journal of Biological Chemistry* 278 (2003) 8154-8162.
- [166] Chouchane, S., Girotto, S., Kapetanaki, S., Schelvis, J. P. M., Yu, S. W., and Magliozzo, R. S., Analysis of heme structural heterogeneity in mycobacterium tuberculosis catalase-peroxidase (katg), *Journal of Biological Chemistry* 278 (2003) 8154-8162.
- [167] Jakopitsch, C., Ruker, F., Regelsberger, G., Dockal, M., Peschek, G. A., and Obinger, C., Catalase-peroxidase from the cyanobacterium *synechocystis pcc 6803*: Cloning, overexpression in *escherichia coli*, and kinetic characterization, *Biological Chemistry* 380 (1999) 1087-1096.
- [168] Erman, J. E., Kinetic studies of fluoride binding by cytochrome-c peroxidase, *Biochemistry* 13 (1974) 34-39.
- [169] Dunford, H. B., Hewson, W. D., and Steiner, H., Horseradish-peroxidase .29. Reactions in water and deuterium-oxide - cyanide binding, compound-i formation, and reactions of compound-i and compound-ii with ferrocyanide, *Canadian Journal of Chemistry-*Revue Canadienne De Chimie** 56 (1978) 2844-2852.

- [170] Johnsson, K., Froland, W. A., and Schultz, P. G., Overexpression, purification, and characterization of the catalase-peroxidase katg from mycobacterium tuberculosis, *Journal of Biological Chemistry* 272 (1997) 2834-2840.
- [171] Yamada, Y., Fujiwara, T., Sato, T., Igarashi, N., and Tanaka, N., The 2.0 Å crystal structure of catalase-peroxidase from haloarcula marismortui, *Nature Structural Biology* 9 (2002) 691-695.
- [172] Bertrand, T., Eady, N. A. J., Jones, J. N., Jesmin, Nagy, J. M., Jamart-Gregoire, B., Raven, E. L., and Brown, K. A., Crystal structure of mycobacterium tuberculosis catalase-peroxidase, *J. Biol. Chem.* 279 (2004) 38991-38999.
- [173] Donald, L. J., Krokhin, O. V., Duckworth, H. W., Wiseman, B., Deemagarn, T., Singh, R., Switala, J., Carpena, X., Fita, I., and Loewen, P. C., Characterization of the catalase-peroxidase katg from burkholderia pseudomallei by mass spectrometry, *J. Biol. Chem.* 278 (2003) 35687-35692.
- [174] Arnao, M. B. A., M.; Del Rio, J. A.; Varon, R.; Garcia-Canovas, F, A kinetic study on the suicide inactivation of peroxidase by hydrogen peroxide., *Biochimica et Biophysica Acta (BBA) - Bioenergetics* 1041 (1990) 43-47.
- [175] Arnao, M. B. A., M.; Del Rio, J. A.; Garcia-Canovas, F, Inactivation of peroxidase by hydrogen peroxide and its protection by a reductant agent., *Biochimica et Biophysica Acta (BBA) - Bioenergetics* 1038 (1990) 85-89.
- [176] Baynton, K. J. B., Jatinder K.; Biswas, Nihar; Taylor, Keith E., Inactivation of horseradish peroxidase by phenol and hydrogen peroxide: A kinetic investigation., *Biochimica et Biophysica Acta (BBA) - Bioenergetics* 1206 (1994) 272-278.

- [177] Nakajima, R., and Yamazaki, I., The mechanism of oxyperoxidase formation from ferryl peroxidase and hydrogen peroxide, *J. Biol. Chem.* 262 (1987) 2576-2581.
- [178] Jakopitsch, C., Wanasinghe, A., Jantschko, W., Furtmuller, P. G., and Obinger, C., Kinetics of interconversion of ferrous enzymes, compound ii and compound iii, of wild-type *Synechocystis* catalase-peroxidase and y249f, *Journal of Biological Chemistry* 280 (2005) 9037-9042.
- [179] Cohn, S., Alternatives to blood in the 21st century, *Critical Care* 8 (2004) S15 - S17.
- [180] Fitzpatrick, C. M., Savage, S. A., Kerby, J. D., Clouse, W. D., and Kashyap, V. S., Resuscitation with a blood substitute causes vasoconstriction without nitric oxide scavenging in a model of arterial hemorrhage, *Journal of the American College of Surgeons* 199 (2004) 693-701.
- [181] Eich, R. F., Li, T. S., Lemon, D. D., Doherty, D. H., Curry, S. R., Aitken, J. F., Mathews, A. J., Johnson, K. A., Smith, R. D., Phillips, G. N., and Olson, J. S., Mechanism of no-induced oxidation of myoglobin and hemoglobin, *Biochemistry* 35 (1996) 6976-6983.
- [182] Olson, J. S., and Maillett, D. H., Designing recombinant hemoglobin for use as a blood substitute, in *Blood substitutes*, in Winslow, R. M., (Ed.), Academic Press, New York, NY, 2005, pp. 354-374.
- [183] Light, W., 3d, and Olson, J., Transmembrane movement of heme, *J. Biol. Chem.* 265 (1990) 15623-15631.
- [184] Light, W., 3d, and Olson, J., The effects of lipid composition on the rate and extent of heme binding to membranes, *J. Biol. Chem.* 265 (1990) 15632-15637.

- [185] Cannon, J. B., Kuo, F. S., Pasternack, R. F., Wong, N. M., and Mullereberhard, U., Kinetics of the interaction of hemin liposomes with heme binding-proteins, *Biochemistry* 23 (1984) 3715-3721.
- [186] Varnado, C. L., Hertwig, K. M., Thomas, R., Roberts, J. K., and Goodwin, D. C., Properties of a novel periplasmic catalase-peroxidase from *escherichia coli* o157:H7, *Archives of Biochemistry and Biophysics* 421 (2004) 166-174.
- [187] Stojiljkovic, I., Kumar, V., and Srinivasan, N., Non-iron metalloporphyrins: Potent antibacterial compounds that exploit haem/hb uptake systems of pathogenic bacteria, *Molecular Microbiology* 31 (1999) 429-442.
- [188] Inoue, E., Takahashi, Y., Imai, Y., and Kamataki, T., Development of bacterial expression system with high yield of *cyp3a7*, a human fetus- specific form of cytochrome p450, *Biochemical and Biophysical Research Communications* 269 (2000) 623-627.
- [189] Faguy, D. M., and Doolittle, W. F., Horizontal transfer of catalase-peroxidase genes between archaea and pathogenic bacteria, *Trends in Genetics* 16 (2000) 196-197.
- [190] Klotz, M. G., and Loewen, P. C., The molecular evolution of catalatic hydroperoxidases: Evidence for multiple lateral transfer of genes between prokaryota and from bacteria into eukaryota, *Molecular Biology and Evolution* 20 (2003) 1098-1112.
- [191] Lathem, W. W., Bergsbaken, T., Witowski, S. E., Perna, N. T., and Welch, R. A., Acquisition of *stce*, a *cl* esterase inhibitor-specific metalloprotease, during the evolution of *escherichia coli* o157:H7, *Journal of Infectious Diseases* 187 (2003) 1907-1914.
- [192] Bandyopadhyay, P., Byrne, B., Chan, Y., Swanson, M. S., and Steinman, H. M., *Legionella pneumophila* catalase-peroxidases are required for proper trafficking and growth in primary macrophages, *Infection and Immunity* 71 (2003) 4526-4535.

- [193] Kengen, S. W., Bikker, F. J., Hagen, W. R., de Vos, W. M., and van der Oost, J., Characterization of a catalase-peroxidase from the hyperthermophilic archaeon *archaeoglobus fulgidus*, *Extremophiles: Life Under Extreme Conditions* 5 (2001) 323-332.
- [194] Kim, J.-A., Sha, Z., and Mayfield, J. E., Regulation of *brucella abortus* catalase, *Infection and Immunity* 68 (2000) 3861-3866.
- [195] Sha, Z., Stabel, T. J., and Mayfield, J. E., *Brucella abortus* catalase is a periplasmic protein lacking a standard signal sequence, *Journal of Bacteriology* 176 (1994) 7375-7377.
- [196] Ruby, E. G., and McFall-Ngai, M. J., Oxygen-utilizing reactions and symbiotic colonization of the squid light organ by *vibrio fischeri*, *Trends in Microbiology* 7 (1999) 414-420.
- [197] Visick, K. L., and Ruby, E. G., The periplasmic, group iii catalase of *vibrio fischeri* is required for normal symbiotic competence and is induced both by oxidative stress and by approach to stationary phase, *Journal of Bacteriology* 180 (1998) 2087-2092.
- [198] Klotz, M. G., Kim, Y. C., Katsuwon, J., and Anderson, A. J., Cloning, characterization and phenotypic-expression in *escherichia-coli* of *catf*, which encodes the catalytic subunit of catalase isozyme *catf* of *pseudomonas-syringae*, *Applied Microbiology and Biotechnology* 43 (1995) 656-666.
- [199] Klotz, M. G., and Hutcheson, S. W., Multiple periplasmic catalases in phytopathogenic strains of *pseudomonas-syringae*, *Applied and Environmental Microbiology* 58 (1992) 2468-2473.

- [200] Slutsker, L., Ries, A. A., Greene, K. D., Wells, J. G., Hutwagner, L., and Griffin, P. M., *Escherichia coli* o157:H7 diarrhea in the united states: Clinical and epidemiologic features, *Annals of Internal Medicine* 126 (1997) 505-513.
- [201] Bhaskar, B., Immoos, C. E., Shimizu, H., Sulc, F., Farmer, P. J., and Poulos, T. L., A novel heme and peroxide-dependent tryptophan-tyrosine cross-link in a mutant of cytochrome c peroxidase, *Journal of Molecular Biology* 328 (2003) 157-166.
- [202] Ghiladi, R. A., Medzihradzky, K. F., and de Montellano, P. R. O., Role of the met-tyr-trp cross-link in mycobacterium tuberculosis catalase-peroxidase (katg) as revealed by katg(m255i), *Biochemistry* 44 (2005) 15093-15105.
- [203] Donald, L. J., Krokhin, O. V., Duckworth, H. W., Wiseman, B., Deemagarn, T., Singh, R., Switala, J., Carpena, X., Fita, I., and Loewen, P. C., Characterization of the catalase-peroxidase katg from burkholderia pseudomallei by mass spectrometry, *Journal of Biological Chemistry* 278 (2003) 35687-35692.
- [204] Jakopitsch, C., Auer, M., Ivancich, A., Ruker, F., Furtmuller, P. G., and Obinger, C., Total conversion of bifunctional catalase-peroxidase (katg) to monofunctional peroxidase by exchange of a conserved distal side tyrosine, *Journal of Biological Chemistry* 278 (2003) 20185-20191.